A Hipparcos census of the nearby OB associations

Zeeuw, P. T.; Hoogerwerf, R. D; Bruijne, J. H. J. de; Brown, A. G. A.; Blaauw, A.

Published in:
The astronomical journal

DOI:
10.1086/300682

Publication date:
1999

A Hipparcos Census of the Nearby OB Associations[1]

P.T. de Zeeuw, R. Hoogerwerf, J.H.J. de Bruijne,
Sterrewacht Leiden, Postbus 9513, 2300 RA Leiden, The Netherlands

A.G.A. Brown,
Instituto de Astronomía U.N.A.M., Apartado Postal 877, Ensenada, 22800 Baja California, México

and

A. Blaauw
Kapteyn Instituut, Postbus 800, 9700 AV Groningen, The Netherlands and
Sterrewacht Leiden, Postbus 9513, 2300 RA Leiden, The Netherlands

Accepted for publication in the Astronomical Journal, January 1999 issue

ABSTRACT

A comprehensive census of the stellar content of the OB associations within 1 kpc from the Sun is presented, based on Hipparcos positions, proper motions, and parallaxes. It is a key part of a long-term project to study the formation, structure, and evolution of nearby young stellar groups and related star-forming regions.

OB associations are unbound 'moving groups', which can be detected kinematically because of their small internal velocity dispersion. The nearby associations have a large extent on the sky, which traditionally has limited astrometric membership determination to bright stars ($V \lesssim 6^{\rm m}$), with spectral types earlier than ∼B5. The Hipparcos measurements allow a major improvement in this situation. Moving groups are identified in the Hipparcos Catalogue by combining de Bruijne's refurbished convergent point method with the 'Spaghetti method' of Hoogerwerf & Aguilar. Astrometric members are listed for 12 young stellar groups, out to a distance of ∼650 pc. These are the 3 subgroups Upper Scorpius, Upper Centaurus Lupus and Lower Centaurus Crux of Sco OB2, as well as Vel OB2, Tr 10, Col 121, Per OB2, α Persei (Per OB3), Cas–Tau, Lac OB1, Cep OB2, and a new group in Cepheus, designated as Cep OB6. The selection procedure corrects the list of previously known astrometric and photometric B- and A-type members in these groups, and identifies many new members, including a significant number of F stars, as well as evolved stars, e.g., the Wolf–Rayet stars γ^2 Vel (WR11) in Vel OB2 and EZ CMa (WR6) in Col 121, and the classical Cepheid δ Cep in Cep OB6. Membership probabilities are given for all selected stars. Monte Carlo simulations are used to estimate the expected number of interloper field stars. In the nearest associations, notably in Sco OB2, the later-type members include T Tauri objects and other stars in the final pre-main sequence phase. This provides a firm link between the classical high-mass stellar content and ongoing low-mass star formation. Detailed studies of these 12 groups, and their relation to the surrounding interstellar medium, will be presented elsewhere.

Astrometric evidence for moving groups in the fields of R CrA, CMa OB1, Mon OB1, Ori OB1, Cam OB1, Cep OB3, Cep OB4, Cyg OB4, Cyg OB7, and Sct OB2, is inconclusive. OB associations do exist in many of these regions, but they are either at distances beyond ∼500 pc where the Hipparcos parallaxes are of limited use, or they have unfavorable kinematics, so that the group proper motion does not distinguish it from the field stars in the Galactic disk.

The mean distances of the well-established groups are systematically smaller than the pre-Hipparcos photometric estimates. While part of this may be caused by the improved membership lists, a recalibration of the upper main sequence in the Hertzsprung–Russell diagram may be called for. The mean motions display a systematic pattern, which is discussed in relation to the Gould Belt.

Six of the 12 detected moving groups do not appear in the classical list of nearby OB associations. This is sometimes caused by the absence of O stars, but in other cases a previously known open cluster turns out to be (part of) an extended OB association. The number of unbound young stellar groups in the Solar neighbourhood may be significantly larger than thought previously.

[1] Based on data from the Hipparcos astrometry satellite.

1. INTRODUCTION

Ever since spectral classifications for the bright stars became available, and in particular with the publication of Cannon and Pickering's monumental Henry Draper Catalog of stellar spectra in 1918–1924, it has been evident that O and B stars are not distributed randomly on the sky — and hence not uniformly among the stellar population of the Galaxy — but instead are concentrated in loose groups. This inspired research on their individual properties, and on their motions and space distribution. Studies of the stellar content, the internal velocity distribution, and the common motion of the group members with respect to the ambient stellar population naturally relied on the capability of identifying the stars belonging to the group, their 'members'. Among extensive early investigations along these lines in the wake of work on 'moving groups' and compact stellar clusters (summarized in Eddington 1914), we note Kapteyn's (1914, 1918) work on 'the brighter Galactic helium stars' — i.e., the B stars — and the work by Rasmuson (1921, 1927). Among the early investigations of the space distribution we note in particular the comprehensive work by Pannekoek (1929), carried out at the time of the breakthrough of the modern concept of the Galaxy as an isolated, rotating system. Pannekoek's summarizing table 15 lists 37 groups of B stars, among which several, called by him 'Lacerta', 'Cep I', 'Cep II', 'ζ Pers', 'Lupus', 'Scorpio', and others, may be considered as 'forerunners' of the objects of modern research. His diagram of the groups of B stars, projected on the Galactic plane (*loc. cit.* p. 65) is a remarkable foreshadow of some of the figures presented in this paper. In the early 1950s the work of W.W. Morgan and collaborators provided the first identification of the Galactic spiral structure in the distribution of stellar 'aggregates' (Morgan, Sharpless & Osterbrock 1952a, b; Morgan, Whitford & Code 1953). Herschel (1847) and Gould (1874) had already noticed that the brightest stars are not distributed symmetrically with respect to the plane of the Milky Way, but seemed to form a belt that is inclined $\sim$18° to it. This became known as the Gould Belt, and was subsequently found to be associated with a significant amount of interstellar material (Lindblad 1967; Sandqvist, Tomboulides & Lindblad 1988; Pöppel 1997).

Ambartsumian (1947) introduced the term 'association' for the groups of OB stars; he pointed out that their stellar mass density is usually less than 0.1 $M_\odot$ pc^{-3}. Bok (1934) had already shown that such low-density stellar groups are unstable against Galactic tidal forces, so that OB associations must be young (Ambartsumian 1949), a conclusion supported later by the ages derived from color-magnitude diagrams. This is in harmony with the fact that these groups are usually located in or near star-forming regions, and hence are prime sites for the study of star formation processes and of the interaction of early-type stars with the interstellar medium (see e.g., Blaauw 1964a, 1991 for reviews). Ruprecht (1966) compiled a list of OB associations, with field boundaries, bright members, and distance. He introduced a consistent nomenclature, approved by the IAU, which we adopt here. Ruprecht's list is based on the massive 'Catalogue of Star Clusters and Associations', put together by him and his group, and maintained for many years (Alter, Ruprecht & Vanýsek 1970; Ruprecht, Balázs & White 1981).

Detailed knowledge of the stellar content, structure, and kinematics of OB associations allows us to address fundamental questions on the formation of stars. What is the initial mass function? What are the characteristics of the binary population? What is the star formation rate and efficiency? Do all stars in a group form at the same time? What causes the distinction between the formation of bound open clusters and unbound associations? What is the connection between the stellar content of associations and the energetics and dynamical evolution of the surrounding interstellar medium? What are the properties of the ensemble of OB associations, and how do these relate to the structure and evolution of the Galaxy? Answers to these questions are essential for the interpretation of observations of extragalactic star-forming regions and starburst galaxies.

Although OB associations are unbound, their velocity dispersions are only a few km s^{-1} (e.g., Mathieu 1986; Tian et al. 1996), and so they form coherent structures in velocity space. The common space motion relative to the Sun is perceived as a convergence of the proper motions of the members towards a single point on the sky (e.g., Blaauw 1946; Bertiau 1958). This can be used to establish membership based on measurements of proper motions. Whereas many such astrometric membership studies have been carried out for open clusters (e.g., van Leeuwen 1985, 1994; van Altena et al. 1993; Robichon et al. 1997), there are few such studies for nearby OB associations because these generally cover tens to hundreds of square degrees on the sky. Ground-based proper motion studies therefore almost invariably have been confined to modest samples of bright stars ($V \lesssim 6^{\rm m}$) in fundamental catalogs, or to small areas covered by a single photographic plate. Photometric studies extended membership to later spectral types (e.g., Warren & Hesser 1977a, b, 1978), but are less reliable due to, e.g., undetected duplicity, or the distance spread within an association. As a result, membership for many associations has previously been determined unambiguously only for spectral types earlier than B5 (e.g., Blaauw 1964a, 1991). Although this covers the important upper main-sequence turnoff region, it is not known what the lower mass limit is of the stars that belong to the association, so that our knowledge of these young stellar groups has remained rather limited.

The Hipparcos Catalogue (ESA 1997) contains accurate positions, proper motions, and trigonometric parallaxes, which are all tied to the same global reference system (ICRS: see ESA 1997, Vol. 1 §1.2.2). This makes these measurements ideally suited for the identification of astrometric members of the nearby OB associations,

with greater reliability, and to much fainter magnitudes than accessible previously. Accordingly, the SPECTER consortium was formed in Leiden in 1982, which successfully proposed the observation by Hipparcos of candidate members of nearby OB associations. An extensive program of ground-based observations was carried out in anticipation of the release of the Hipparcos data (for a summary, see de Zeeuw, Brown & Verschueren 1994; §2.3). Here we present the results of our census of the nearby associations based on the Hipparcos measurements.

We have developed a new procedure to identify moving groups in the Hipparcos Catalogue in an objective and reliable way. It combines a refurbished convergent point method (de Bruijne 1998) and the so-called 'Spaghetti method' of Hoogerwerf & Aguilar (1998), and in this way significantly reduces the number of misidentifications. We have estimated the remaining number of interlopers by means of Monte Carlo simulations. The Hipparcos measurements are most valuable for the nearest associations. The individual parallaxes have typical errors of ∼1 mas, and hence are of little value beyond ∼500 pc. However, the proper motions can be quite significant to much larger distances. For this reason we apply our procedure to fields centered on the known associations and suspected groups at pre-Hipparcos estimated distances of less than 1 kpc from the Sun.

This paper is organized as follows. In §2 we summarize the original selection of fields, and the resulting Hipparcos sample, and in §3 we describe our member selection procedure. Then we discuss the results for each of the fields, starting with the Scorpio–Centaurus–Lupus–Crux complex in §4. §5 is devoted to the Vela region. In §6 we discuss Canis Major, Monoceros, and Orion. Then follow Taurus, Perseus, Cassiopeia, and Camelopardalis (§7), and Lacerta, Cepheus, Cygnus, and Scutum (§8). In §9 we derive mean distances and motions for the nearby associations. We summarize our overall conclusions in §10, and also outline the next steps. Appendices give details of the member selection, of pitfalls in the determination of mean distances, and lists of association members. The selection procedure for the Scorpio–Centaurus–Lupus–Crux complex (§4) is described in detail. It provides an example of how we have analysed the other fields, for which we restrict ourselves to a concise description of the pre- and post-Hipparcos results.

Preliminary results of this census were reported in de Bruijne et al. (1997), Hoogerwerf et al. (1997) and de Zeeuw et al. (1997). These are superseded by the results presented here. Detailed studies of the physical properties of the stars in the nearby OB associations will be presented elsewhere.

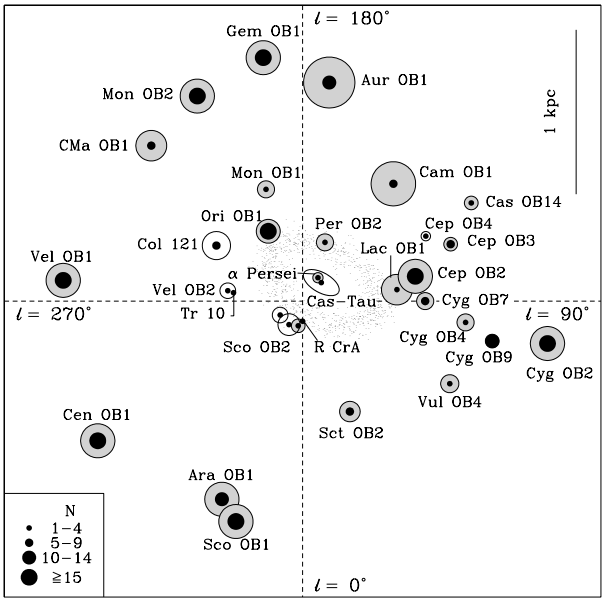

Figure 1: Pre-Hipparcos locations of the OB associations within ∼1.5 kpc, projected onto the Galactic plane, as listed by Ruprecht (1966). The Sun is at the center of the dashed lines which give the principal directions in Galactic longitude, ℓ. The size of the circles represents the projected dimension of the associations, enlarged by a factor 2 with respect to the distance scale. The size of the central dots indicates the degree of current or recent star formation activity, as given by the number N of stars more luminous than absolute magnitude $M_V \sim -5^{\rm m}$ (Humphreys 1978). Associations discussed in this paper which are absent from Ruprecht's list are represented as open circles: Scorpius OB2 subgroups 3 and 4 (Blaauw 1946); Vela OB2 (Brandt et al. 1971); Trumpler 10 (Lyngå 1959, 1962); Collinder 121 (Feinstein 1967); Cassiopeia–Taurus (Blaauw 1956); Cepheus OB4 (MacConnell 1968); R Corona Australis (Marraco & Rydgren 1981). The distribution of small dots indicates the Gould Belt (§9.2). Figure 29 presents the post-Hipparcos map of the nearby OB associations.

2. THE NEARBY OB ASSOCIATIONS

2.1. The Solar neighbourhood

Properties of the OB associations within 1.5 kpc from the Sun were reviewed by Blaauw (1964a, 1991). Figure 1 shows the pre-Hipparcos locations of these associations, as given in the official IAU list (Ruprecht 1966). It also includes a few associations and subgroups discussed here, but absent from Ruprecht's list. The large variety in stellar content, projected dimension, clumpiness, age, and connection to the interstellar medium introduces biases in the identification of the associations. For example, associations containing several luminous supergiants can be detected out to several kpc (e.g., Cep OB1 in §8.2; Humphreys 1978; Garmany & Stencel 1992), whereas associations without such stars can easily escape attention. Ruprecht's list is based on Ambartsumian's definition which requires the presence of O stars and an open

cluster as 'nucleus' (e.g., Alter et al. 1970). As a result the list is incomplete, e.g., two of the subgroups of Sco OB2 are not included (§4). Many of the groups in Figure 1 are associated with concentrations of molecular material (e.g., Dame et al. 1987). Most associations within 500 pc from the Sun belong to the Gould Belt system (§9.2).

2.2. *Hipparcos Proposal 141*

When the call for proposals for the Hipparcos mission was released in 1982, the pre-launch specifications indicated absolute proper motions and parallaxes with 1σ accuracies of 1.5–2 mas (yr^{-1}), a limiting magnitude of $V{\sim}11^{\mathrm{m}}$, and a total mean stellar density of about 3 stars per square degree. This clearly promised a major step forward in the study of the nearby OB associations. Accordingly, the SPECTER consortium submitted a proposal to ESA to include in the Hipparcos Input Catalogue candidate members of the known OB associations (or subgroups) out to a distance of 1 kpc. We took generous boundaries around the known locations. Table 1 lists the associations, gives their pre-Hipparcos distance $D_{\rm clas}$, the field boundaries in Galactic coordinates (ℓ, b), and the proposed number $N_{\rm prop}$ of candidate members per association or subgroup.

We selected all O and B stars from the Catalogue of Stellar Identifications (CSI: Jung & Bischoff 1971) within the assocation boundaries, as well as later-type stars within certain magnitude limits defined by the (pre-Hipparcos) distances of the associations, so as to exclude foreground and background stars. This resulted in 13961 candidate member stars. We divided this sample initially into three categories. Priority 1 contained stars of spectral type O and B and stars that were considered as established or probable members of the associations based on proper motion, radial velocity or photometric work by previous authors. The remaining stars were divided into two nearly equal groups, by assigning them priority 2 or 3 depending on whether their CSI number is odd or even. We took this seemingly peculiar step because the number density of our proposed objects was uncomfortably close to the limit of 3 per square degree. We therefore suggested to the Input Consortium that in order to satisfy the constraint on the number density of objects, while preserving the statistical completeness of our sample, all priority 3 stars could be dropped, if necessary.

The SPECTER proposal was approved as number 141, with the comment that for groups beyond 600 pc the parallax measurements would not be very significant, and that — as we had expected — the number density of the fainter proposed stars was larger than was possible to accept for the Hipparcos Input Catalogue. This resulted in the inclusion of 9150 of our candidate members in the Hipparcos Input Catalogue (Turon et al. 1992), amongst which were nearly all the priority 1 stars. Table 1 lists the number $N_{\rm HIC}$ of the originally proposed stars that were accepted per field, together with the total number $N_{\rm HIP}$ of stars observed by Hipparcos in the same field.

Table 1. The nearby OB associations

Name	$D_{\rm clas}$	ℓ_-	ℓ_+	b_-	b_+	$N_{\rm prop}$	$N_{\rm HIC}$	$N_{\rm HIP}$
Sco OB2_1	170	330	3	−19	7	2522	1650	3320
Sco OB2_2*	160	337	3	7	32	1233	908	1796
Sco OB2_3*	170	313	337	5	31	1737	1202	2215
Sco OB2_4*	160	292	313	−10	16	1531	1161	2787
Sco OB2_5	170	273	292	−20	5	1337	973	2225
Col 121	630	222	244	−15	−3	562	424	1001
Ori OB1	500	197	215	−26	−12	1318	750	968
Mon OB1	715	201	205	−3	3	86	46	94
Per OB2	400	156	164	−22	−13	207	130	218
α Persei*	170	140	155	−11	−3	619	361	517
Cam OB1	900	130	153	−3	8	862	320	919
Cep OB4	845	116	120	3	7	46	18	60
Cep OB3	960	108	113	1	7	169	97	157
Cep OB2	700	96	108	−1	12	651	345	676
Lac OB1	600	94	107	−19	−7	561	344	709
Cyg OB7	740	84	96	−5	9	249	181	680
Cyg OB4	1000	81	85	−9	−6	15	10	51
Sct OB2	730	20	26	−3	2	45	28	82
Cas–Tau**	140		all sky			49	49	
Runaways			all sky			162	153	
Total						13961	9150	18475

Note. — Pre-Hipparcos distance estimate $D_{\rm clas}$ (from Ruprecht 1966; Sco OB2_1, 2_3, 2_4, and 2_5 from Blaauw 1946; Col 121 from Feinstein 1967; Cep OB4 from MacConnell 1968; Cas–Tau from Blaauw 1956), field boundaries in Galactic coordinates (ℓ, b), and number $N_{\rm prop}$ of candidate members proposed for observation with Hipparcos in 1982. $N_{\rm HIC}$ is the number of candidates accepted for inclusion in the Hipparcos Input Catalogue. $N_{\rm HIP}$ is the total number of stars in the Hipparcos Catalogue within the field boundaries. Some of the fields contain more than one association. In this paper, we also study fields in Corona Australis (§4.6) and in Vela (§5). *Sco OB2_2: Upper Scorpius (US); Sco OB2_3: Upper Centaurus Lupus (UCL); Sco OB2_4: Lower Centaurus Crux (LCC); α Persei: Per OB3. **Ruprecht lists Cas–Tau as a semi-doubtful association, and gives a distance of 1400 pc.

Even though we had distinguished priority 2 and 3 stars to allow cutting of the sample by a factor 2 in a statistically unbiased way, the final selection turned out to contain both, so that statistical inferences, especially for stars fainter than the completeness limit, should be made with care. For example, in some areas the inclusion of many B-type stars resulted in a bias against stars of type A and later, so as to stay within the limits on number density (Figure 2).

We reproposed our program in 1992, and took the opportunity to modify the field boundaries slightly, and to include the groups R CrA and Vel OB2. The preliminary results of our census, reported in de Bruijne et al. (1997), Hoogerwerf et al. (1997), and de Zeeuw et al. (1997), are based on the resulting sample of 12842 stars, made available to us in late 1996. During this investigation it became clear that in some cases the associations seemed to 'spill over' the previously chosen boundaries in ℓ, b, and V. Now that the entire Hipparcos Catalogue is available, we can investigate the full set of stars in the association fields, and also study the surrounding areas, and we do so here.

The Hipparcos Catalogue also includes 153 of our original 162 proposed candidate runaway OB stars. The study of these stars is of interest for the question of their origin: supernova explosions in high-mass binaries, or dynamical ejection, or both (Blaauw 1961, 1993; Poveda, Ruiz & Allen 1967). We are in the process of retracing the three-dimensional paths of the runaways and the OB associations in the Galactic potential in order to identify the parent associations, and the age of the runaways. This

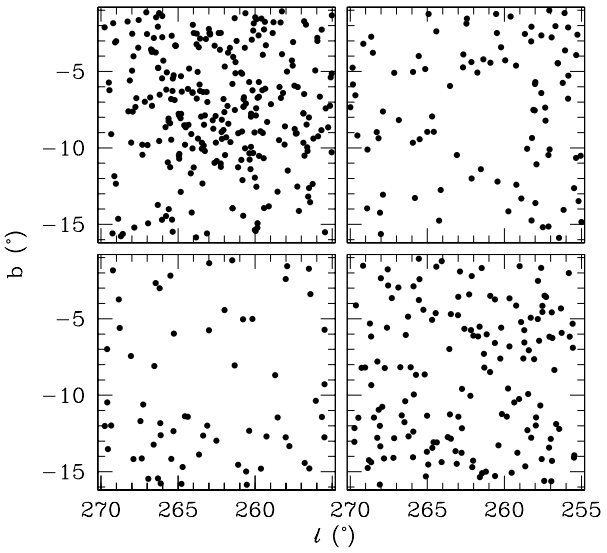

Figure 2: An example of selection effects in the Hipparcos Catalogue. The four panels show all stars in the field $255° \leq \ell \leq 270°$ and $-16° \leq b \leq -1°$ in Vela (§5.1) with $V > 7^{\rm m}$ and spectral types O and B (top left; 277 stars), A (top right; 93 stars), F (bottom left; 62 stars), and G (bottom right; 153 stars). The relative shortage of A, F, and G stars is caused by the large numbers of B stars that were included, combined with the requirement that the mean number density does not exceed about 3 per square degree.

is also of considerable interest for studies of high-mass binary evolution (van Rensbergen, Vanbeveren & de Loore 1996) and of high-mass X-ray binaries (Kaper et al. 1997). We will report on this investigation elsewhere.

2.3. Photometry

The SPECTER consortium carried out extensive photometric observations of the southern associations between 1982 and 1989, with the Walraven *VBLUW* photometer on the 91cm Dutch telescope at ESO (Lub & Pel 1977). As the total number of originally proposed candidate stars in the southern fields approached 10 000, we concentrated on the priority 1 and 2 stars as defined in Proposal 141, and obtained *VBLUW* measurements for a total of 5260 objects (de Geus, Lub & van der Grift 1990). A preliminary analysis for the priority 1 stars in Sco OB2 and in Ori OB1 was reported by de Geus, de Zeeuw & Lub (1989) and Brown, de Geus & de Zeeuw (1994), respectively.

The final set of candidates included in the Hipparcos Input Catalogue is a mix of our original priority 2 and 3 objects (§2.2). By the time this was known our Walraven program was concluded, so that we do not have *VBLUW* photometry for the entire sample. The Walraven photometer was retired before the release of the Hipparcos Input Catalogue. Our member selection should not favor stars of either priority, so the *VBLUW* photometry is incomplete also for the finally selected member stars. Published *uvbyβ* and *UBV* photometry is incomplete as well (Hauck & Mermilliod 1990; Mermilliod & Mermilliod 1994). Here we will therefore generally restrict ourselves to the V and $B-V$ values listed in the Hipparcos Catalogue. We are taking steps to obtain homogeneous intermediate band photometry for all the associations.

3. SELECTION METHOD

The stars in an OB association have nearly identical space motions, and can be recognized as a coherent structure in velocity space. We identify the members of these moving groups by using Hipparcos positions, proper motions *and* parallaxes. We do this by combining two member selection methods. One is a modification of the classical convergent point method, outlined in §3.1. The other method is new, and we summarize it in §3.2. Then we describe the selection procedure and membership definition (§3.3), and discuss how we estimate the contamination by field stars (referred to as interlopers, §3.4), the problems caused by marginally resolved long-period binaries (§3.5), the derivation of mean distances (§3.6), and the prospects for resolving the internal structure and motions (§3.7).

3.1. Convergent point method

The common space motion of stars in a moving group results in converging proper motions on the sky. We employ a modern implementation of a classical convergent point method (Brown 1950; Jones 1971), which uses the Hipparcos positions and proper motions, but not the parallaxes. The method is described and tested in full by de Bruijne (1998). We first summarize the classical method, and then describe the main modifications.

The classical convergent point method considers a set of stars j at positions $(\ell, b)_j$, with proper motions $(\mu_\ell \cos b, \mu_b)_j$, and errors $(\sigma_{\mu_\ell \cos b}, \sigma_{\mu_b})_j$. The first step is to discard stars with insignificant proper motions, i.e., with

$$t \equiv \frac{\mu}{\sigma_\mu} \equiv \frac{\sqrt{\mu_\ell^2 \cos^2 b + {\mu_b}^2}}{\sqrt{\sigma^2_{\mu_\ell \cos b} + \sigma^2_{\mu_b}}} \leq t_{\rm min}, \qquad (1)$$

where $t_{\rm min}$ was typically chosen to be equal to 3–5 (Jones 1971). The next step is to search for the maximum likelihood coordinates $(\ell, b)_{\rm cp}$ of the convergent point by minimizing

$$\chi^2 = \sum_{j=1}^{N} t^2_{\perp j}, \qquad (2)$$

where N is the number of stars in the sample, and $t_{\perp j}$ is the value for star j of the quantity $t_\perp$, defined as

$$t_\perp \equiv \mu_\perp / \sigma_\perp. \qquad (3)$$

Here $\mu_\perp$ is the component of the proper motion perpendicular to the direction towards the convergent point, and $\sigma_\perp$ is its measurement error.

In case of a common space motion, the proper motion vectors will be directed towards the convergent point, so that for all moving group members the expectation value for $\mu_\perp$ equals 0. The sum (2) is distributed as χ^2 with N–2 degrees of freedom. If, after minimization with respect to $(\ell, b)_{\rm cp}$, the value of χ^2 is unacceptably high, the star with the highest value of $\mu_\perp/\sigma_\perp$ is rejected, after which minimization is repeated until a satisfactory value of χ^2 is obtained. Subsequently, all non-rejected stars are identified as members. This procedure allows for simultaneous convergent point determination and member selection, and has been applied with success to, e.g., the Hyades (van Bueren 1952; Perryman et al. 1998), and Sco OB2 (Jones 1971).

De Bruijne's (1998) modification of the convergent point method consists of three steps. First, unlike previous astrometric catalogs, the Hipparcos Catalogue gives the full covariance matrix for the measured astrometric parameters. It is therefore possible to include the full error propagation. Second, even for infinitely accurate measurements, moving group members would not have proper motions directed exactly towards the convergent point because of the intrinsic velocity dispersion in the group. As a result, selecting only stars with $t_\perp = 0$ will not identify all members. For this reason definition (3) of $t_\perp$ is changed to

$$t_\perp \equiv \frac{\mu_\perp}{\sqrt{{\sigma_\perp}^2 + {\sigma^\star_{\rm int}}^2}}, \qquad (4)$$

where $\sigma^\star_{\rm int}$ is an estimate of the intrinsic one-dimensional velocity dispersion in the group, expressed in proper motion units. Accordingly, the definition (1) of t is changed to

$$t \equiv \frac{\mu}{\sqrt{{\sigma_\mu}^2 + {\sigma^\star_{\rm int}}^2}}. \qquad (5)$$

Third, the current workstations are powerful enough to drop the classical approach of evaluating the sum (2) on a grid. In order to find the maximum likelihood convergent point, a global, direct minimization routine can be applied. De Bruijne (1998) defines a membership probability $p_{\rm cp}$ as $p_{\rm cp} = 1 - p$, where p is the probability that the perpendicular component of the proper motion has a value different from zero, given the covariance matrix. He shows that

$$p_{\rm cp} = \exp(-t_\perp^2/2). \qquad (6)$$

The above procedure is biased towards inclusion of stars at larger distances. It selects members based on the absolute value of $t_\perp$, which is a function of distance: nearby stars generally have large proper motions, and are more likely to be rejected than those at larger distances, which generally have smaller proper motions. Our combined member selection method (§3.3; Figure 4) effectively deals with this bias.

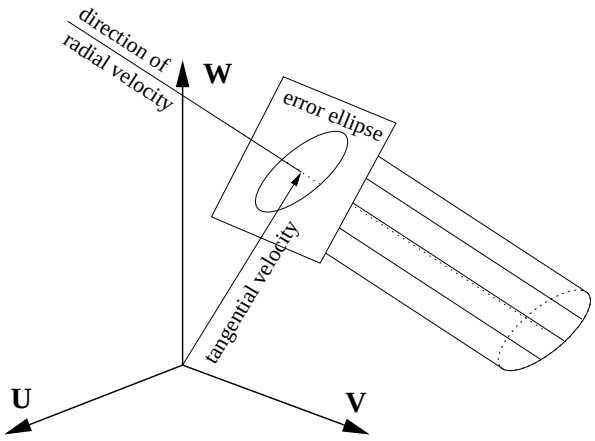

Figure 3: The five astrometric parameters of a star measured by Hipparcos define an elliptical cylinder in velocity space. The offset from the origin is determined by the tangential velocity, which follows from the proper motion and the parallax; the orientation is set by the direction of the radial velocity (i.e., by the position on the sky). The finite thickness of the cylinder is caused by the measurement errors. All cylinders of stars in a moving group intersect. U, V, and W are the velocity components in standard Galactic Cartesian coordinates: U is directed towards the Galactic center, V in the direction of Galactic rotation, and W towards the north Galactic pole.

3.2. Spaghetti method

In order to make optimal use of the Hipparcos data, we also apply a kinematic member selection method developed by Hoogerwerf & Aguilar (1998, hereafter HA), which uses, besides positions and proper motions, also parallaxes. We briefly summarize the main steps.

The Hipparcos measurements constrain a star to lie on a straight line in velocity space: the proper motion and parallax determine the offset from the origin (tangential velocity), while the sky position of the star determines its direction (cf. Figure 3). The covariance matrix of the astrometric parameters transforms this line into a probability distribution in velocity space, which HA describe as a two-dimensional Gaussian. Surfaces of equal probability are elliptic cylinders. HA denote these as 'spaghetti'. The cylinders of a set of stars with the same space motion all intersect in one point. Thus, HA identify moving groups by searching for maxima in the density of cylinders in velocity space. This 'spaghetti density' in velocity space is simply the sum over all stars in the sample of the individual probability distributions.

Measurement of the stellar radial velocities would reduce each elliptic cylinder to an ellipsoidal probability distribution in velocity space. In practice, high-quality radial velocities are available only for a small subset of the stars in our sample, and we therefore decided not to use them in the member selection.

In case of infinitely accurate astrometric measurements, moving group members would not necessarily have cylinders coinciding exactly at the space motion of the group

because of the intrinsic velocity dispersion in the group. This broadens the associated peak in velocity space. Measurement errors broaden it further. HA therefore place a sphere at the position of this peak, with a radius $\sigma_{\rm sp}$ given by

$$\sigma_{\rm sp}^2 = \sigma_{\rm med}^2 + \sigma_{\rm int}^2, \qquad (7)$$

where $\sigma_{\rm med}$ is an estimate of the typical error in tangential velocity for a star at the distance of the moving group, taken as the median value of the semi-major axis length of the 1σ cylinders of all stars in the range of distances where moving group members can be expected (Appendix A), and $\sigma_{\rm int}$ is an estimate of the one-dimensional velocity dispersion in the moving group. At a given distance D in kpc, $\sigma_{\rm int}$ and $\sigma^\star_{\rm int}$ (eq. 4) are related through $\sigma_{\rm int} = A\,\sigma^\star_{\rm int} D$, where $A = 4.74$ km yr s^{-1} and $\sigma_{\rm int}$ is in units of mas yr^{-1}.

HA compute for each star the integral of its probability distribution over three-dimensional velocity space restricted to the volume of the sphere with radius $\sigma_{\rm sp}$ defined in eq. (7), and denote this quantity by S. All stars with S larger than a certain cutoff $S_{\rm min} = 0.1$ are accepted as members. This value is based on extensive Monte Carlo simulations of associations, described in HA. S cannot be interpreted as a simple probability as it depends on distance. Stars with small parallaxes, at the far side of a group, will have smaller values of S than those with large parallaxes at the near side, because the error in tangential velocity, i.e., the thickness of the cylinder, depends on parallax.

3.3. Combined method and search strategy

We combine the results of the two methods described above to define our membership list: we consider as secure members those stars that are selected by both methods. Figure 4 illustrates the power of this combined approach. The left panel shows the secure members for Vel OB2 (§5.1). Both the proper motions and parallaxes show a coherent structure confirming Vel OB2 as a physical group. The additional stars selected by the Spaghetti method only (middle panel) have parallaxes in the same range as those of the secure members. These stars are rejected by the convergent point method because the proper motions are inconsistent with the convergent point, even though the tangential velocities used by the Spaghetti method are consistent with that of the group within the errors. This occurs because the errors on the tangential velocity components include the parallax error, which dominates for the more distant groups like Vel OB2. The fraction of such rejected Spaghetti members drops to a few per cent in the nearest associations. In turn, some of the stars selected by the convergent point method are rejected by the Spaghetti method because the corresponding tangential velocities are inconsistent with the cluster motion, even though the proper motions are consistent with the convergent point. These stars have deviating parallaxes (right panel); the convergent point method is clearly biased towards selecting stars with small parallaxes (§3.1).

Many radial velocity and proper motion studies of moving groups have been carried out for open and globular clusters (e.g., van Leeuwen 1994; Cudworth 1998). These systems are centrally concentrated and gravitationally bound, have small internal velocity dispersions $\sigma_{\rm int}$ (less than 1 km s^{-1} for most open clusters), and a finite radius set by the Galactic tidal field. As a result, kinematic membership is well-defined: in practice all stars that have velocities within $3\sigma_{\rm int}$ of the mean motion are considered members. It is sometimes possible to identify 'fellow-travelers', which at one time may have belonged to the cluster, but have spilled over the tidal radius relatively recently (e.g., Grillmair et al. 1995; Perryman et al. 1998).

By contrast, OB associations are low-density dispersed stellar groups which have formed recently, but are unbound. The dispersion in stellar velocities is at most a few km s^{-1} (Mathieu 1986; Tian et al. 1996), but the velocity distribution may have substructure: there may be subgroups with significantly smaller dispersions and/or slightly different space velocities. The overall space motion can be detected kinematically, but the definition of membership is less well-defined, as it is not clear *a priori* what should be taken as $\sigma_{\rm int}$ in eqs (4), (5), and (7). A value that is too large will result in the inclusion of many interloper field stars. A value that is too small may well exclude many of the stars that were formed at the same time, and in the same region. We take $\sigma_{\rm int}$ to be 3 km s^{-1}. This value is somewhat larger than the expected velocity dispersion in the OB associations, and hence it reduces the number of genuine members that is discarded by our selection procedure (but see §3.5). Monte Carlo simulations show that a choice for $\sigma_{\rm int}$ consistent with the modeled intrinsic velocity dispersion will typically miss less than ∼10 per cent of the members (de Bruijne 1998; Hoogerwerf & Aguilar 1998). If we used the convergent point or the Spaghetti method separately, this high reliability would come at the price of an increased number of interlopers. We rely on the combination of the two methods to minimize the number of accidental interlopers (Figure 4).

It is difficult to define a membership probability for stars selected by the Spaghetti method (§3.2). We therefore use $P = p_{\rm cp}$ defined in eq. (6) as membership probability for the stars selected by the combined method. In view of the above, this probability should be interpreted with care.

The Hipparcos Catalogue is essentially complete to $V = 7\overset{\rm m}{.}3$–$9\overset{\rm m}{.}0$, depending on Galactic latitude and spectral type. A few binaries and stars in crowded fields brighter than this limit are missing. It follows that many genuine association members do not appear in the Catalogue, especially for later spectral types and/or associations at large distances. Therefore, we decided on a search strategy in which we identify the association among the early-type stars in the Hipparcos Catalogue. This provides the common motion. We then find the association members among the later spectral types by selecting those stars that are consistent with the motion of the secure early-type mem-

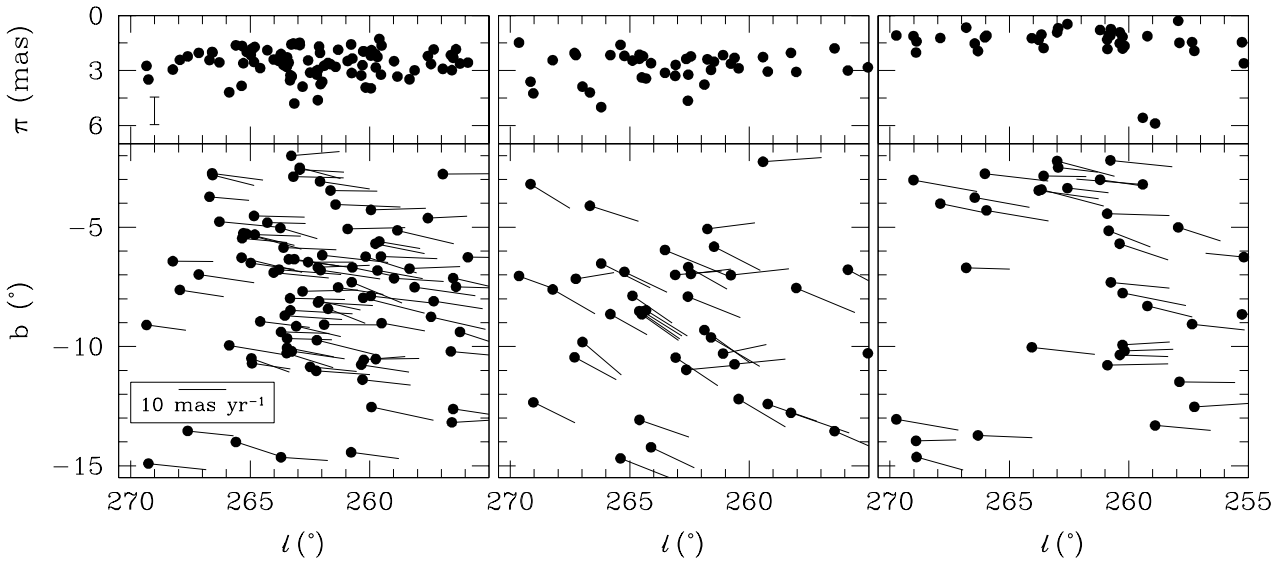

Figure 4: Left: positions and proper motions (bottom) and parallaxes (top) for the 93 secure members of Vela OB2 (§5.1), selected by the convergent point method *and* the Spaghetti method. Middle: same diagram for 41 additional stars selected by the Spaghetti method only. The directions of the proper motions differ considerably from those in the left panel. The group of comoving stars around $(\ell, b)\sim(264\overset{\circ}{.}5, -8\overset{\circ}{.}5)$ consists of members of NGC2547. Right: same diagram for 37 other stars selected by the convergent point method only. The proper motions are parallel to those in the left panel, but the parallaxes differ considerably, with most of them being significantly smaller. Two stars move in the opposite direction. The vertical bar in the left top panel corresponds to the average $\pm 1\sigma$ parallax range for the stars shown.

bers. The full procedure is described step-by-step in Appendix A.

3.4. Contamination by field stars

Our kinematic selection method will accept some field stars as association members. Here we describe our method for estimating the expected number of these interlopers.

3.4.1. Principles

We consider a specific association, select all entries from the Hipparcos Catalogue within the chosen field boundaries (Table A1), and optionally (see §3.4.2) delete the entries corresponding to the secure members. Next, we delete all proper motions. Then we replace these by synthetic values, consistent with the field star distribution in the Solar neighbourhood. We draw these randomly from the kinematic model of the Galactic disk derived from the Hipparcos Catalogue by Dehnen & Binney (1998). By construction, the magnitude, parallax, position, and spectral-type distribution are reproduced consistent with those in the Hipparcos Catalogue. We then apply our selection procedure to 100 of these Monte Carlo realisations in the same manner as for the corresponding association, to search for comoving stars at the known space motion of the group. The resulting median number of comoving stars is an estimate of the expected number of interlopers. We summarize the results in Table A2.

3.4.2. Removal of secure members?

A non-trivial aspect is whether or not to remove the secure members from the field before performing the interloper analysis. Either option leads to systematic errors. Two facts are important: (i) the ratio of the number of association members and the number of field stars in the Hipparcos Catalogue decreases strongly from spectral type O to M; and (ii) the ratio of the number of association members observed by Hipparcos and the total number of association members is a function of distance, and strongly decreases towards later spectral types due to the completeness limit of the Catalogue.

Removing the secure members, including a number of interlopers, from a sample leads to an underestimate of the expected number of interlopers because the analysis takes into account too few stars. Not removing the secure members leads to an overestimate of the expected number of interlopers because the analysis takes into account too many stars, namely the field stars *and* the genuine association members. In both cases, the systematic under/overestimate is significant for the earliest spectral types, and unimportant beyond spectral type A–F; the precise transition depends on the distance of the association. If one assumes that the stars in our membership lists are primarily genuine association members, the option leading to the smallest systematic errors is to remove the secure members before performing the analysis. Table A2 presents the results for both options.

3.4.3. The $B-V$ versus age degeneracy

The velocity distribution in the Galactic disk is a function of stellar age. Dehnen & Binney (1998) used the B–V color listed in the Hipparcos Catalogue as a simple age indicator for main-sequence stars. Our simulations accordingly use the $B-V$ color of each star to assign it the appropriate proper motion. However, for giants and supergiants, age and $B-V$ are not uniquely related. Assignment of kinematics to stars based on $B-V$ color without regard to luminosity class gives 'old' kinematics to relatively young giants and supergiants, leading to systematic effects. OB associations generally have small space motions relative to the Sun, and are thus observed in velocity space around the reflex of the Solar motion plus a small offset due to differential Galactic rotation. At similar distances as the association, any unrelated population of evolved young giants and supergiants will be clustered around the same velocity as the association. These stars are then wrongly assigned 'old' kinematics, spreading them around in velocity space. This leads to an underestimate of the number of interlopers.

In Table A2, we list for each field and for each spectral type the percentage of stars explicitly classified as main-sequence star (luminosity class V). As expected, this percentage is roughly constant for spectral types O through A–F and decreases going from F to M due to the completeness limit of the Catalogue. The low percentages found in the northern associations in Perseus, Cepheus and Lacerta are due to the specific spectral classifications used by the Hipparcos consortium, which in this region often lack an indication of luminosity class (cf. ESA 1997, Vol. 1 §2.1, pp 134–135). Although the percentages are lower limits to the actual values, they show that the expected number of interlopers for spectral types F–G and later should be interpreted with care (cf. ESA 1989, Vol. 2 §7.3, pp 90–94).

3.4.4. Solar neighbourhood

Dehnen & Binney's (1998) determination of the local velocity distribution is based on a kinematically unbiased sample of Hipparcos main-sequence stars with relative parallax errors better than 10 per cent. Using a median parallax accuracy of 0.97 mas, this translates the term 'local' to a volume centered on the Sun with a radius of 80–100 pc. However, even the nearest association, Lower Centaurus Crux, lies outside this volume (§4.4). Furthermore, it is part of the Gould Belt, which exhibits peculiar kinematics (§9.2). An improved interloper analysis will require a more extended model of the velocity distribution, which includes the Gould Belt.

3.4.5. Selection effects in the Hipparcos Catalogue

The Hipparcos Catalogue contains ∼52 000 stars brighter than the completeness limit ($V = 7\overset{\mathrm{m}}{.}3$–$9\overset{\mathrm{m}}{.}0$, depending on Galactic latitude and spectral type). The remaining ∼66 000 stars were explicitly proposed to be observed by Hipparcos, and thus constitute a special set. Two large-scale effects are the inclusion of high proper-motion stars, and the inclusion of additional F- and G-type stars in two strips from the north to the south Galactic pole (at $\ell\sim0°$ and $\ell\sim180°$) for the purpose of Galactic structure studies (ESA 1989, Vol. 2 §7.3, pp 94–100). Dehnen & Binney's (1998) model does not take these effects into account, so it is to be expected that our synthetic data sets based on their model differ kinematically from the Hipparcos measurements beyond the completeness limits of the Catalogue. Tests indeed reveal differences, particularly in the fourth Galactic quadrant in a strip of width 60° centered on the Galactic plane. In this region, we estimate the resulting uncertainties in the expected number of interlopers to be a factor of 2 at maximum.

3.5. Binaries

The Hipparcos observations were carried out over 3.3 years. The measured motions of long-period binaries that are marginally resolved can differ by many mas yr^{-1} from the mean motion of the system (Lindegren 1997). Genuine association members of this kind can therefore be missed by our selection method (even with our generous choice of $\sigma_{\rm int}$, see §3.3), and some field binaries may accidentally masquerade as members. This problem is most significant for nearby binaries with massive components (Wielen et al. 1997).

Our kinematic member selection method is objective and consistent, and is based only on the Hipparcos positions, parallaxes and proper motions. At this stage we do not want to include physical properties of the stars as further criteria for membership, so as not to bias subsequent discussion of the stellar content of the associations. We therefore do not discuss on a star-by-star basis whether its assignment as a member should be trusted or not based on its spectral type, colors, radial velocity, or multiplicity, also because this additional information is generally not of homogeneous quality. We make one exception to this approach, namely for the few cases where our selection method rejects stars which were previously considered to be solid astrometric members, based on proper motions derived from measurements in fundamental catalogs, over time spans much longer than three years. We do not include these stars in our member lists (Table C1), but identify them in the text. For many of these the Hipparcos Catalogue turns out to give indications for 'perturbed' proper motions. The majority of these systems may therefore well be association members.

3.6. Mean distances

Use of the Hipparcos trigonometric parallaxes of the secure members to determine mean distances to the associations or their subgroups requires some care, as the inverse of the parallax is a biased distance indicator (Smith & Eichhorn 1996; Brown et al. 1997b), and the conversion of mean

parallax to mean distance for a group of stars depends on the distribution of stars within the group. We show in Appendix B that for all spherical groups the expectation value of the mean of the measured parallaxes is equal to the true mean parallax, and corresponds to the true distance of the group. For elongated associations the bias in the mean parallax is small, typically less than 1 per cent. Hipparcos parallaxes measured in regions of high stellar density (in the Catalogue) have to be interpreted with care (Lindegren 1989; Robichon et al. 1997). This is not a problem for the low-density associations (Appendix B).

Interlopers generally have parallaxes similar to those of true members (otherwise they would have been rejected; cf. Figure 4), so these should not influence the mean distances significantly. However, the observed distribution of parallaxes may not be representative of the true underlying parallax distribution of an association. Magnitude limits bias the selected members, and furthermore some stars in the Hipparcos Catalogue have a negative measured parallax. Our member selection method rejects these, which introduces a bias towards a smaller mean distance. In order to estimate the magnitude of these effects, we have carried out Monte Carlo simulations, set up as follows. We considered associations with radius 25 pc, and then created 200 members at random positions in a homogeneous sphere. We chose masses, and corresponding magnitudes, using a power-law initial mass function with exponent -1.7 (cf. Brown et al. 1994), and a minimum and maximum mass of 1 $M_\odot$ and 120 $M_\odot$, respectively. We took the parallax error distribution as a function of magnitude from the Hipparcos Catalogue (ESA 1997, Vol. 1, figure 3.2.39), using a standard deviation on the median parallax error of 0.2 mas for $V \leq 10^{\rm m}$ and 0.4 mas for $V > 10^{\rm m}$. We then retained all stars with $V < 7\overset{\rm m}{.}3$, and discarded fainter stars consistent with the magnitude distribution in the Hipparcos Catalogue. We also discarded all stars with $\pi \leq 0$ mas. We carried out this process as a function of distance, by constructing 100 random realisations in intervals of 50 pc each. The effect of the magnitude limit turns out to be negligible, but, as expected, the bias caused by the exclusion of stars with negative parallaxes increases with distance, and reaches nearly 30 per cent at a distance of 1 kpc. This bias depends sensitively on the magnitude of the parallax errors. For a mean parallax error of 0.97 mas with a standard deviation of 0.2 mas independent of magnitude, the bias is only 15 per cent at 1 kpc.

We give the mean distances derived from the mean parallax of the secure association members in §§4–8. In all cases, these are corrected for the above mentioned bias, and the error quoted is the formal error on the mean. The results are summarized in Table 2.

3.7. Internal structure and motions

The OB associations studied here have distances larger than 100 pc, and linear dimensions of order 50 pc or less. It is impossible to resolve the depth of the associations with the median parallax error of 0.97 mas. Estimates of the individual stellar distances (after member selection) can be improved by deriving so-called secular parallaxes from the measured proper motions (e.g., Jones 1971). A sophisticated method to determine the improved parallaxes and space motions was presented by Dravins et al. (1997). We will investigate its application to the nearby associations in a future paper.

OB associations will expand due to their unbound nature (Ambartsumian 1949). The expansion can be detected if and only if the correct mean streaming motion of the association with respect to the Sun is subtracted from the observed proper motions *and* radial velocities. What remains is the true expansion. Proper motions alone cannot distinguish between a radial streaming motion and contraction or expansion (e.g., Blaauw 1964b). Thus, knowledge of the radial streaming velocity is essential for an unambiguous proof of expansion. This requires radial velocities with errors smaller than the expected expansion velocities, a few km s^{-1}. These are generally not available, so that even with Hipparcos quality proper motions the expected expansion of OB associations, and thus the kinematic ages, cannot be determined (see also Brown, Dekker & de Zeeuw 1997). Our member selection method is not influenced by either radial streaming or expansion/contraction (Blaauw 1952b; de Bruijne 1998; Hoogerwerf & Aguilar 1998). However, the resulting space motions, and convergent points, not only reflect the mean streaming motion of the association but may also include an extra component in radial velocity.

4. THE SCORPIO–CENTAURUS–LUPUS–CRUX COMPLEX

In this section, and the ones that follow, we report the results of applying our member selection method to the fields centered on the nearby associations, starting with Sco OB2 in the region of the constellations Scorpius, Centaurus, Lupus, and Crux, and continuing along the Galactic plane in the direction of decreasing ℓ. We have surveyed the literature, and in each case first review pre-Hipparcos work on association membership. While in some cases this has established a list of commonly accepted astrometric and/or photometric members, for other associations there is considerable confusion about membership, and sometimes even on the existence of an underlying association. Our adopted fields contain all suspected early-type members, and are small enough to minimize the number of interlopers. Table A1 summarizes the field boundaries, and specifies the other parameters used in the member selection.

We review pre-Hipparcos work on Sco OB2 in §4.1, and present our analysis of the Hipparcos data for the three subgroups of this association in detail in §§4.2–4.4. We then briefly consider the entire Sco OB2 complex (§4.5), and conclude with an investigation of an adjacent field,

centered on the nearby star-forming region near R CrA (§4.6).

The presentation in this section also serves as an example of how we have investigated the other fields of the census, for which we restrict ourselves to a concise summary of the pre- and post-Hipparcos results (§§5–8). Unless stated otherwise, we use spectral types, and V and $B-V$ photometry reported in the Hipparcos Catalogue.

4.1. Sco OB2

In the lengthy paper 'On the individual parallaxes of the brighter Galactic Helium stars in the southern hemisphere, together with considerations on the parallax of stars in general', Kapteyn (1914) investigated the secular parallaxes of 319 OB stars brighter than $V{\sim}6^{\rm m}$ contained in L. Boss' Preliminary General Catalog in the region $216°{\lesssim}\ell^I{\lesssim}360°$, $-30°{\lesssim}b^I{\lesssim}30°$ ('old' Galactic coordinates)[2]. He recognized the Sco OB2 association as a moving group of ∼150 stars spread over $70°\times40°$ on the sky (cf. Plummer 1913). Later kinematic studies confirmed Sco OB2 as a moving group (e.g., Rasmuson 1921; Plaskett & Pearce 1928, 1934; Canavaggia & Fribourg 1934; Kulikovsky 1940; but see Smart 1936, 1939; Petrie 1962). Blaauw (1946; 114 members), Bertiau (1958; 77 bright members and 37 additional faint B-type members), and Jones (1971; 47 members), made detailed kinematic studies of Sco OB2, resulting in a total of 157 classical proper motion members with spectral types earlier than ∼B9, of which 153 were observed by Hipparcos. Several photometric studies suggested membership for another 243 stars to spectral type ∼A8–F0, 215 of which are included in the Hipparcos Catalogue (Hardie & Crawford 1961; Garrison 1967; Gutiérrez–Moreno & Moreno 1968; Glaspey 1971, 1972). Numerous authors have investigated radial and rotational velocities, and the properties of the binary distribution (e.g., Blaauw & van Albada 1963, 1964; van Albada & Sher 1969; Rajamohan 1976; Levato et al. 1987; Verschueren, David & Brown 1996; Brown & Verschueren 1997; Brandner & Köhler 1998).

Blaauw (1960, 1964a) divided the association in three separate concentrations or subgroups: Upper Scorpius (US), Upper Centaurus Lupus (UCL), and Lower Centaurus Crux (LCC), and derived an expansion age of ∼20 Myr for the entire complex (Blaauw 1964b). He estimated the kinematic age of US to be ∼5 Myr (Blaauw 1978). At $b{\sim}20°$, US is well-separated from the early-type Galactic field star distribution and is most concentrated, whereas UCL and LCC are spread over a considerably larger area on the sky (see Figure 9). As a result, UCL and LCC have received remarkably little attention compared to US; they are not mentioned in Ruprecht's (1966) list of nearby OB associations (§2.1).

De Geus (1992) summarized the characteristics of the interstellar medium related to Sco OB2. Whereas little interstellar matter is associated with the subgroups UCL and LCC, filamentary material connected to the Ophiuchus cloud complex ($345°\lesssim\ell\lesssim10°$, $0°\lesssim b\lesssim25°$) is observed towards US. This is also reflected in spatial variations of extinction in this region. The densest part of this complex, the ρ Oph dark cloud, is a site of ongoing low-mass star formation (e.g., Grasdalen, Strom & Strom 1973; Greene & Young 1992; Wilking et al. 1997b), as well as interaction with the early-type stars of US.

De Geus et al. (1989) analyzed Walraven as well as published Strömgren photometry of the priority 1 stars in Sco OB2. The derived extinctions were compared with the IRAS 100μm emission, and it was shown that the Ophiuchus dark clouds are on the near side of US, at ∼125 pc. These authors derived ages of ∼5 Myr for US, ∼13 Myr for UCL, and ∼10 Myr for LCC by isochrone fitting in the Hertzsprung–Russell diagram. It follows that stars with spectral types beyond the mid-F range may not yet have reached the main sequence. Extensive Hα and X-ray surveys of the Sco OB2 region indeed have revealed several dozens of pre-main sequence objects (e.g., Walter et al. 1994; Feigelson & Lawson 1997; Preibisch et al. 1998; Sciortino et al. 1998).

Finally, we remark that ζ Oph (HIP81377, O9.5V) has long been recognized as a runaway star originating in Sco OB2 (e.g., Blaauw 1952b, 1961, 1991; van Rensbergen et al. 1996). We will discuss it elsewhere.

4.2. Upper Scorpius

Figure 5 summarizes the results of our selection procedure for US. The first row displays the Hipparcos measurements for all stars in our US field (cf. Table A1). The panels show no clear sign of a physical group, except for the vector point diagram (panel two), which contains a concentration around $(\mu_\ell\cos b,\mu_b){\sim}(-25,-10)$ mas yr^{-1} superimposed upon the broader Galactic disk distribution. The second row of Figure 5 shows only the 86 stars that were proposed as members of US, based on pre-Hipparcos kinematic and photometric studies (§4.1). They are mostly B- and A-type stars concentrated towards the centre of the field, with the majority contained in the same clump in the vector point diagram. Their parallax distribution is narrower than the one in the first row, and is peaked around 7 mas. The characteristics of the set of members identified by our selection method are presented in the third row of Figure 5. There is considerable overlap with the classical members, but there are also significant differences. The vector point diagram of these secure members is more concentrated than that of the classical members, and the parallax distribution is narrower. This is most likely due to a reduced contamination by field stars. The observed spread and the elongated shape in the vector point diagram are consistent with the combined effects of observational errors, our choice of $\sigma_{\rm int}$, and projection on the sky. Finally, the panels in the bottom row of Figure 5 show the not-selected stars, and demonstrate that our procedure does

[2]The approximate relation between (ℓ^I,b^I) and (ℓ,b) is $\ell\approx\ell^I+32\fdg9$, and $b\approx b^I$.

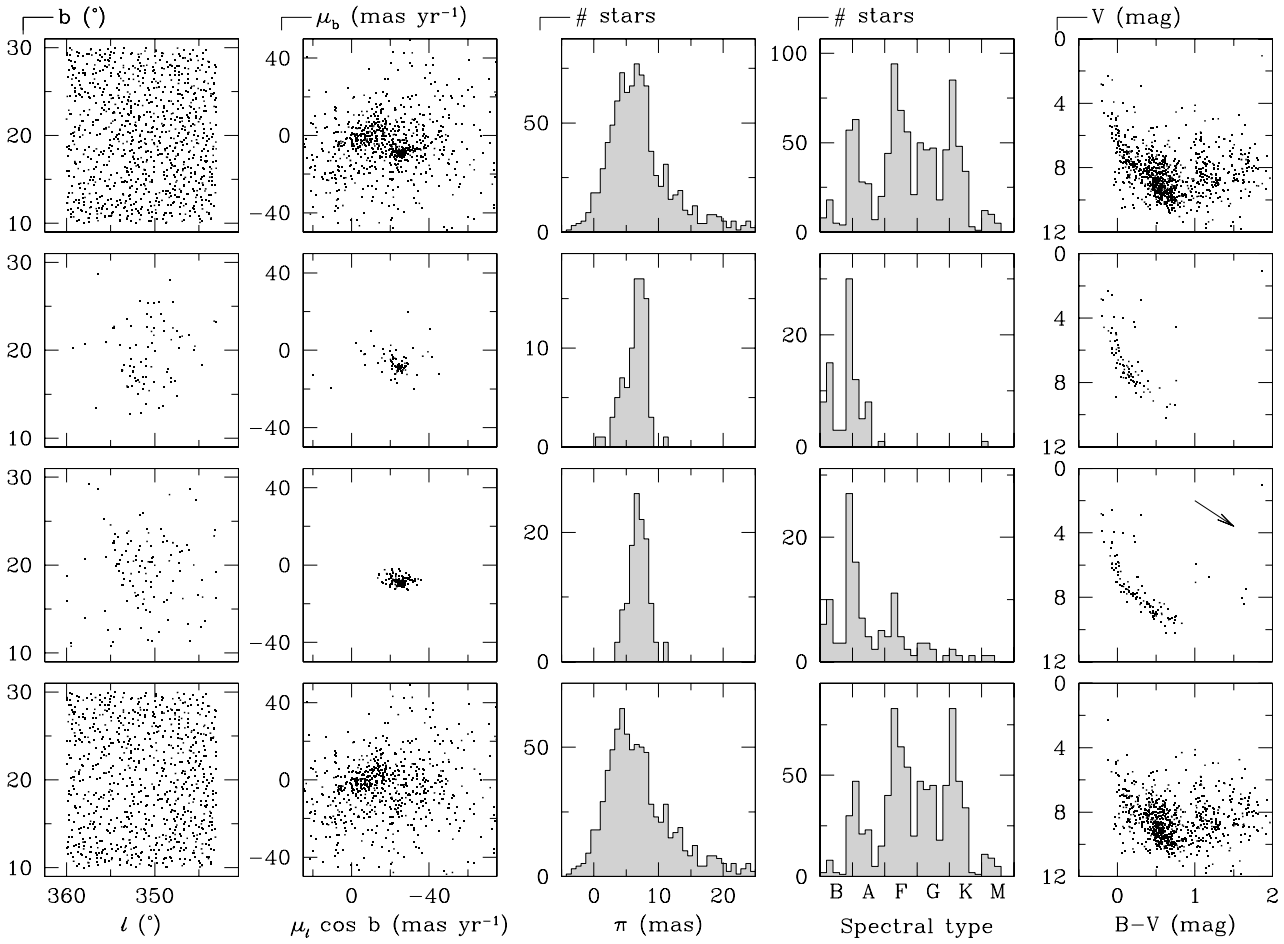

Figure 5: Hipparcos measurements for Upper Scorpius (from the top row down): (1) all 945 Hipparcos stars in the region (cf. Table A1); (2) the 86 pre-Hipparcos members; (3) the 120 Hipparcos members; (4) the remaining stars after member selection. The columns show (from left to right): (1) positions in Galactic coordinates; (2) Galactic vector point diagram; (3) trigonometric parallax distribution; (4) spectral type distribution; (5) color-magnitude diagram, not corrected for reddening. The arrow indicates the direction of reddening for the standard value $R = 3.2$ of the ratio of total to selective extinction. The stars within the apparent concentration around $(\mu_\ell \cos b, \mu_b) \sim(5, -5)$ mas yr^{-1} in the first and fourth panels of the second column do not form a moving group.

not leave 'holes' in the distributions of positions, proper motions, and parallaxes. This indicates that our method has separated US cleanly from the field stars.

We find a total of 120 secure members of US: 49 B, 34 A, 22 F, 9 G, 4 K, and 2 M-type stars. Of these, 53 were previously classified as member (39 kinematic, 14 photometric), while 67 are new. We confirm the evolved supergiant Antares (α Sco, HIP80763, M1Ib), as well as the stars ρ Oph (HIP80473, B2V), χ Oph (HIP80569, B2Vne), and 48 Lib (HIP78207, B8Ia/Iab), as members. The latter two are classical proper motion members with peculiar positions in the Hertzsprung–Russell diagram (e.g., de Geus et al. 1989). We select 2 A stars with peculiar spectra (HIP78494, A2m...; HIP79733, A1m...), and reject the doubtful classical proper motion member o Sco (HIP80079, A4II/III; see Blaauw, Morgan & Bertiau 1955; de Geus et al. 1989). We also do not select the classical proper motion member δ Sco (HIP78401). However, this star is a binary with a separation of 0.″13 (16 AU at $\pi = 8.12$ mas). Hipparcos detected a change in the position angle of the binary components of 18° yr^{-1}, which indicates a period of ∼20 yr. Therefore, the Hipparcos proper motion, observed during the mission lifetime of ∼3.3 yr, does not necessarily reflect the center-of-mass proper motion (§3.5). The typical differences between the center-of-mass and observed proper motions are on the order of 2 mas yr^{-1} (e.g., Wielen et al. 1997), enough to explain why δ Sco is not selected.

The mean distance of US is 145±2 pc, where the error is the formal error on the mean, and the correction applied for the bias caused by exclusion of stars with negative parallaxes is negligible (§3.6). This value is consistent with the most recent photometric determination of 160±40 pc by de Geus et al. (1989). The accuracy of the individual parallaxes does not allow us to resolve the internal structure. If the association extends about as far along the line of sight as it does on the sky (∼14°), the parallax spread is ∼1.6 mas, corresponding to ∼0.$^{\rm m}$5. Taking into account

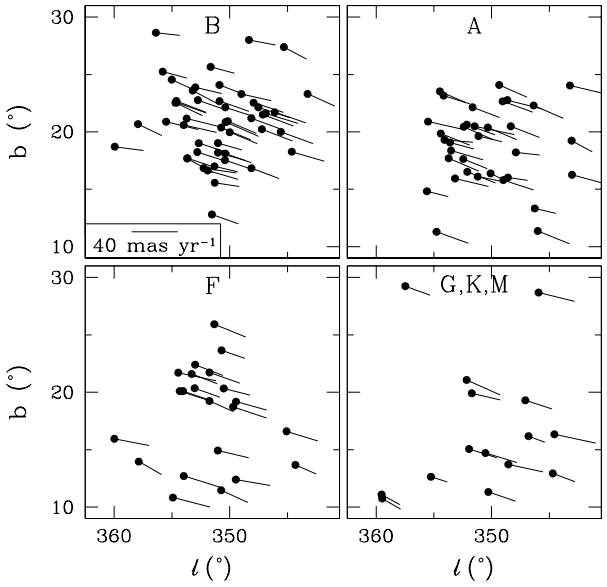

Figure 6: Positions and proper motions for the Hipparcos members of Upper Scorpius, as a function of spectral type: 49 B, 34 A, 22 F, 9 G, 4 K, and 2 M-type stars. The selected F, G, K, and M stars co-move with the B and A stars. The distribution of F stars is similar to that of the early-type stars, suggesting that the stellar content of the association has now been established to spectral type F. Some of the later-type stars could be interlopers.

the individual measurement error of ∼1 mas, this is consistent with the observed width of the parallax distribution.

Figure 6 shows the positions and proper motions for all secure members, as a function of spectral type. There is a clear concentration in the early-type stars. Some of the stars that lie away from this main concentration could be interlopers. We have estimated the expected number of interlopers by means of the Monte Carlo simulations described in detail in §3.4. The result is given in Table A2, and shows that the observed clustering in the F-star distribution is significant. The concentration of F-type members coincides with a similar concentration of X-ray selected pre-main sequence stars, around $(\ell, b)\sim(350°, 20°)$ found by Walter et al. (1994) and Preibisch et al. (1998). These generally have $V\sim12^{\rm m}$–$17^{\rm m}$, and are too faint for Hipparcos, so no reliable kinematic link is possible. The one exception may be provided by the US member HIP77960 (SAO183927, A4IV/V), which is listed as the possible optical identification of the X-ray detected candidate pre-main sequence object Sco–014 (Sciortino et al. 1998). The majority of the G- to M-type members probably do not belong to US, although only 4 interlopers are predicted for these spectral types. However, this number is an underestimate because of the large fraction of giants and supergiants in the Hipparcos Catalogue (§3.4.3).

The secure US members span a much larger range in spectral type than the classical members, which are confined to stars earlier than ∼A8–F0. The distribution of secure members in the color-magnitude diagram extends to fainter magnitudes than for the classical members (right panels in Figure 5). The main sequence is not very narrow; we infer that this is caused by the distance spread along the line of sight (∼$0\overset{\rm m}{.}5$), by unresolved binaries, and probably by significant differential reddening, especially for the bright early-type members (including ρ Oph, σ Sco, π Sco, and ν Sco, all of which are associated with nebulosities; de Geus et al. 1989). Many fainter members are likely missing, due to the completeness limit of the Hipparcos Catalogue. Even so, the new late-type members allow a much improved definition of the lower part of the main sequence (cf. §4.5).

4.3. Upper Centaurus Lupus

We started the analysis of UCL by applying our selection method to the Hipparcos objects in the classical 'field 3' defined by Blaauw (1946). This resulted in the detection of a moving group, with members spread over nearly the entire field. We subsequently modified it to the field given in Table A1, to be sure that we included the entire subgroup (cf. Figure 9). The results are summarized in Figure 7, which is similar to Figure 5, except that the improvement in the member list for UCL provided by Hipparcos is more dramatic than for the much better studied US subgroup. Our member selection method identifies 221 members in this field, with a mean distance of 140±2 pc: 66 B, 68 A, 55 F, 25 G, 6 K, and 1 M-type star. Of these, only 58 were previously classified as member (24 kinematic, 34 photometric), while 163 are new. We discarded 78 classical members. The parallax distribution and vector point diagram of the new members both show a significantly smaller spread than those of the classical members. The new UCL members are not spread uniformly over the sky but seem to be concentrated in 'clumps'. Although some of this 'clumping' could be caused by selection effects in the Hipparcos Catalogue, it seems likely that UCL has substructure (§4.5). The number of expected interlopers (Table A2) indicates that some of the G and K stars may well be non-members.

The mean distance of UCL is consistent with the value 160±40 pc found by de Geus et al. (1989). Just as for US, the width of the parallax distribution is consistent with the measurement errors and the angular extent of ∼27°, which at this distance corresponds to ∼3.6 mas ($1\overset{\rm m}{.}1$) if UCL is roughly spherical.

The panels in the fourth row of Figure 7 show smooth distributions of Galactic disk field stars in position, proper motion, and parallax. The color-magnitude diagram of the non-members contains five stars with $V \lesssim 4^{\rm m}$ which follow the main sequence of the secure members remarkably well. With the exception of ζ Cen, these are classical proper motion members. This suggests that μ^1 Sco (classified as 'V'-type by Hipparcos[3]), β Lup, η Cen (B1Vn+A), and ι Lup,

[3]We use the nomenclature for binaries that corresponds to the five parts of the Double and Multiple Systems Annex of the Hipparcos Catalogue, where 'C' indicates component solutions, 'G' indicates

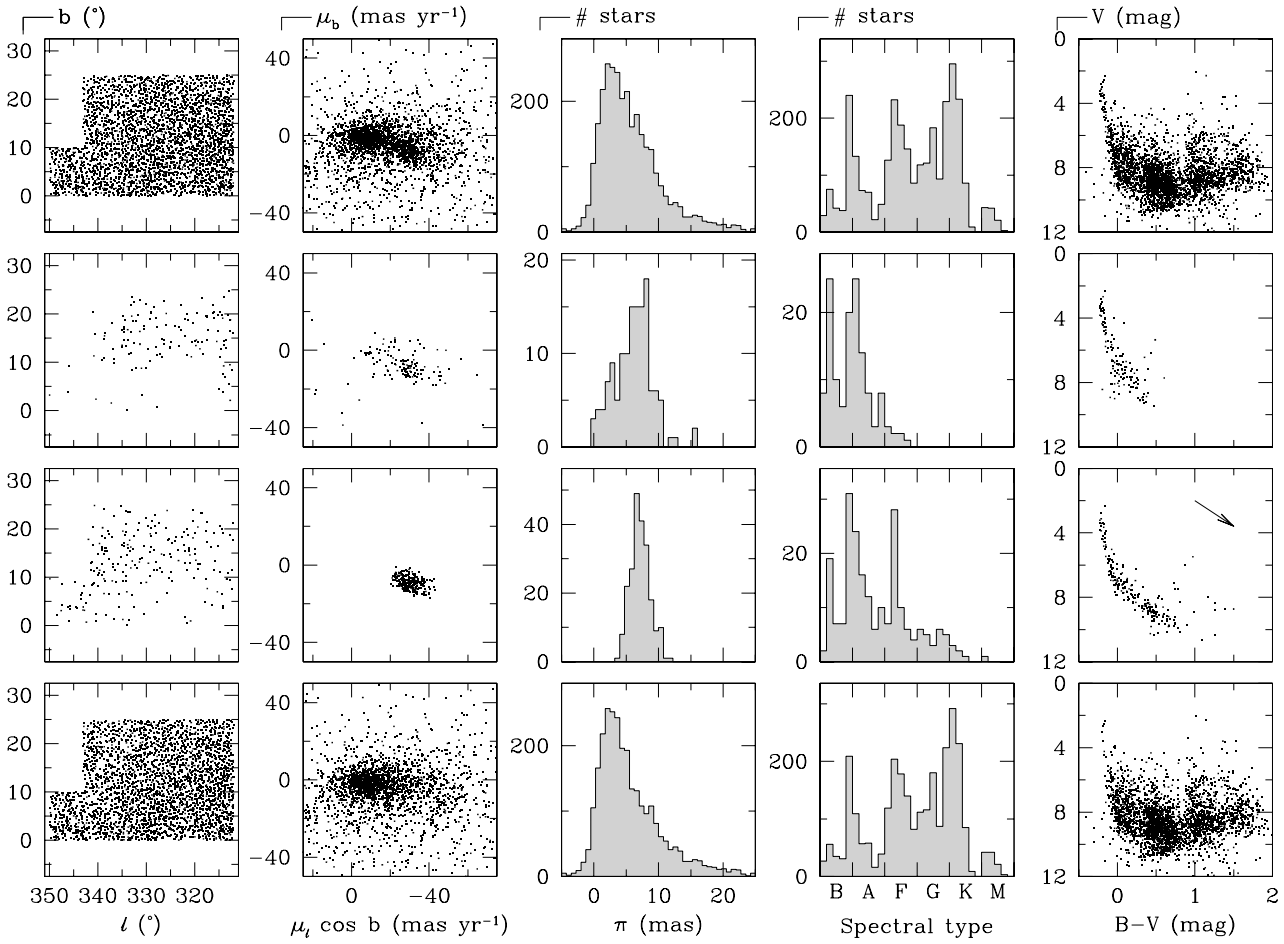

Figure 7: As Figure 5, but for the 3132 stars in the field of Upper Centaurus Lupus. The stars within the apparent concentration around $(\mu_\ell \cos b, \mu_b) \sim (-20, -15)$ mas yr^{-1} in the second panel of the first row do not form a moving group.

could be members of UCL, although their kinematic properties as observed by Hipparcos are not consistent with the mean motion of UCL. We suspect that perturbations of the stellar motion due to marginally resolved multiplicity could be important (§3.5), but note that the SIMBAD radial velocity for ι Lup differs significantly from that of UCL (Table 2).

The color-magnitude diagram of the secure members of UCL is cleaner than that of US, which we attribute to the absence of significant differential extinction (de Geus et al. 1989). The vertical spread of the main sequence is consistent with the expected distance range of $\sim 1\overset{\mathrm{m}}{.}1$, and the presence of unresolved binaries. The main sequence extends nearly two magnitudes fainter than in the pre-Hipparcos diagram, and indeed includes not only 8 stars with peculiar and/or magnetic spectra, but also HIP77157 (HT Lup, $V = 10\overset{\mathrm{m}}{.}31$, $B-V = 1\overset{\mathrm{m}}{.}264$, Ge) and HIP82747 (AK Sco, $V = 9\overset{\mathrm{m}}{.}21$, $B-V = 0\overset{\mathrm{m}}{.}746$, F5V), which are binary T Tauri stars (e.g., Gregorio–Hetem et al. 1992), and HIP74797, which is the A component of the binary system CCDM J15172–3435, the B component of which is a pre-main sequence T Tauri binary system (Brandner et al. 1996). We also select another four pre-main sequence stars: HIP75924 (G6V), HIP73777 (K(1)V+G), HIP77524 (K0V:), and HIP78684 (G8V) (Neuhäuser & Brandner 1998).

The star-forming region associated with the Lupus clouds, at a distance of 140±20 pc, contains several tens of low-mass pre-main sequence stars with estimated ages of ∼3 Myr (e.g., Hughes, Hartigan & Clampitt 1993; Hughes et al. 1994; Chen et al. 1997; Wichmann et al. 1997b). However, most of them have $V \gtrsim 12^{\mathrm{m}}$, and only 5 were observed by Hipparcos (HT Lup, and HIP78094, 78317, 79080, 79081). Wichmann et al. (1997a) derive a distance of 190±27 pc, based on Hipparcos parallaxes, and suggest that these stars are members of UCL (cf. Murphy, Cohen & May 1986). We select only HT Lup as secure UCL member.

4.4. Lower Centaurus Crux

We started our analysis of LCC in Blaauw's (1946) 'field 4', and then extended the field boundaries to those given in Table A1 to be sure of including the entire subgroup

an acceleration solution, 'O' an orbital solution, 'V' a variability-induced mover, and 'X' a stochastic solution.

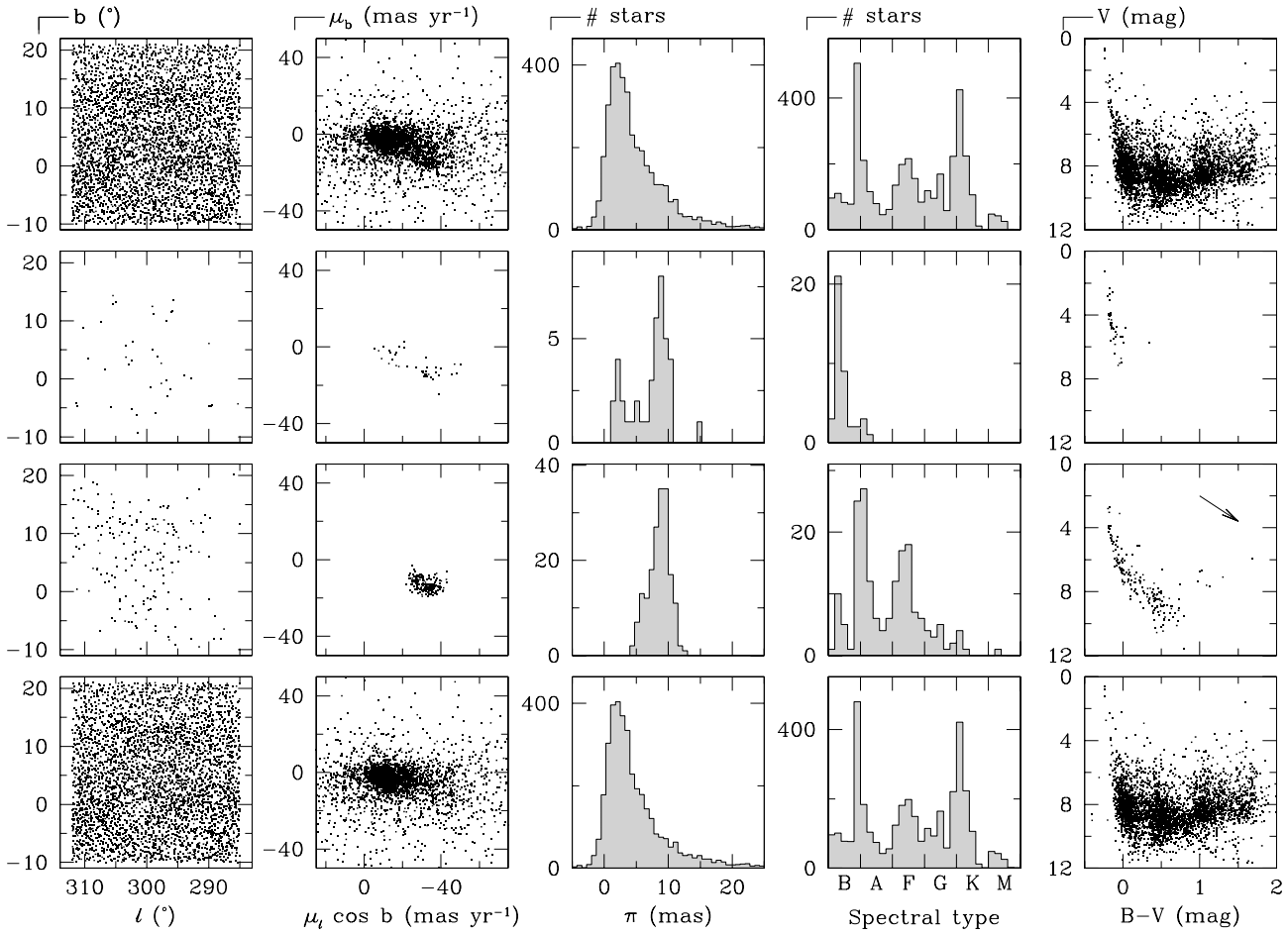

Figure 8: As Figure 5, but for the 3897 stars in the field of Lower Centaurus Crux. The stars in the concentration at $(\ell, b)\sim(290^\circ, -5^\circ)$ in the first and fourth panel of the first column are members of the open cluster IC2602 (cf. Hoogerwerf & Aguilar 1998).

(cf. Figure 9). Our selection procedure is summarized in Figure 8, which is organized in the same way as Figures 5 and 7. LCC was never studied extensively, and only 41 classical members are known, all with spectral type earlier than B6. Identification of later-type members in this rich field in the Galactic disk was particularly difficult, and suggests that interlopers are present even among the brightest members. The second and third panels of row two in Figure 8 indeed show many deviating proper motions and parallaxes. We confirm only 19 (16 kinematic, 3 photometric) of the classical members, but identify a total of 180 secure members: 42 B, 55 A, 61 F, 15 G, 6 K, and 1 M-type star, so that Hipparcos has transformed this sparse subgroup into a moving group that is very similar to UCL. The members are not spread uniformly over the field, and show some evidence for substructure.

The panels in the bottom row of Figure 8 indicate a clean separation of LCC from the field star distribution, but just as in the case of UCL and US, the color-magnitude diagram of the non-members contains a number of bright ($V \lesssim 4^{\rm m}$) early-type stars which were discarded by our selection method, and which deserve attention. The classical proper motion member δ Cen (HIP59196, B2IVne) is a γ Cas-type eruptive variable identified by Hipparcos as a 'variability-induced mover' (see footnote 2). Another is β Crux (HIP62434, B0.5III), rejected as LCC member by Jones (1971). It was observed by Hipparcos as 'G'-type binary, and is probably an astrometric binary with a period $\gtrsim$10 yr. HIP59449 (B3V) is another 'G'-type binary. We suspect that these are in fact members of LCC. The stars β Cen (HIP68702, B1III, Agena) and HIP60718 (B0.5IV) are Hipparcos 'component binaries', but were never proposed as members of LCC, and neither was HIP51576 (B4Vne). We do not select them either. HIP66657 (B1III, 'G'-type binary) and HIP61199 (B5V, γ Mus) were already rejected by Jones (1971). Finally, HIP52419 (B0Vp, 'O'-type binary) is a member of IC2602 (Hoogerwerf & Aguilar 1998).

LCC is significantly closer than US and UCL: the Hipparcos mean distance of 118±2 pc agrees well with earlier photometric estimates (de Geus et al. 1989). The parallax distribution is marginally broader than for UCL, but again does not allow us to resolve the internal structure of the subgroup. The expected distance spread correspond-

ing to the ∼25° extent on the sky is ∼3.7 mas (or $0\overset{m}{.}9$). Taking into account the individual measurement errors, this is consistent with the observed width of the parallax distribution.

Chereul, Crézé & Bienaymé (1997) used a different method to search for moving groups in the Hipparcos Catalogue, and applied it to nearby A dwarfs with pre-Hipparcos distances less than 125 pc. They identified a moving group of 33 stars at a mean distance of 105 pc in 'Lupus–Centaurus', in a field which roughly coincides with our LCC field. These are clearly LCC members, but the sample definition biases them towards the near side of the subgroup, and explains the somewhat smaller mean distance than we find.

The color-magnitude diagram of our secure LCC members, not corrected for reddening, is shown in the right-hand panel of the third row of Figure 8. The vertical spread of the main sequence is consistent with the combined effects of some differential reddening, the distance range, and unresolved binaries. The main sequence extends a full four magnitudes further towards fainter objects than the one for the classical 'members' shown in the panel above it, and indeed extends into the regime where we would expect some pre-main sequence objects. Unfortunately, none of the pre-main sequence members of LCC found by Feigelson & Lawson (1997) appear in the Hipparcos Catalogue. However, we do select HIP56420 ($V = 11\overset{m}{.}56$, $B-V = 0\overset{m}{.}789$, $\pi = 7.20 \pm 2.92$ mas, Gp), which might be a T Tauri star.

The LCC field also contains a concentration of stars in the direction $(\ell, b)\sim(290°, -5°)$ (bottom left panel in Figure 8). This is the open cluster IC2602 (age 8–30 Myr; Whiteoak 1961; Braes 1962; Stauffer et al. 1997). Blaauw (1964a) suggested that IC2602 may belong to LCC. Hoogerwerf & Aguilar (1998) show that the Spaghetti method (§3.2) identifies IC2602 flawlessly as a separate group, containing 23 Hipparcos members at ∼144 pc (cf. Mermilliod et al. 1997), with a motion that differs significantly from that of LCC. We do not discuss it further here.

4.5. The Sco OB2 complex

Figure 9 illustrates the motions of all the Sco OB2 members we have identified, and also gives the subgroup boundaries defined by Blaauw (1946, p. 43). UCL and LCC clearly extend beyond the classical boundaries, and contain stars from Blaauw's 'fields 1 and 5' (Sco OB2_1 and Sco OB2_5 in Table 1). We do not find astrometric evidence for additional subgroups of Sco OB2 in these fields.

The individual membership probabilities P of the selected stars (§3.3) are listed in Table C1. The cumulative distributions are displayed in Figure C1, and range from ∼50 to 100 per cent. The black dots in Figure 9 indicate all members with $P \geq 95$ per cent. These cover nearly the same area on the sky as the full set of members, but the outlying members of US, and some of UCL and LCC, all have low values of P. The stars in the concentrations near $(\ell, b)\sim(342°, 3°)$, $(338°, 15°)$ and $(334°, 16°)$ have high probabilities, which suggests that UCL has substructure.

Application of our member selection method to the entire field shown in Figure 9 results in the identification of one coherent structure: Sco OB2. US stands out in the distribution of Sco OB2 members on the sky, and the parallax distribution clearly distinguishes UCL and LCC. The differences between the Hertzsprung–Russell diagrams of the groups (de Geus et al. 1989) also indicate that a division of Sco OB2 into three separate subgroups is warranted. Our field boundary separating UCL from US has, somewhat arbitrarily, been chosen in such a way that US comprises the stellar concentration centered on $(\ell, b)\sim(352°, 20°)$ with radius ∼5° (§4.2), separated by a sparsely populated zone from the main body of UCL (Figure 9). Analysis of the secular parallaxes (e.g., Dravins et al. 1997) will allow an improved description of the internal structure of Sco OB2.

Accurate intermediate-band Walraven *VBLUW* photometry is available for 1870 of the 7974 Hipparcos stars in the Sco OB2 field (de Geus et al. 1990). These include 261 of the 521 Hipparcos members. *UBV* photometry is available for 327, and *uvbyβ* for 235, of the Hipparcos members (Hauck & Mermilliod 1990; Mermilliod & Mermilliod 1994; cf. Slawson, Hill & Landstreet 1992). We postpone a discussion of the physical properties of the stars in Sco OB2 based on this and other material to a future paper, but refer to de Zeeuw et al. (1997; figure 2) for an illustration of the improved quality of the color-color diagrams due to the refined and extended astrometric membership lists. Completion of the photometry will allow to correct for differential reddening, to improve the provisional determination of the initial mass function by Brown (1998), to determine whether an up-turn of the main sequence occurs in the F-star regime, as expected for groups of this age, and to investigate if small-scale structure is associated with age differences.

4.6. Corona Australis

Pre-Hipparcos: Blaauw's (1946) 'field 1' contains the Corona Australis cloud complex located at $(\ell, b)\sim(360°, -18°)$, at 150±50 pc (Gaposchkin & Greenstein 1936). It is also called Corona Austrina (Botley 1980), and contains sites of active intermediate- and low-mass star formation extending a few degrees on the sky, which have been studied extensively (e.g., Rossano 1978; Loren 1979; Goss et al. 1980; Brown 1987; Cappa de Nicolau & Pöppel 1991; Harju et al. 1993; Andreazza & Vilas–Boas 1996; cf. Figure 10). The densest molecular core contains the emission-line star R CrA (A5IIe var). The stellar content of the CrA complex was studied through Hα emission-line surveys, infrared surveys, and X-ray observations (Knacke et al. 1973; Glass & Penston 1975; Vrba, Strom & Strom 1976; Marraco & Rydgren 1981; Wilking et al. 1985, 1992, 1997a; Koyama et al. 1996; Walter et al. 1997). These studies revealed a mixed, predominantly pre-main sequence, stellar content: several embedded and/or Herbig stars (e.g.,

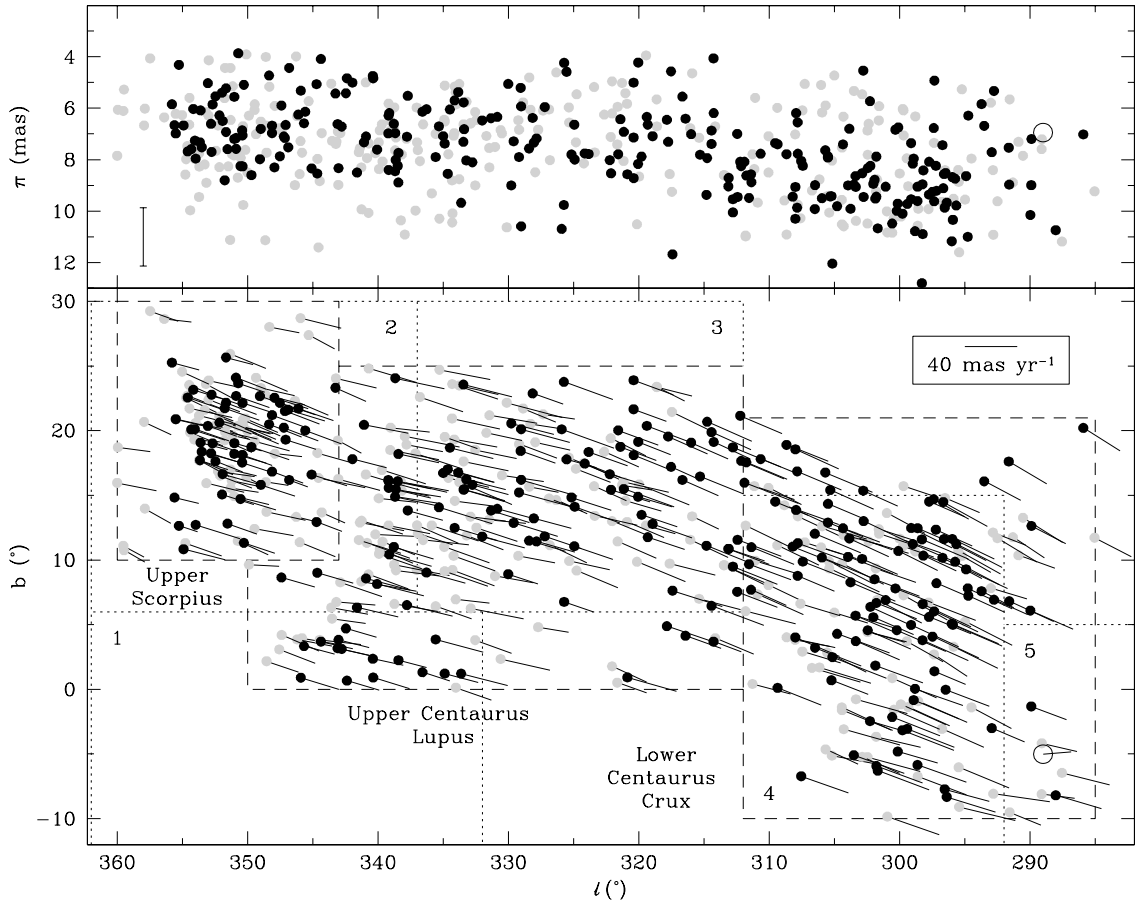

Figure 9: Positions and proper motions (bottom), and parallaxes (top), for 521 members of Sco OB2 selected from 7974 stars in the Hipparcos Catalogue in the area bounded by the dashed lines. The vertical bar in the top panel corresponds to the average $\pm 1\sigma$ parallax range for the stars shown. The black dots indicate stars with membership probability $P \geq 95$ per cent. Gray dots indicate the remaining members. Many members near the association boundary have a low membership probability. The dotted lines are the schematic boundaries of the classical subgroups Upper Scorpius (2, US), Upper Centaurus Lupus (3, UCL), Lower Centaurus Crux (4, LCC), and the candidate subgroups (1 and 5) defined by Blaauw (1946). US is identified as a subgroup based on the concentration of members on the sky, and LCC can be distinguished from US and UCL based on its significantly smaller distance. The large open circle represents the open cluster IC2602.

R CrA, T CrA, HD176386, TY CrA) with the associated reflection nebulae NGC6729 and NGC6726/6727, as well as a loose association of T Tauri stars (e.g., Herbig & Rao 1972), Herbig–Haro objects (Strom, Strom & Grasdalen 1974; Strom, Grasdalen & Strom 1974; Wilking et al. 1997a), and the embedded infrared Coronet cluster associated with R CrA (Taylor & Storey 1984). The pair HR7169/HR7170 and SAO210888 may not have formed in the CrA cloud complex (Marraco 1978; Marraco & Rydgren 1981; Wilking et al. 1992). Strömgren photometry for HR7169/7170 and HD176386 indicates a mean distance of approximately 130 pc.

New results: We have investigated whether there is astrometric evidence for a moving group associated with the CrA star-forming region. We have performed our membership analysis on Hipparcos data in the field $345° < \ell < 15°$, $-30° < b < 0°$. The few bright B0–B3 stars in the field were already noted by Blaauw (1946, 1964a), who suggested they might belong to a putative nearly dispersed 'subgroup 1' of the Sco OB2 association, at an estimated distance of ∼170 pc. We find no evidence for the existence of a moving group. Changing the field size does not alter this conclusion. Figure 10 shows the distribution of all OB stars in the field $345° < \ell < 15°$, $-30° < b < -10°$ with measured parallaxes $4 < \pi < 12$ mas. Nearly all of these are B8–B9 stars with parallaxes $\pi \lesssim 6$ mas; their proper motions simply reflect the Solar motion.

The five stars observed by Hipparcos associated with the CrA clouds by themselves also provide insufficient evidence for a moving group: R CrA (HIP93449) is faint ($V = 11\overset{\mathrm{m}}{.}57$): the measured parallax ($\pi = 121.75 \pm 68.24$ mas) and proper motions are not significant, and the 'stochastic binary' and 'suspected non-single' flags are set. The pair HR7169/7170 (HIP93368/93371) has an uncertain parallax. The remaining two, SAO210888 (HIP93689) and HD176386 (HIP93425), have parallaxes consistent with the classical distance estimate of ∼130 pc, and similar

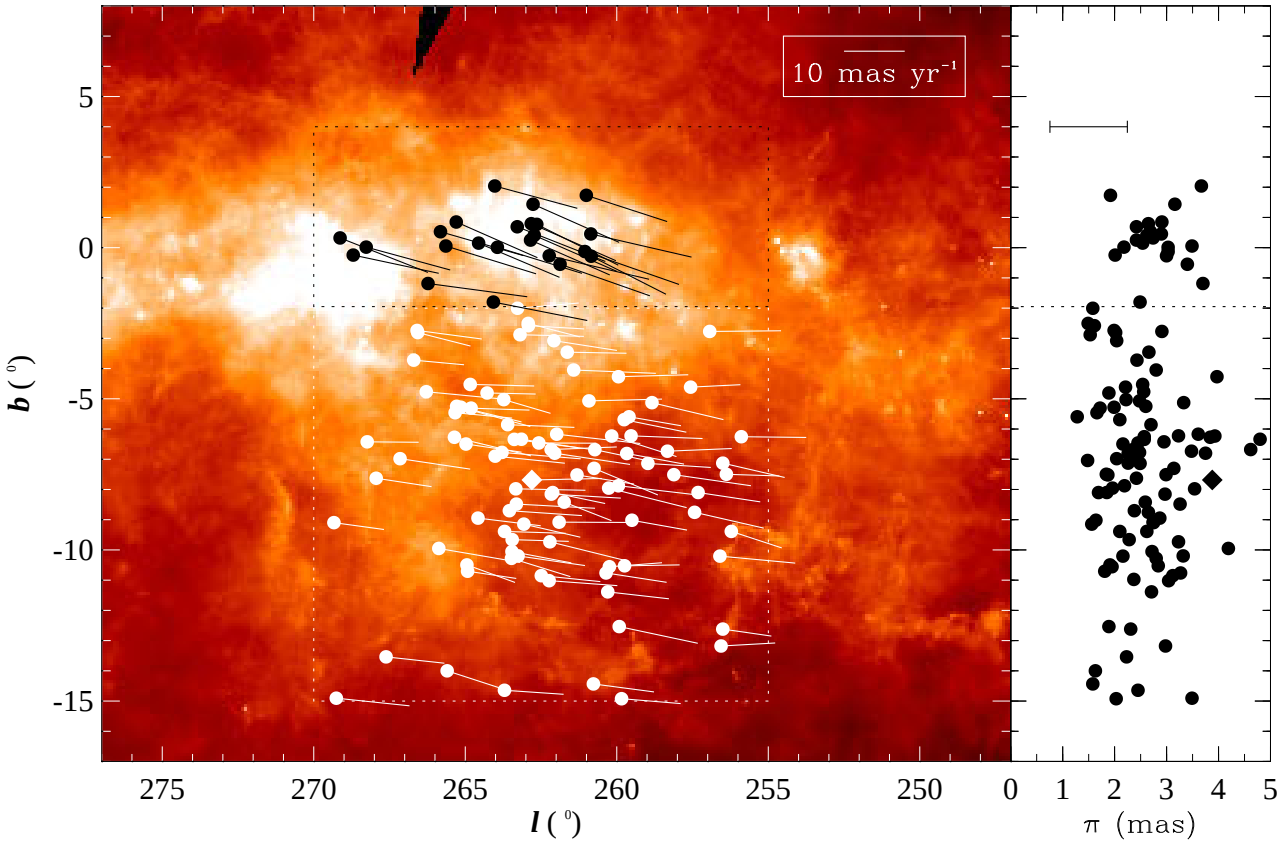

Figure 11: Left: positions and proper motions for the Hipparcos members of Vela OB2 (white) and Trumpler 10 (black). The diamond denotes the Wolf–Rayet star γ^2 Velorum (WR11). The dotted lines indicate the field boundaries (cf. Table A1). The gray-scale represents the IRAS 100μm skyflux. The IRAS Vela shell is the ring-like structure centered on $(\ell, b)\sim(263^\circ, -7^\circ)$ with a radius of $\sim 6^\circ$ surrounding Vel OB2. The intense emission in the area $260^\circ \lesssim \ell \lesssim 273^\circ$, $-2^\circ \lesssim b \lesssim 2^\circ$ corresponds to the Vela molecular ridge. Right: parallax distribution for Vel OB2 and Tr 10

proper motions. If these belong to a moving group associated with the CrA complex, then the other members must be fainter than the magnitude limit of the Hipparcos Catalogue.

5. VELA

Blaauw's (1964a) map of the early-type stars along the Galactic plane (his figure 3) contains a concentration of O–B3 stars brighter than $V_{\rm pg} = 7^{\rm m}$ in a field in Vela centered on old Galactic coordinates $(\ell^I, b^I)\sim(230^\circ, -10^\circ)$, which had already been noted by Kapteyn (1914). This field of low interstellar extinction out to $\sim$1 kpc contains a number of nearby stellar groups, sometimes referred to as the Vela Sheet (cf. Eggen 1980). Here we discuss Vel OB2 and Tr 10.

5.1. Vela OB2

Pre-Hipparcos: In his 1914 paper, Kapteyn not only identified Sco OB2, but also discussed a group of bright stars in Vela (his §6, p. 63) and, based on proper motions, listed 15 probable members (his table XIV) for this so-called Vela Group. Lacking radial velocities for 14 of these stars, Kapteyn concluded that 'the reality of the group seems ... probable, though not beyond a doubt'. The widely-spread radial velocities for 12 of the 15 stars used by Blaauw (1946, his §22, p. 101) did not allow confirmation of Kapteyn's Vela Group. It is not listed as an OB association by Ruprecht (1966). Brandt et al. (1971) noted the presence of 17 bright early-type stars within a few degrees of the Wolf–Rayet WC8+O9I binary system γ^2 Velorum (HIP39953, WR11). These authors took the similar distance moduli for 10 of these stars (including γ^2 Vel) as evidence for an OB association at $\sim$450 pc: Vel OB2. Straka (1971, 1973) investigated SAO proper motions and Bright Star Catalog radial velocities for these 10 stars. Only 5 of them, including the multiple system γ^1–γ^2 Vel, turned out to share a common space motion. Abt et al. (1976) discussed astrometric and photometric observations of 7 stars around γ^2 Vel, and concluded that γ^1 Vel and CD$-$46 3848 are probably associated with γ^2 Vel, and that γ^2 Vel, as well as HD68157 and HD68324 (HIP39970), are members of Vel OB2. Photometric evidence for the existence of an association at $\sim$450 pc was provided by Upton (1971),

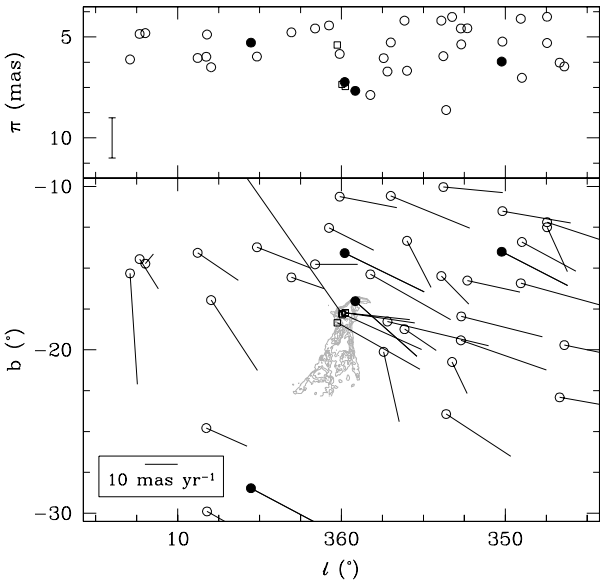

Figure 10: Positions and proper motions (bottom) and parallaxes (top) for all OB stars in the field $345° < \ell < 15°$, $-30° < b < -10°$ with parallaxes $4 < \pi < 12$ mas. Filled circles denote O–B3 stars. Open squares denote the 5 classical CrA members observed by Hipparcos, which fall inside the shaded region representing the IRAS 100μm flux measurements. The parallaxes for R CrA and HR7170 fall outside the plotted range. The deviating proper motion of the star R CrA is insignificant.

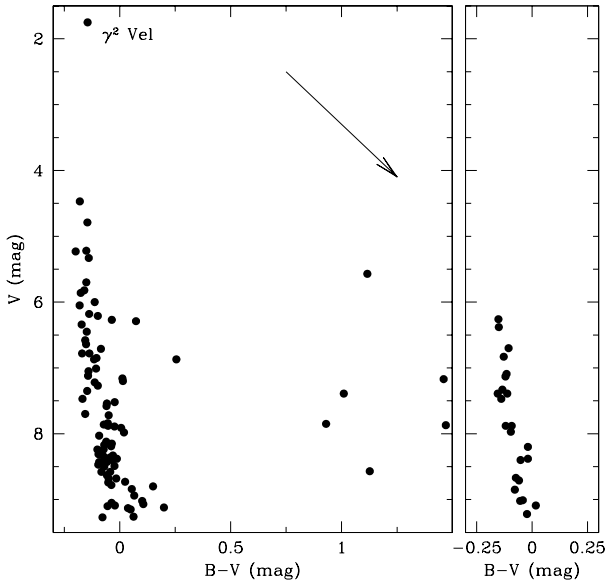

Figure 12: Left: color-magnitude diagram, not corrected for reddening, for the Vela OB2 members. The stars with $B-V > 0\overset{\mathrm{m}}{.}5$ are 3 G- and 3 K-giants. Right: color-magnitude diagram for the Trumpler 10 members.

Straka (1973), and Eggen (1986)[4].

New results: Our selection confirms only 4 of the 10 Brandt et al. stars as members. One of the 6 remaining stars, γ^1 Vel (HR3206), was not observed by Hipparcos. However, our member selection procedure identifies 89 new members for Vel OB2, which brings the total number to 93: γ^2 Vel, 81 B, 5 early-A, and 3 G- and 3 K-type giants. Figure 11 shows the distribution of positions and parallaxes of the selected stars. The abrupt cutoff of the membership list beyond spectral type B9 is artificial: inclusion of many B-type stars in the Hipparcos Catalogue, and the restriction on the stellar density of 3 stars per square degree, cause an absence of stars in Vela of later spectral types, starting already with spectral type A (cf. Figure 2 and §3.4). Vel OB2 has a space motion which does not clearly separate the association from the field star population. Therefore, the expected number of interlopers is high: ∼30 B stars and ∼5 A stars.

Figure 12 (left panel) shows the color-magnitude diagram[5] for our Hipparcos members. No reddening correction has been applied; we suspect this contributes significantly to the horizontal width of the main sequence. The earliest spectral type on the main sequence is B1, suggesting an age of $\lesssim$10 Myr.

We find Collinder 173 (Collinder 1931; Catalog of Open Clusters [1997]: $[\ell, b] = [261\overset{\circ}{.}32, -8\overset{\circ}{.}06]$; diameter ∼6°) to be identical to Vel OB2 ($[\ell, b]$∼[263°, −7°]; diameter ∼10°). Collinder estimated the number of Col 173 members to be 70, and quoted a distance of only 55 pc(!). Eggen (1980, 1983, 1986) found photometric evidence for 29 members of Col 173, including our secure Vel OB2 member γ^1–γ^2 Vel, and derived a photometric distance of 350–525 pc (cf. ∼500 pc [Buscombe 1963]; 380±144 pc [Lyngå & Wramdemark 1984]). He derived a motion for 8 'cluster' members similar to that of our Vel OB2 group. Only 7 of the 29 Eggen members are listed in the Hipparcos Catalogue: we find that 3 of them are secure members of Vel OB2.

The γ^2 Vel system contains WR11, the nearest known Wolf–Rayet star, and its distance is important for the absolute magnitude calibration of WR stars. Classical distance estimates range from ∼170–550 pc (Brandt et al. 1971; Sahu 1992; van der Hucht et al. 1997); the most commonly assumed distance is 450 pc. Even though its parallax of 3.88±0.53 mas places γ^2 Vel at the near edge of Vel OB2, the direction and magnitude of the proper motion leave little doubt about its membership. Schaerer, Schmutz & Grenon (1997) combined the Hipparcos parallax with single star evolutionary models, and derived a weak upper limit of ∼6–10 Myr for the age of the O9I companion of WR11.

[4]Eggen (1982) also mentions Vel OB2, but uses this designation for another group of stars.

[5]Three widely different $B-V$ values for the A0V star HIP38816 ($V = 9\overset{\mathrm{m}}{.}26$) are available: (i) the Hipparcos Catalogue lists a ground-based $B-V = 1\overset{\mathrm{m}}{.}020 \pm 0\overset{\mathrm{m}}{.}020$; (ii) the SIMBAD database gives $B-V = -0\overset{\mathrm{m}}{.}9$; (iii) Tycho photometry ($B_T = 9\overset{\mathrm{m}}{.}399 \pm 0\overset{\mathrm{m}}{.}024$, $V_T = 9\overset{\mathrm{m}}{.}330 \pm 0\overset{\mathrm{m}}{.}032$, $B_T - V_T = 0\overset{\mathrm{m}}{.}069$) can be converted into a Johnson $B-V$ color using eq. 1.3.24 in ESA (1997; Vol. 1 §1.3, Appendix 4, p. 60), resulting in $B-V = 0\overset{\mathrm{m}}{.}062$. As neither POSS plates nor IRAS maps reveal associated interstellar medium features which could affect the $B-V$ color, we adopt $B-V = 0\overset{\mathrm{m}}{.}062$, which places the star on the main sequence.

We obtain a mean distance of 410±12 pc for Vel OB2. The new members are concentrated on the sky around $(\ell, b) \sim (263°, -7°)$ within a radius of ∼5°. Sahu (1992) reported the detection of the so-called IRAS Vela shell in the IRAS Sky Survey Atlas maps (cf. Sahu & Blaauw 1994). This is an expanding shell, centered on Vel OB2, with a projected radius of ∼6° (Figure 11). Assuming that (i) the center of the IRAS Vela shell has a distance of 450 pc, (ii) Vel OB2 is a 'standard association' with a 'normal' initial mass function, and (iii) Vel OB2 has an age of 20 Myr, Sahu showed that the observed kinetic energy of the IRAS Vela shell is of the same order of magnitude as the total amount of energy injected into the interstellar medium through the combined effects of stellar winds and supernovae. Our astrometric identification of Vel OB2 as a rich OB association, and the improved distance determination, will allow a considerable refinement of Sahu's analysis once photometry and radial velocities are available for all our Hipparcos members.

5.2. Trumpler 10

Pre-Hipparcos: Based on relative proper motion data for 29 stars, Lyngå (1959, 1962) identified 19 probable members of the sparse open cluster Trumpler 10 (Tr 10; Catalog of Open Clusters [1997]: $[\ell, b] = [262.°81, 0.°64]$; diameter 14′). Photometry indicated a maximum age of ∼30 Myr and a distance of ∼420 pc. Levato & Malaroda (1975) derived a distance of 440±50 pc for a subset of these stars. Based on 15 members, Eggen (1980) found a distance of 468±65 pc; this value is biased because all stars out to 350 pc were considered foreground objects. Lyngå & Wramdemark (1984) found 363±68 pc for 11 photometric members. Stock (1984) carried out an extensive proper motion study of 979 stars near Tr 10 down to $V = 12^{\rm m}$, and concluded that the existence of a single cluster in this field was doubtful.

New results: During our investigation of the Vela region, our member selection procedure not only identified Vel OB2 in the Hipparcos Catalogue, but it also 'rediscovered' Tr 10. This resulted in a moving group of 23 stars: 22 B-type stars (earliest spectral type B3V) and 1 A0V star. We confirm 4 of the 7 classical members (Lyngå; Levato & Malaroda; Eggen) contained in the Catalogue. The mean distance is 366±23 pc. The members are spread over ∼8° in the sky (∼50 pc at this distance; Figure 11). Figure 12 shows the color-magnitude diagram for our 23 Hipparcos members. Even though the measurements are not corrected for reddening, the main sequence is remarkably tight. Tr 10 is seen in projection in front of the Vela molecular ridge (e.g., May, Murphy & Thaddeus 1988; Murphy & May 1991). This group is clearly older than Vel OB2, and our provisional age estimate based on the earliest spectral type is ∼15 Myr.

The many selected stars outside the classical diameter of 14′ cannot all be interlopers: we expect only 3–5 B-type interlopers and 1 A star (Table A2). We conclude that Tr 10 is in fact not a tight open cluster, but instead an intermediate age OB association.

6. CANIS MAJOR, MONOCEROS AND ORION

The region $245° > \ell > 195°$ contains two nearby OB associations (Ruprecht 1966), Mon OB1 and Ori OB1, and the interesting group Col 121, which we discuss first. Ori OB1 lies in a direction near the Solar antapex, and its space motion does not stand out in the proper motion distribution, while its distance of ∼400 pc makes it difficult to determine membership from the Hipparcos parallaxes alone. We also discuss the well-studied association CMa OB1, which lies in the same region but at a distance of ∼1 kpc.

6.1. Collinder 121

Pre-Hipparcos: Collinder (1931) studied the structural properties and spatial distribution of Galactic open clusters, and discovered a cluster of 20 stars at ∼590 pc in an area of $1° \times 1°$ on the sky: Col 121. Schmidt–Kaler (1961) noted a large number of evolved early-type stars in a field of $10° \times 10°$ centered on the bright supergiant *o* CMa (HIP33152, K3Iab) located in the central part of Col 121. Using photometry, radial velocities, and proper motions, he assigned membership of Col 121 to 10 of these stars, and derived a mean distance of 630 pc. Feinstein (1967) found 12 photometric members within 30′ of the cluster center: 11 main-sequence stars and one evolved star, *o* CMa. He extended this list with 14 bright, mostly evolved, and 12 faint stars inside a circle of 10° radius centered on the cluster. These include some of the Schmidt–Kaler stars, in particular the supergiants δ CMa (HIP34444, F8Ia) and σ CMa (HIP33856, K4III), and the Wolf–Rayet star WR6 (EZ CMa, HIP33165, WN5). Feinstein also put the cluster at 630 pc. In another photometric study, Eggen (1981) suggested a division of the stars in this direction into two groups: an open cluster-like group of 13 stars at 1.17 kpc, identified as Col 121, and a group of 18 stars at 740 pc resembling an OB association.

New results: Figure 13 shows the proper motions for the 43 stars of the combined list of members proposed by Collinder, Schmidt–Kaler, Feinstein and Eggen which are listed in the Hipparcos Catalogue (5, 10, 34 and 13 stars, respectively). Evidence for a moving group can be seen in the proper motions, but our selection procedure rejects 25 of the 43 stars.

We select 103 stars in our Col 121 field (Table A1) with a mean distance of 592±28 pc; 1 WR, 1 O, 85 B, 8 A, 1 F, 1 G, 3 K, and 3 M-type. We reject σ CMa, but include δ and *o* CMa as member. Only 6 of the 14 bright members and 5 of the 12 faint members of Feinstein are selected by our procedure. One bright Feinstein member (HIP34489) has a negative parallax, while HIP34045 (B8II) and HIP35205 (M2III) have parallaxes larger than 7 mas and discordant proper motions. The classical member HIP35904 (B5Ia;

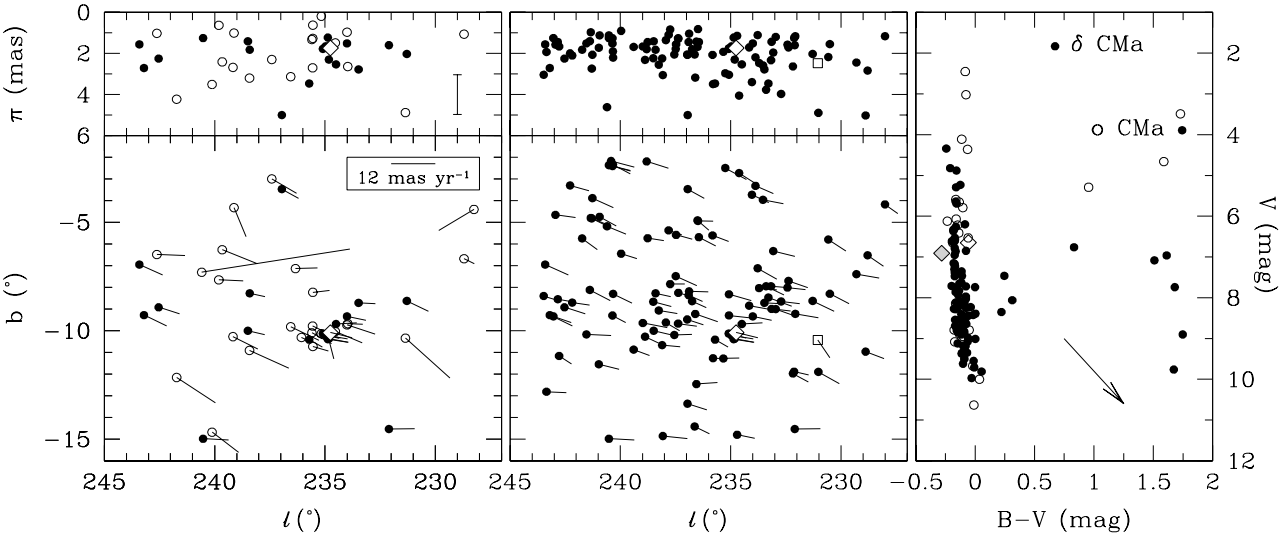

Figure 13: Left: positions and proper motions (bottom) and parallaxes (top) of the pre-Hipparcos members of Collinder 121. Filled circles are confirmed members. Open circles indicate stars rejected by our selection procedure. Three of the latter fall outside the plotted parallax range. Two of these have discrepant proper motions as well. The confirmed member EZ CMa (WR6) is indicated by an open diamond. Middle: same diagram for all stars selected as member of Col 121, illustrating the dramatic change from pre- to post-Hipparcos. The open square represents the open cluster NGC2287: its position, proper motion and parallax is an average of the measurements for 9 members observed by Hipparcos in an area of $0\overset{\circ}{.}5$ diameter. We expect ∼30 interlopers in the Col 121 membership list (see Table A2). These may be mostly the stars above $b{\sim}{-}6^\circ$ and below $b{\sim}{-}12^\circ$ which lie outside the main concentrations. Right: color-magnitude diagram, not corrected for reddening, for the Col 121 members (filled circles), and rejected classical members (open circles). The unusual position of EZ CMa (open diamond) may be caused by systematic effects in the *Hp* to V and $B_T{-}V_T$ to $B{-}V$ transformation (cf. ESA 1997, Vol. 1 §1.3, Appendix 4 and §2.1, pp 107–108). Feinstein (1967) obtained $V = 6\overset{\mathrm{m}}{.}91$, $B{-}V = -0\overset{\mathrm{m}}{.}28$ (gray diamond).

η CMa) is not selected because of its small, but significant, parallax: $\pi = 1.02 \pm 0.44$ mas. HIP33347 (B3Ib/II), HIP33856 (K4III), and HIP33977 (B3Ia) have incompatible or insignificant proper motions. We select 4 of the 7 stars in Eggen's distant group and 2 of the 6 stars in his nearby group, suggesting that his proposed division in two groups is unphysical. We do not confirm the possible connection between Col 121 and NGC2287 proposed by Eggen (1981): the directions of the mean proper motions of these two groups differ by more than 45 degrees (see Figure 13).

Figure 13 (right panel) presents the Hipparcos color-magnitude diagram, not corrected for reddening, for the secure members. It shows that Col 121 contains a number of evolved stars. The abrupt cutoff of the main sequence near $V = 10^{\mathrm{m}}$ is caused by the completeness limit of the Hipparcos Catalogue. Some of the late-type stars may well be interlopers. The presence of an O star and early-type B stars indicates this is a young group, of age ∼5 Myr.

Howarth & Schmutz (1995) put a lower limit of 1800 pc on the distance of EZ CMa. This would imply that it is at least 320 pc away from the Galactic plane. If it were a runaway star (as proposed by Skinner, Itoh & Nagase 1998) born in the Galactic plane, its observed proper motion in b, $\mu_b = -1.46 \pm 0.6$ mas yr^{-1}, puts a lower limit on its age of ∼30 Myr, which is unlikely for a Wolf–Rayet star (e.g., Maeder & Meynet 1994). Although a distance of 1.8 kpc is marginally consistent with $\pi = 1.74{\pm}0.76$ mas, the proper motion and parallax of EZ CMa agree perfectly with those of Col 121, leaving little doubt about its membership, and hence about its distance. It follows that EZ CMa is ∼10 times less luminous than estimated by Howarth & Schmutz.

Col 121 has completely changed its appearance compared to the classical membership lists. Figure 13 clearly suggests two subgroups, $(\ell, b){\sim}(233^\circ, -9^\circ)$ and $(238^\circ, -9^\circ)$. A possible third subgroup lies at $(\ell, b){\sim}(243^\circ, -9^\circ)$. We expect ∼30 interlopers among the B- and A-type stars in this large field (Table A2). It is likely that most of these lie outside the main concentrations, where the membership probabilities are high (Table C1). The linear dimensions of this complex are 100 pc × 30 pc, similar to that of the Sco OB2 association. The color-magnitude diagram also resembles that of Sco OB2, after taking into account the four times larger distance, in the sense that the earliest spectral type and amount of extinction are similar. A full analysis of the stellar content of this OB association is clearly warranted.

6.2. Canis Major OB1

Pre-Hipparcos: The high density of early-type stars in the Canis Major region ($222\overset{\circ}{.}0 < \ell < 226\overset{\circ}{.}0$, $-3\overset{\circ}{.}4 < b < 0\overset{\circ}{.}7$) led Ambartsumian (1949) to propose the existence of the OB association CMa OB1. Markarian (1952) identified

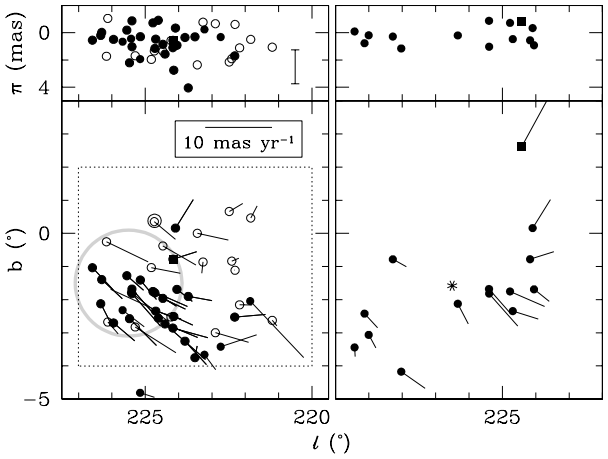

Figure 14: Left: positions and proper motions (bottom) and parallaxes (top) for 30 classical members of Canis Major OB1–R1 (filled symbols). The 16 open symbols show all Hipparcos O–B5 stars with $\pi \leq 5$ mas in the field $220° \leq \ell \leq 227°$, $-4° \leq b \leq 2°$ (dotted lines), which are not classical members. The large open circle at $(\ell, b) = (224\overset{\circ}{.}72, 0\overset{\circ}{.}38)$ denotes the open cluster NGC2353. HIP33735 ($\ell = 221\overset{\circ}{.}85$; $\pi = 6.16 \pm 1.29$ mas) falls outside the upper panel. HIP34536 (filled square) is Herbst & Assousa's (1977) runaway star, and the gray circle denotes their supernova shell. Right: Comerón et al.'s (1998) 14 CMa OB1–R1 members. The new candidate runaway star HIP35707 is the filled square; its proper motion is 17 mas yr $^{-1}$. The asterisk denotes the projected expansion center. The field has been shifted $2\overset{\circ}{.}5$ in Galactic longitude with respect to the left panel.

11 probable members, and derived an angular diameter of $\sim 4°$ and a very uncertain distance of 960 pc[6]. Ruprecht (1966) assumed that the young open cluster NGC2353 (age $\sim$12.6 Myr [Hoag et al. 1961]; age $\sim$76 Myr [Fitzgerald, Harris & Reed 1990]) constitutes a stellar concentration in CMa OB1 (cf. Ambartsumian 1949, 1954), and therefore listed its distance as the open cluster distance of 1315 pc (Becker 1963).

Based on *UBV* measurements, Clariá (1974a, b) found 44 members of CMa OB1, derived a distance of 1150±140 pc and an age $\sim$3 Myr, and confirmed its physical relation to the association of reflection nebulae CMa R1 (Racine 1968; Herbst, Racine & Warner 1978) and to the open cluster NGC2353 (cf. Eggen 1978). The CMa OB1 members are the main exciting stars of the HII regions S292, S296, and S297, which are physically related to the R association. Star formation in this CMa OB1–R1 complex was initiated recently: very young objects are present, among which the classical Herbig emission-line stars Z CMa (HIP34042) and HD53367 (HIP34116). An upper limit of 3 Myr for the age of the complex was derived from the main-sequence lifetime of the massive O-star progenitor of the carbon star W CMa (HIP34413, CII...; Herbst, Racine & Richer 1977).

Herbst & Assousa (1977; cf. Reynolds & Ogden 1978; Machnik et al. 1980) found that CMa R1 lies on the outer edge of an Hα emission ring, centered on $(\ell, b) = (225\overset{\circ}{.}5, -1\overset{\circ}{.}5)$ with a radius of $\sim 1\overset{\circ}{.}5$. The form of the ring, its position with respect to CMa R1, the small age of CMa R1, the detection of the ring in radio wavelengths, an expanding HI shell at the same location, and the runaway star HD54662 (HIP34536, O6), possibly related to a supernova explosion (Blaauw 1961), led these authors to suggest that this ring is a supernova shell with an age of $\sim$0.5 Myr.

New results: Based on Hipparcos proper motions (alone) for 14 O and early B-type stars, corrected for Solar motion and Galactic rotation, and *assuming* a distance of 1150 pc, Comerón, Torra & Gómez (1998) claim the detection of an expanding structure, with center $(\ell, b) = (226\overset{\circ}{.}5, -1\overset{\circ}{.}6)$, and an expansion age of 1.5 Myr. According to these authors, the expansion of 15 km s^{-1}, and the spatial arrangement of the stars, confirm that a supernova was responsible for the formation of CMa OB1–R1. Furthermore, they propose a new candidate for the runaway star related to the supernova: HIP35707 (O9V), which has a residual tangential velocity of 90 km s^{-1} (at the assumed distance of 1150 pc, cf. $\pi = -0.81 \pm 0.84$ mas) directed away from the expansion center, and a corresponding runaway age of $\sim$1 Myr.

Our member selection procedure is unable to detect a moving group in the CMa OB1–R1 field because of the small (often barely significant) proper motions and parallaxes of the candidate members. Figure 14 (left panel) shows the 30 classical members of CMa OB1–R1 contained in the Hipparcos Catalogue, 24 of which have spectral type O–B5 (Racine 1968, and Herbst et al. 1978 [10]; Clariá 1974b [19]; Welin 1979 [1; Ape emission-line shell star HIP33436]). The 16 open symbols show all remaining Hipparcos O–B5 stars with parallaxes $\pi \leq 5$ mas in the field $220° \leq \ell \leq 227°$, $-4° \leq b \leq 2°$, a region somewhat larger than Ruprecht's and Clariá's fields. The parallax distribution shows that the majority of stars lies beyond $\sim$500 pc. The right panel is slightly shifted in ℓ with respect to the left panel, and shows the 14 CMa OB1–R1 members suggested by Comerón et al. (1998).

6.3. Monoceros OB1

Pre-Hipparcos: The Mon OB1 association mainly consists of the open cluster NGC2264 and the R association Mon R1, as well as a rich molecular cloud complex (Herbst 1980) with numerous emission-line objects (e.g., Herbig & Rao 1972; Cohen & Kuhi 1979; Ogura 1984) and one detected outflow object (Margulis et al. 1990). NGC2264 is an open cluster at $\sim$950 pc with $\sim$150 members brighter than $V = 15^{\rm m}$, and age $\sim$3 Myr (Pérez 1991). The up-turn around spectral type A0 in the color-magnitude diagram suggests that low-mass stars are still contracting toward the zero-age main sequence (e.g., Walker 1956; Vasilevskis, Sanders & Balz 1965). The R association Mon R1 is located only 2° from NGC2264, and is part of the same cloud complex (Racine 1968; Herbst et al. 1982). Mon R1 shows a similar up-turn of the main sequence for the A-type

[6]Schmidt (1958) copied Markarian's distances but lists 950 pc.

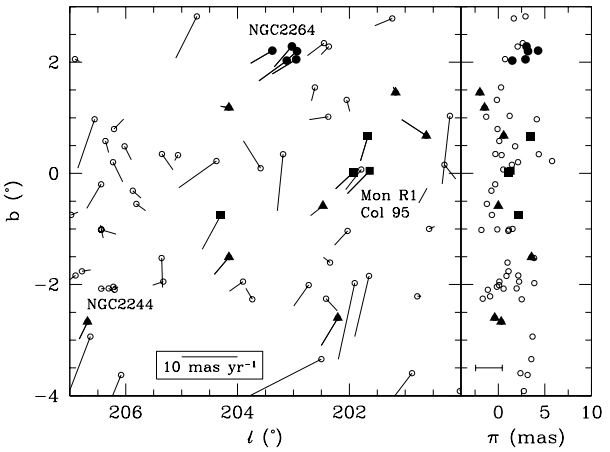

Figure 15: Positions and proper motions (left) and parallaxes (right) of the classical Monoceros OB1 members in the Hipparcos Catalogue (filled symbols), and all stars earlier than A0 with parallaxes $\pi < 10$ mas (open circles). One star lies outside the plotted parallax range ($\pi = -5.93 \pm 6.94$ mas). The classical NGC2264 members (Walker 1956) are denoted by filled circles. Their parallaxes, $\pi \sim 3$ mas, do not fit the distance estimate of ∼1 kpc (e.g., Walker 1956; Pérez 1991). The filled squares are the classical Mon R1 members (Racine 1968, Herbst et al. 1982). The proper motion and parallax of HIP31065 ($[\ell, b] \sim [202°, 0°]$, open circle) indicate that it may belong to Mon R1 (also known as Col 95). The filled triangles are the additional Mon OB1 members proposed by Turner (1976). NGC2244, the open cluster associated with the Rosetta nebula, is also indicated.

stars. Turner (1976) published a new list of 14 photometric Mon OB1 members distributed over an area of $4° \times 8°$, including the concentrations of NGC2264 and Mon R1. The area contains two large HII regions, one centered on NGC2264, the other on NGC2244 (the Rosetta nebula), and a supernova remnant, the Monoceros Ring. NGC2244 is part of the Mon OB2 association at 1.4 kpc (Ruprecht 1966). Several expanding shells have been observed in the Mon OB1 region. Blitz (1978) reported an HI shell, expansion velocity of ∼15 km s^{-1}, adjacent to the molecular clouds. The shell is similar to the HI shell observed in CMa OB1 (§6.2). Kutner et al. (1979) reported a ring structure in the Mon R1 molecular clouds which appears to be kinematically distinct from the Mon OB1 molecular cloud complex. They also found evidence for an expanding HI shell associated with the molecular ring, and estimated an expansion age of 1–3 Myr.

New results: The Hipparcos data do not allow a rigorous kinematic member selection. The parallel proper motions of the 5 NGC2264 members contained in the Catalogue confirm NGC2264 as a moving group (Figure 15). However, four of these have parallaxes larger than 2.5 mas, corresponding to a distance $\lesssim$400 pc, which is much smaller than previous estimates. One of these stars is S Mon (HIP31978, O7). Due to the small angular size of the cluster the Hipparcos measurements are correlated and must be treated with care. The 4 Mon R1 members observed by Hipparcos have parallaxes of $\sim 1.3 \pm 1.0$ mas, consistent with the classical distance of 1 kpc. Of the 10 stars in the Catalogue suggested by Turner (1976) one is a member of Mon R1 and two belong to NGC2264. The proper motions of the remaining 7 stars do not show a clear sign of a moving group, and their parallaxes vary between −1.97 and 3.57 mas (Figure 15).

6.4. Orion OB1

Pre-Hipparcos: Of all OB associations, Ori OB1 undoubtedly has received most attention (e.g., Warren & Hesser 1977a, b, 1978; Goudis 1982; Brown, Walter & Blaauw 1998). It is related to the Orion molecular cloud complex, which is a site of active star formation (e.g., McCaughrean & Burkert 1998). Blaauw (1964a) divided Ori OB1 into four subgroups: 1a, northwest of the Belt stars; 1b, the Belt region, including the Belt stars; 1c, the Sword region; and 1d, the Orion Nebula cluster region, including the Trapezium stars.

The most recent photometric census of Ori OB1 was carried out by Brown et al. (1994), who determined membership, distances (1a: 380±90 pc; 1b: 360±70 pc; 1c: 400±90 pc; 1d: undetermined due to nebulosity and small number of stars), ages (1a: 11.4±1.9 Myr; 1b: 1.7±1.1 Myr; 1c: 4.6±2 Myr; 1d: <1 Myr), and found the initial mass function for subgroups 1a, 1b, and 1c to be a single power law: $\xi(\log M) \mathrm{d} \log M \propto M^{-1.7 \pm 0.2} \mathrm{d} \log M$. These authors showed that the total energy output of the association over its lifetime can explain the observed Orion–Eridanus HI shell surrounding Ori OB1 (cf. Burrows et al. 1993; Brown, Hartmann & Burton 1995). In a proper motion study of the Orion Nebula cluster, Tian et al. (1996) derived an upper limit on the velocity dispersion of ∼2 km s^{-1} (assuming a distance of 470 pc), and concluded that the cluster is unbound.

Early evidence for pre-main sequence objects in Orion was discussed by Haro (1953) and Walker (1969). Hα and X-ray surveys (e.g., Nakano, Wiramihardja & Kogure 1995; Alcalá et al. 1996; Walter, Wolk & Sherry 1998) have uncovered hundreds of emission-line and X-ray sources in Ori OB1, of which many are likely to be pre-main sequence stars (Alcalá, Chavarría–K. & Terranegra 1998; Brown et al. 1998). The population of low-mass pre-main sequence stars clustered around σ Ori (HIP26549; O9.5V...) in subgroup 1b has a similar age as the high-mass members of the subgroup (Walter et al. 1998). At $V > 12^{\mathrm{m}}$, these stars are too faint to be included in the Hipparcos Catalogue.

New results: Unfortunately, the relative motion of the Ori OB1 association is mostly directed radially away from the Sun. This makes it very hard to detect the association with our selection procedure using the Hipparcos measurements, as is illustrated in Figure 16. However, Ori OB1 is such a well-studied association that Brown et al. (1998) decided to analyse the Hipparcos data in a provisional way in order to constrain its distance. They show that a rough

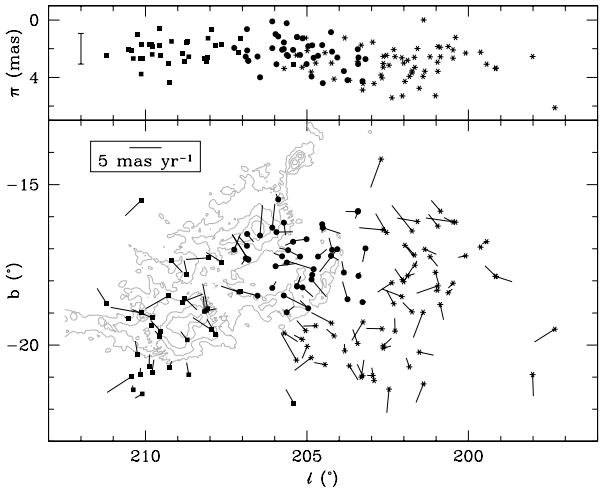

Figure 16: Positions and proper motions (bottom) and parallaxes (top) in the subgroups of Orion OB1, for the stars selected according to the proper motion criterion given in eq. (8). The proper motions are small because Ori OB1 lies near the direction of the Solar Antapex. The parallaxes in subgroup 1a (asterisks) are generally larger than those in 1b (filled circles) and 1c (filled squares). The contours present the 100μm IRAS flux map.

selection of Ori OB1 members can be made by requiring:

$$(\mu_\alpha \cos\delta - 0.44)^2 + (\mu_\delta + 0.65)^2 \leq 25, \qquad (8)$$

where the units are mas yr^{-1}. The resulting set of stars overlaps the Brown et al. (1994) list of photometric members by 96 per cent. Figure 16 shows the stars located close to the Orion molecular clouds, selected according to eq. (8). The parallaxes of the members of subgroup 1a are significantly larger than those of 1b and 1c (Figure 16). Taking the parallax distributions at face value, the mean distances to the subgroups (cf. §3.6) are: 336±16 pc for 1a, 473±33 pc for 1b and 506±37 pc for 1c, where the quoted errors are the formal errors on the mean distances. The actual uncertainty is larger due to the simplified member selection. Deriving more accurate distance estimates requires better knowledge of membership. The only firm conclusion we can draw at this point is that 1a is located significantly closer to the Sun than 1b and 1c. The implications of the smaller distance of 1a are discussed by Brown et al. (1998).

7. PERSEUS, TAURUS, CASSIOPEIA AND CAMELOPARDALIS

The Perseus region contains the well-studied association Per OB2, as well as the α Persei cluster, listed as Per OB3 by Ruprecht (1966). It may be related to the old Cas–Tau association, which we discuss here also. Cam OB1 lies at a larger distance, but in the same general direction.

7.1. Perseus OB2

Pre-Hipparcos: Blaauw (1944; cf. Blaauw 1952a) noticed the presence of 15 O–B3 stars concentrated in a region of 6° diameter in Perseus: Per OB2, sometimes called the ζ Persei association or moving cluster after its brightest member. Other special classical members are: ξ Per (doubtful member because of deviating radial velocity; $v_{\rm rad}$ = 67.1 km s^{-1}), X Per (high-mass X-ray binary), o Per, 40 Per, HD23060 (unknown radial velocity), AG Per (double-lined eclipsing binary), HD21483 (star in nebulosity with deviating radial velocity), and BD+31 643 (heavily reddened B star with β Pic-like circumstellar disk [Kalas & Jewitt 1997; Lissauer 1997]). Blaauw (1944) derived a photometric distance of 267 pc, a mean radial velocity of 19.4 km s^{-1}, and a mean space motion of 21.7 km s^{-1}.

In a subsequent study, Blaauw (1952a; cf. Delhaye & Blaauw 1953) deduced a kinematic expansion age of 1.3 Myr. The star o Per was omitted from the analysis as it did not obey the expansion. Delhaye & Blaauw (1953) suggested that the proper motions of o Per, as well as of X Per and HD23478, deviate from the cluster mean because these stars are actually multiple systems in which an invisible, massive companion is still contracting towards the main sequence. Lesh (1969) repeated Blaauw's expansion analysis using new proper motions for 9 bright Per OB2 members, and obtained an expansion age of 1.3±0.1 Myr. The right ascension proper motions of the stars o Per and 40 Per deviated strongly from the expansion pattern and were not taken into account.

Later studies of the stellar content of Per OB2 were mainly photometric (e.g., Morgan et al. 1953; Harris 1956; Hardie, Seyfert & Grenchik 1957; Seyfert, Hardie & Grenchik 1960; Borgman & Blaauw 1964; Rydgren 1971; Guetter 1977; Černis 1993). The derived ages range from 2 to 15 Myr (e.g., Klochkova & Kopylov 1985; de Zeeuw & Brand 1985; Giménez & Clausen 1994).

Blaauw (1952a) discussed the embedded, nebulous open cluster IC348 ∼8′ south of o Per as a possible concentration in Per OB2 (Gingrich 1922; Hubble 1922a, b; Greenstein 1948; Harris, Morgan & Roman 1954, 1955; Strom, Strom & Carrasco 1974; Černis 1993). Proper motions revealed 8 members, the brightest of which is BD+31 643 (B5V). The proper motions used by Fredrick (1954, 1956) showed that '... o Per is not a member of the nucleus and perhaps is not even a member of the association'. Later discoveries of Hα emission-line T Tauri stars (Herbig 1954), reflection nebulae (Racine 1968), infrared sources (Ladd, Lada & Myers 1993), X-ray selected T Tauri stars (Preibisch, Zinnecker & Herbig 1996), and photometrically detected pre-main sequence stars have led to the recognition that star formation in IC348 has been going on continuously for 3–7 Myr (e.g., Strom et al. 1974; Lada & Lada 1995; Trullols & Jordi 1997).

The Per OB2 region is rich in patches of bright and dark nebulosities. The interstellar material in Perseus is distributed in various layers at various distances, and the obscuring material has a patchy, inhomogeneous dis-

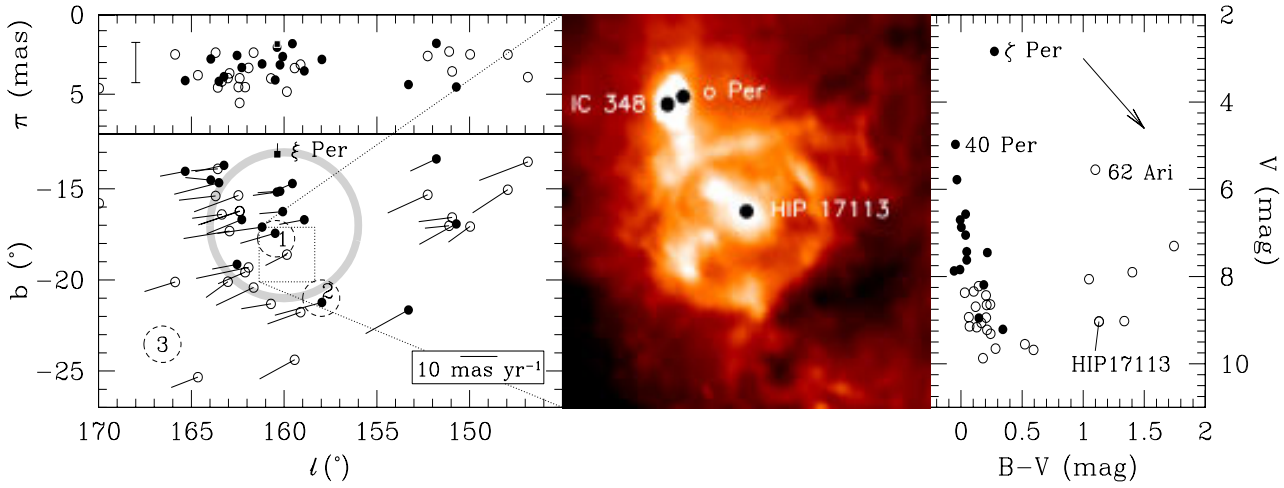

Figure 17: Left: positions and proper motions (bottom) and parallaxes (top) for the 41 Perseus OB2 members. Filled circles indicate OB-type members (17 stars), while open circles refer to later-type members (24 stars). The filled square denotes the runaway ξ Per. The related HII region NGC1499 ('California nebula') lies $\sim$1° above ξ Per (e.g., Bohnenstengel & Wendker 1976). The gray ring denotes the expanding HI shell detected by Sancisi et al. (1974). The small dashed circles indicate the positions of (1) IC348, (2) NGC1333, and (3) the Pleiades. The 3° × 3° dotted box is centered on HIP17113 ($\ell = 159\overset{\circ}{.}85, b = -18\overset{\circ}{.}61$), and is enlarged in the middle panel. Middle: IRAS 60μm map of the cores IC348 (with overlapping dots at the positions of the stars HIP17465 and 17468) and B3/L1468–1470 in the Per OB2 molecular cloud. The position of the bright star o Per is shown for reference. HIP17113 seems to be related to a ring in the interstellar medium with a radius of $\sim 0\overset{\circ}{.}6$. Right: color-magnitude diagram, not corrected for reddening, for 40 of the 41 Per OB2 members (without HIP17561). Symbols as in the left panel. HIP20324 has $B-V = 2\overset{\mathrm{m}}{.}020$. The main sequence is broadened by differential reddening, stellar multiplicity, and a distance spread of $\sim 0\overset{\mathrm{m}}{.}4$.

tribution (e.g., Heeschen 1951; Lynds 1969; Rydgren 1971; Černis 1990, 1993; Krelowski, Megier & Strobel 1996). Some of the material at 140 to 180 pc might simply be an extension of the Taurus dark clouds to the northwest (Černis 1990, 1993; Cernicharo, Bachiller & Duvert 1985). The elongated chain of dark, molecular condensations called the Per OB2 molecular cloud (e.g., Sargent 1979) hosts several isolated, opaque molecular cores, of which only IC348 and NGC1333 (e.g., Lada et al. 1974; Lada, Alves & Lada 1996), separated by $3\overset{\circ}{.}5$, contain young B stars. Several hundreds of pre-main sequence objects are known in and around IC348 and NGC1333 (e.g., Herbig 1954; Herbig & Rao 1972; Preibisch et al. 1996; Trullols & Jordi 1997; Preibisch 1997). They generally have $V \sim 15^{\mathrm{m}}$–20^{m}, and were hence not observed by Hipparcos.

A physical relation between Per OB2 and the Per OB2 molecular cloud has never been proven beyond doubt, due to the uncertain distance estimates to the cloud, which range from 150 to 500 pc (Rydgren 1971; Strom et al. 1974). However, Sancisi (1970; cf. Sancisi et al. 1974) found complex gas and dust clouds, which were interpreted as an expanding supernova remnant shell of interstellar matter physically connected with Per OB2 and Gould's Belt. Sancisi (1974; cf. Loren 1976; Hartquist & Morfill 1983) suggested that the stars in Per OB2 formed 1–4 Myr ago in the densest parts of this shell (e.g., Öpik 1953). Indirect 'evidence' for this supernova explosion is provided by the existence of the runaway O star ξ Per (HIP18614; Blaauw 1961, 1964a).

New results: We find 41 Hipparcos members of Per OB2: 17 B, 16 A, 2 F, 2 G, 3 K, and 1 M-type. All 17 classical members (Blaauw 1944, 1952a) were observed by Hipparcos. We confirm only 8 of them, among which ζ Per (HIP18246, B1Ib), 40 Per (HIP17313, B0.5V), and AG Per (HIP19201, B5V:p; but see Giménez & Clausen 1994). Three of the 9 rejected classical proper motion members have unreliable or insignificant astrometric parameters: HIP17631 (B3IV...), X Per (HIP18350, O9.5pe; also known as 'non-conventional member' [e.g., Borgman & Blaauw 1964; Wackerling 1972; Sargent 1979]), and BD+31 643[7] (HIP17465, B5V; brightest member of IC348, of which Gingrich 12 [HIP17468, A2] is another member). Another three were already suspected to be peculiar or even non members: o Per (HIP17448, B1III; see e.g., Delhaye & Blaauw 1953; Fredrick 1954, 1956; Sargent 1979; Snow et al. 1994), HD21483 (HIP16203, B3III; cf. Schreur 1970; Sargent 1979), and the runaway ξ Per (HIP18614, O7.5Iab:).

The early-type members give a mean distance of 318±27 pc, somewhat smaller than most previous values. The interloper analysis predicts one or two spurious B-type members and $\sim$10 A-type members. Figure 17 (left panel) shows the positions and parallaxes of the 41 members. The late-type members clumped around $(\ell, b) \sim (151°, -16°)$, and separated by $\sim 5°$ from the main body of the cluster, could be interlopers. The Per OB2 molecular cloud

[7] The parallax and proper motion of HIP17468 have been fixed to those of HIP17465 as indicated by H60 = F.

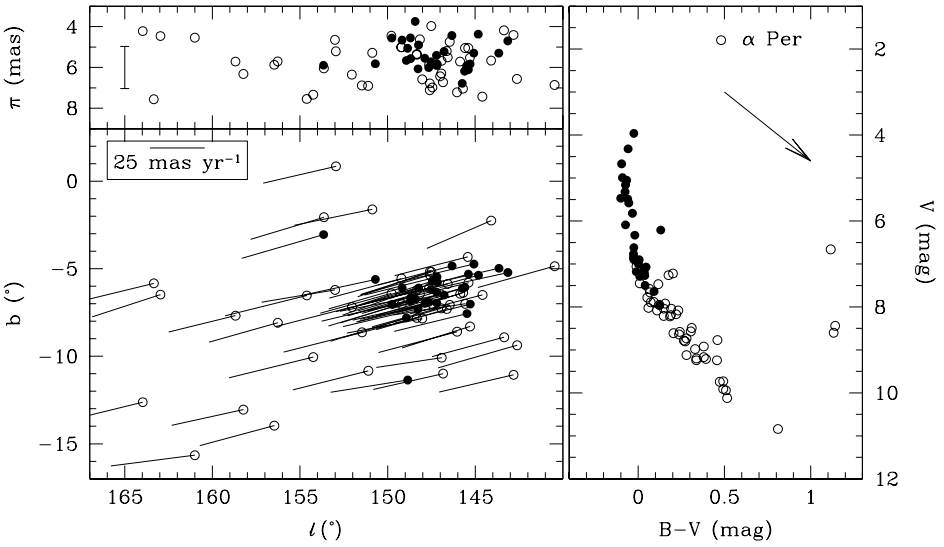

Figure 18: Left: positions and proper motions (bottom) and parallaxes (top) of the α Persei (Perseus OB3) members. Filled circles indicate B-type stars, and open circles the later spectral types. Right: color-magnitude diagram, not corrected for reddening, for the α Persei members. Symbols as in the left panels. The main sequence extends from B3Ve ($V = 3\overset{\mathrm{m}}{.}96$) to G3V ($V = 10\overset{\mathrm{m}}{.}84$).

roughly connects the dashed circles (1; IC348) and (2; NGC1333).

Figure 17 (right panel) shows the color-magnitude diagram, not corrected for reddening. The brightest member, ζ Per (B1Ib), is an evolved star, leaving 40 Per (B0.5V) as the brightest main-sequence member. The large and variable extinction in the Perseus region (e.g., Lynds 1969; Černis 1990, 1993), combined with a large fraction of spectroscopic binaries (e.g., Giménez & Clausen 1994) is probably responsible for the broad main sequence. The 7 stars with $B - V > 1^{\mathrm{m}}$ include all members later than spectral type F (the brightest is 62 Ari [HIP15696, G5III], most likely an interloper) and HIP17113. The Hipparcos Catalogue lists HIP17113 as an F2 star, with $V = 9\overset{\mathrm{m}}{.}03$ and $B-V = 1\overset{\mathrm{m}}{.}13$ based on Tycho photometry. The SIMBAD database gives a spectral type B5, with $V = 10\overset{\mathrm{m}}{.}6$ and $B-V = -0\overset{\mathrm{m}}{.}1$ based on aperture photometry. The IRAS 60μm map (Figure 17) shows that the star appears to be located at the center of a ring (or shell) of radius $\sim 0\overset{\circ}{.}6$ (3.3 pc at an assumed distance of 318 pc). The star seems to be surrounded by interstellar material related to the molecular globule B3/L1468–1470 (Barnard 1927; Lynds 1962). We suspect this has influenced the photometric measurements reported in SIMBAD.

7.2. *Cassiopeia–Taurus and α Persei (Per OB3)*

Pre-Hipparcos: The Cassiopeia–Taurus group was identified and studied by Blaauw (1956). He proposed 49 members of spectral type B5 and earlier, in an area of $140^\circ \times 100^\circ$, which showed remarkably parallel motions. Blaauw concluded that this group formed an old, nearly dissolved, association at $\sim$140 pc, with an expansion age of $\sim$50 Myr. Based on the similar velocity and distance of the Cas–Tau group and the cluster α Persei, Blaauw suggested that the two belonged to the same physical group. Rasmuson (1921) already reported an extended stream of stars around α Persei that shared its motion. Using new radial velocities, Petrie (1958) claimed that Cas–Tau is not a physical group. Crawford (1963) suggested that either the group did not exist, or that there was a large contamination by non members, based on a large scatter in the intrinsic color versus Hβ relation.

The α Persei moving group was discovered independently by B. Boss (1910), Eddington (1910) and Kapteyn (1911) after publication of the Preliminary General Catalog by L. Boss. They noted a group of $\sim$16 bright early-type stars with large proper motions, well-separated from the early-type field population. Later studies extended and refined the list of members to $V \lesssim 12^{\mathrm{m}}$ and spectral types earlier than G5, using photometric, proper motion and radial velocity measurements (e.g., Roman & Morgan 1950; Harris 1956; Heckmann, Dieckvoss & Kox 1956; Heckmann & Lübeck 1958; Artyukhina 1972; Fresneau 1980). CCD photometry identified $\sim$300 candidate members to $V \sim 19^{\mathrm{m}}$ (e.g., Stauffer et al. 1985; Stauffer, Hartmann & Jones 1989; Prosser 1992). Meynet, Mermilliod & Maeder (1993) estimated an age of $\sim$50 Myr for this group.

New results: Only 52 of the 170 stars in the classical list of bright α Persei members (Heckmann & Lübeck 1958) are contained in the Hipparcos Catalogue. Our selection method rejects 13 of these, but adds another 40, resulting in a total of 79 members: 30 B, 33 A, 12 F, 2 G, and 2 K-type, nearly all of them with large membership probability (Table C1). We confirm α Per (HIP15863, F5Ib) itself as member. Two of the 13 rejected stars fall outside the proper motion window for the secure members as defined in Table A1, and 7 have parallaxes smaller than 4 mas,

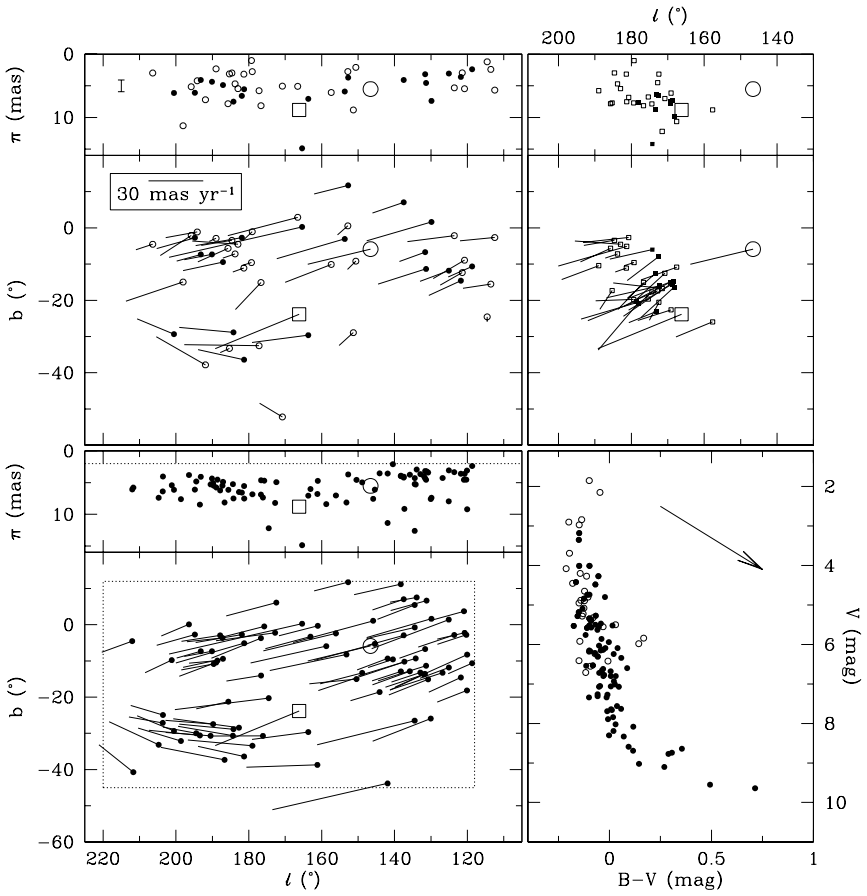

Figure 19: Upper left panels: positions, proper motions, and parallaxes for 47 classical members of the Cassiopeia–Taurus association proposed by Blaauw (1956). The two classical members α Ara (HIP85792) and η UMa (HIP67301) lie outside these panels (see §7.2). Filled circles are confirmed Cas–Tau members. Open circles are stars rejected by our selection procedure. The large open circle and open square represent the α Persei and Pleiades cluster, respectively. Lower left panels: positions, proper motions, and parallaxes for 83 Cas–Tau members in the field $118° \leq \ell \leq 220°$ and $-45° \leq b \leq 12°$ with $\pi > 2$ mas. Field and parallax limits are indicated as dotted lines. Lower right panel: color-magnitude diagram, not corrected for reddening, for the 83 Cas–Tau members (filled circles), and rejected classical members (open circles). Upper right panels: positions, proper motions, and parallaxes for 12 T Tauri stars (filled squares; Frink et al. 1997), and 21 B-type members (open squares; Walter & Boyd 1991), associated with the Tau–Aur star-forming region.

and discordant proper motions. Three of the remaining stars are labeled as binary in the Hipparcos Catalogue (two 'G'-type and one component 'C' solution). Most of the members are located in a region of $3° \times 3°$, consistent with the 1.°25 and 2.°5 radii for the 'nucleus' and 'corona', respectively, found by Artyukhina (1972). However, we find a 'halo' of 10°, consisting mostly of A-type stars (Figure 18). We expect ∼5 interloper A stars (Table A2) which may partly explain this extended component of the moving group (but see below). We select 10 of the 16 stars proposed by Eddington (1910). This high success rate is mainly due to the small distance (177±4 pc), and large tangential streaming velocity (∼30 km s^{-1}) with respect to the Sun.

The α Persei main sequence in the color-magnitude diagram shown in the right-hand panel of Figure 18 is remarkably narrow. It is the result of nearly negligible differential reddening, and a small distance spread. The turnoff at the bright end is consistent with an age of ∼50 Myr. The absence of late-type members is only apparent, and is due to the completeness limits of the Hipparcos Catalogue.

Unlike previous fundamental catalogs, the Hipparcos Catalogue is free of regional systematic errors, which makes it possible to establish reliable kinematic membership of groups covering a large area on the sky, such as Cas–Tau. We first applied our selection procedure to all OB stars in the field $118° \leq \ell \leq 220°$ and $-45° \leq b \leq 12°$. We excluded the secure α Persei members in order to prevent confusion between the Cas–Tau group and α Persei. To avoid a large contamination by distant objects in this very large field we confined the search to all stars with parallaxes $\pi > 2$ mas. We did not consider later-type stars for the same reason. The refurbished convergent point method (§3.1) recognizes Cas–Tau as a moving group and finds a convergent point $(\ell_{\rm cp}, b_{\rm cp}) = (243.°6, -13.°1)$. The Spaghetti method (§3.2) finds multiple peaks in velocity

space. The highest peak corresponds to the field B stars at a velocity of $(U,V,W) = (-10.19, -6.36, -7.08)$ km s^{-1}. However, there is a significant secondary peak at a velocity $(U,V,W) = (-13.24, -19.69, -6.38)$ km s^{-1}, which corresponds to Cas–Tau. The resulting convergent point and streaming velocity with respect to the Sun are $(\ell_{\rm cp}, b_{\rm cp}) = (236\fdg1, -15\fdg1)$ and $S = 24.6$ km s^{-1}, respectively. The convergent points found by both methods are remarkably similar to each other and to the results of Blaauw (1956), $(\ell_{\rm cp}, b_{\rm cp}) = (233\fdg9, -12\fdg0)$ and $S = 23.9$ km s^{-1}, Petrie (1958), $(\ell_{\rm cp}, b_{\rm cp}) = (225\fdg1, -10\fdg2)$ and $S = 20.1$ km s^{-1}, and Eggen (1961), $(U,V,W) = (-15.1, -19.6, -5.6)$ km s^{-1}.

We select 83 stars which are consistent with the derived convergent point and space velocity (Figure 19). The expected number of interlopers in the large field is ∼50 (Table A2). While this number is substantial, it is significantly smaller than 83, which strengthens the conclusion that Cas–Tau is a physical group. Our procedure selects 16 of the 49 classical Cas–Tau members proposed by Blaauw. One other classical member (HIP19343) is a secure member of α Persei. Six classical members brighter than $V = 4^{\rm m}$ are rejected by our selection scheme. Two of these are foreground objects: η UMa (HIP67301; B3V; $[\ell, b] = [100\fdg69, 65\fdg32]$; $\pi = 32.39$ mas; $V = 1\fm85$) and α Ara (HIP85792; B2Vne; $[\ell, b] = [340\fdg75, -8\fdg82]$; $\pi = 13.46$ mas; $V = 2\fm84$). Another three have indications of binarity (HIP4427, HIP18532, HIP26451). The distances of the Cas–Tau stars vary systematically with ℓ, ranging between 125 and 300 pc. This is not unexpected, given the large physical size and unknown orientation of this group.

The color-magnitude diagram of the 83 B-type Cas–Tau members is narrower than the similar diagram for the classical members. The expected distance spread is $\sim 1\fm9$. Three of the six highly reddened stars ($B-V > 0\fm25$) are located within 5° of each other, and are probably obscured by the same 'cloud complex' ($[\ell, b] \sim [133°, 6°]$).

The motion of the α Persei cluster is consistent with that of Cas–Tau, which thus confirms the physical relation between the two groups. It also suggests that the halo of α Persei members mentioned above is the inner region of the Cas–Tau group. These results provide kinematic support for the hypothesis that the α Persei cluster and the Cas–Tau association have a common origin, with α Persei surviving as a bound structure. This is in harmony with the age estimates of ∼50 Myr for both the cluster and the association.

The Taurus–Auriga clouds lie in this same area, near $(\ell, b) \sim (170°, -20°)$, at a distance of ∼140 pc (e.g., Kenyon, Dobrzycka & Hartmann 1994). It is natural to ask whether this well-known site of low-mass star formation is also kinematically related to the Cas–Tau association. Walter & Boyd (1991) searched for B stars with similar kinematics as the low-mass stars in the Tau–Aur clouds. They identified 29 such stars; 21 are listed in the Hipparcos Catalogue, and 7 of these are in the original Cas–Tau list of Blaauw (1956). We reject all of the latter, and select only 2 of the remaining 14 as Cas–Tau members. Figure 19 shows that the proper motions of the Walter & Boyd stars have a large dispersion in magnitude and direction. Frink et al. (1997) used proper motions with accuracies of ∼5 mas yr^{-1} to identify a moving group of pre-main sequence objects in Tau–Aur. Twelve of their objects are listed in the Hipparcos Catalogue. The directions of the Hipparcos proper motions of these stars are reasonably similar, but they differ by ∼40° from that of the Cas–Tau members. We conclude that the star-forming region in Tau–Aur and the old Cas–Tau association are distinct stellar groups.

7.3. Camelopardalis OB1

Morgan et al. (1953) investigated the luminous star content in Camelopardalis, and found evidence for an 'aggregate', Cam OB1, of 8 early-type stars at a distance of ∼900 pc. Ruprecht (1966) extended this list with 2 stars. The 10 members are spread over an area of 15° × 3° on the sky. The corresponding physical dimensions, 240 pc × 50 pc, make a common origin for these stars implausible (cf. Garmany & Stencel 1992). Humphreys (1978) compiled a list of 19 luminous stars for Cam OB1 based on positions, photometric distances and, when available, radial velocities. She derived a distance of ∼1 kpc. However, these stars are distributed over an even larger area on the sky than the 10 stars of Ruprecht. Haug (1970) found 39 luminous Cam OB1 members in an area of 4° × 2° at ∼1 kpc, associated with the HII region S202 located at $(\ell, b) \sim (140°, 2°)$ at ∼800 pc (Brand & Blitz 1993). Digel et al. (1996) also associated Cam OB1 with S202 based on the velocity of the stellar association and the CO emission from the cloud complex containing S202. The region around S202 is an active star-forming complex containing outflow objects and HII regions (Blitz, Fich & Stark 1982; Snell et al. 1984; Campbell, Persson & McGregor 1986), as well as the R association Cam R1 (∼870 pc; Racine 1968). Some of the Cam OB1 members according to Morgan et al., Ruprecht, and Humphreys are identified as Cam R1 members by Racine.

The Hipparcos parallaxes of the classical members are consistent with a distance of ∼1 kpc (Figure 20). The proper motions of the classical members are small, and do not allow identification of a moving group. The field also contains three open clusters: NGC1502 (at ∼900 pc), IC1848 (at ∼2.5 kpc), and IC1805 (at ∼2.2 kpc) (Mermilliod 1998).

Camelopardalis embraces a star-forming region of considerable dimensions, which clearly requires a detailed study of its internal structure and kinematics, comparable to what Hipparcos allows us to do for the nearest associations. This will be complicated by the fact that Camelopardalis lies in the direction of the Perseus spiral arm, so that the large number of early-type stars and giants might be caused by accidental alignments along the line of sight.

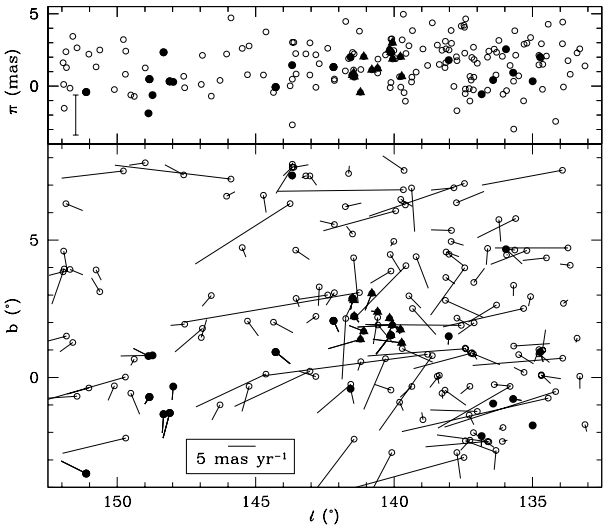

Figure 20: Positions and proper motions (bottom) and parallaxes (top) of the classical Camelopardalis OB1 members in the Hipparcos Catalogue, filled symbols, and all OB-type stars with parallaxes $\pi < 5$ mas, open circles. Filled triangles denote the Cam OB1 members from Haug (1970). The concentrations at $(\ell, b)\sim(143\overset{\circ}{.}5, 7\overset{\circ}{.}5)$, $(137\overset{\circ}{.}5, 1\overset{\circ}{.}0)$, and $(135\overset{\circ}{.}0, 1\overset{\circ}{.}0)$ are three distant open clusters: NGC1502, IC1848, and IC1805, respectively.

8. LACERTA, CEPHEUS, CYGNUS AND SCUTUM

The Cepheus and Cygnus region is rich in luminous young stars, molecular cloud complexes and active star-forming regions. The most striking example is the Cygnus X complex, which is ∼10° in diameter, at a distance of ∼1 kpc (e.g., Wendker, Higgs & Landecker 1991). Ruprecht (1966) lists 5 OB associations in Cepheus and 9 in Cygnus. All associations in Cygnus, except Cyg OB4 and 7, are most likely physically connected to the Cygnus Superbubble and are located beyond 1 kpc. We start by studying Lac OB1, which has remarkably little associated interstellar medium. Then we discuss Cep OB2, 3, and 4, a new group in Cepheus, which we refer to as Cep OB6, as well as Cyg OB4 and Cyg OB7. We conclude this section with the one remaining nearby association of Table 1, Sct OB2.

8.1. Lacerta OB1

Pre-Hipparcos: Blaauw's (1952a) detection of expansion of Per OB2 confirmed Ambartsumian's hypothesis that OB associations are young, unbound groups. Stimulated by these results, Blaauw & Morgan (1953; cf. Blaauw 1952c) found similar evidence for a young aggregate containing 29 candidate O–B5 members in the field $60° < \ell^I < 75°$, $-20° < b^I < -5°$: Lac OB1. Among the members were the O9V star 10 Lac (HIP111841), and the β CMa-type variables 12 Lac (HIP112031) and 16 Lac (HIP113281). The B2V and B3V stars gave a distance of 460 pc. Based on 25 members, a disputed expansion age of 4.2 Myr was derived: because of systematic errors in the right ascension proper motion components, the analysis used declination values alone, which possibly contained systematic errors as well (van Herk 1959). A re-analysis with new data by Woolley & Eggen (1958) could not confirm the expansion of Lac OB1 (cf. Steffey 1973). Lesh (1969) used new proper motions for 10 stars (Delhaye, unpublished) to obtain an expansion age of 2.5 ± 0.5 Myr.

Based on proper motions and radial velocities (Delhaye & Blaauw, unpublished), Blaauw (1958) divided Lac OB1 in an old dispersed subgroup 'a' (15 stars; 16–25 Myr), and a younger concentrated subgroup 'b' (11 stars; 12–16 Myr, see Blaauw 1964a, 1991). The Hertzsprung–Russell diagram was consistent with this division: the members of subgroup 'a' were somewhat brighter on average, and consequently older, than those of 'b', while also lacking the earliest spectral types. These results were confirmed by Crawford (1961) and Lesh (1969). Lesh also derived different distances for the subgroups: 368 pc for 'a' and 603 pc for 'b' (cf. Crawford & Warren 1976: 417 and 479 pc, respectively). Nonetheless, the reality of 'a' has always been controversial (e.g., Lesh 1969). Consequently, most studies focused on 'b', often referred to as Lac OB1. Ruprecht's (1966) field, $96\overset{\circ}{.}0 < \ell < 98\overset{\circ}{.}0$, $-18\overset{\circ}{.}7 < b < -15\overset{\circ}{.}6$, indeed refers to subgroup 'b' exclusively. Besides polarization studies (e.g., Krzemínski & Oskanjan 1961), radial velocity (e.g., Blaauw & van Albada 1963; Bijaoui, Lacoarret & Granes 1981) and rotational velocity (e.g., Abt & Hunter 1962) studies, several photometric and spectroscopic investigations were conducted (e.g., Harris 1955; Seyfert & Hardie 1957; Blaauw 1958; Hardie & Seyfert 1959; Crawford 1960, 1961; Adelman 1968, 1973; Lesh 1968; Crawford & Warren 1976; Levato & Abt 1976; Guetter 1976).

New results: We find 96 Hipparcos members: 1 O, 35 B, 46 A, 1 F, 8 K, 3 M-type, 1 star without spectral classification (HIP111762), and the carbon star HIP116681 at the edge of our field. We confirm 16 of the 29 Blaauw & Morgan (1953) members (among which are 10, 12, and 16 Lac). The two B2V stars HIP110790 and HIP110849 labeled as 'Field star?' in Blaauw & Morgan's table 1 are both selected as members. We also confirm HD215227 (HIP112148, B5:ne; Harris 1955), HD213976 (HIP111429; Odenwald 1988; Olano, Walmsley & Wilson 1994), but reject HD211835 (HIP110177, B3:Ve; e.g., Crampton 1968), HD215304 and HD213421 (HIP112215, A1V, and HIP111106, Ap, respectively; Crawford & Warren 1976). Only 1 of the 4 (HD209961, HIP109082, B2V) spectroscopic binaries discussed by van Albada & Klomp (1969) is selected. Several other studies have put forward 'special' candidate members (e.g., Crawford 1961; Slettebak, Bahner & Stock 1961; Adelman 1968; Kodaira, Greenstein & Oke 1970; Levato & Abt 1976; Guetter 1976; Malaroda 1981; Garmany & Stencel 1992): we confirm membership of the emission-line star HD216851 (HIP113226, B3V:n), the shell star HD213801 (HIP111337, B9V), and the red supergiants HD213310 and HD216946 (HIP111022, M0II, and HIP113288, K5Ibvar, respectively). We do not confirm most candidate members with peculiar and/or mag-

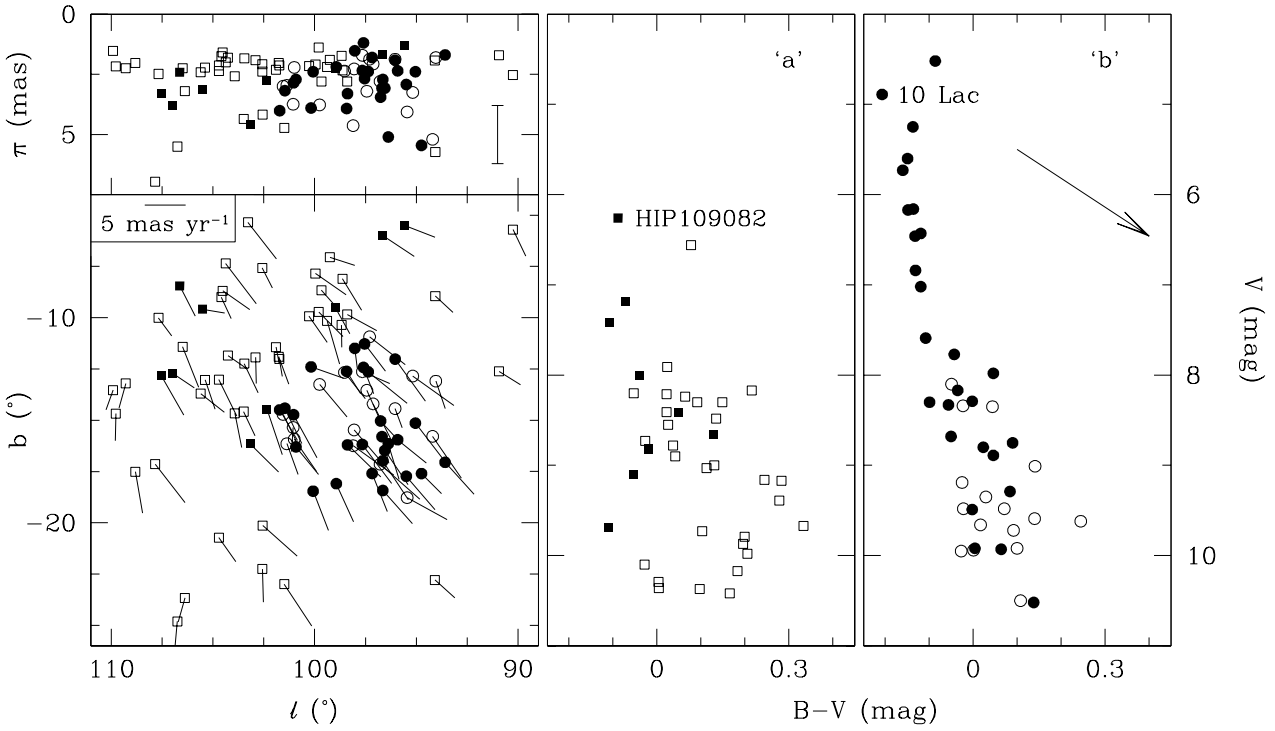

Figure 21: Left: positions and proper motions (bottom) and parallaxes (top) for the 96 Lacerta OB1 members. Circles (27 filled: OB stars; 18 open: later-type) indicate stars inside the circle with radius 5° centered on $(\ell, b) = (97.^\circ0, -15.^\circ5)$, subgroup 'b'. Squares (9 filled: OB stars; 42 open: later-type) denote stars outside the circle, subgroup 'a'. Middle: color-magnitude diagram, not corrected for reddening, for subgroup 'a'. Twelve stars (the star without a spectral type, the carbon star, all 3 M-, and 7 of the 8 K stars) have $B-V > 0.^m4$. Right: similar diagram for subgroup 'b'. HIP113145 (A2) and HIP113237 (K2) have $B-V > 0.^m4$, and are not shown.

netic spectra. The very metal-poor horizontal branch star candidate member BD+39 4926 (HIP112418, B8) has a negative parallax.

Our field (Table A1) comprises the classical subgroups 'a' and 'b'. Fourteen of the 17 O–B5 members lie in subgroup 'b', which for convenience we represent as a circle centered on $(\ell, b) = (97.^\circ0, -15.^\circ5)$ with radius 5° (Figure 21). The corresponding color-magnitude diagram also confirms the existence of 'b'. The main sequence is narrow, and indicates that the effects of differential reddening are small. The deviating star at the bright end of the main sequence is 10 Lac. Although it is a spectral-type standard, it is well-known for its peculiar properties (e.g., Lamers et al. 1997). The brightest member is an evolved star (HIP111104, B2IV).

Based on Hertzsprung–Russell diagrams and photometric distances, several authors have concluded that most A-type stars observed in the direction of Lacerta are not main-sequence association members (e.g., Seyfert & Hardie 1957; Howard 1958; but see Coyne, Burley–Mead & Kaufman 1969 and Weaver 1970), although most studies were incomplete at the visual magnitude of ∼A0V stars (e.g., Guetter 1976). The Hipparcos A-type members show a nearly uniform distribution on the sky. The ∼25 expected A-type interlopers, the lack of structure in the color-magnitude diagram, and the presence of only a few B stars in subgroup 'a', make its existence unlikely.

We find a mean distance of 368±17 pc for all 96 members, and 358±22 pc for the 45 stars in subgroup 'b'. These values are significantly smaller than most previous distance estimates, including the classical value given by Ruprecht (1966; cf. Table 1). We suspect that this is caused by the significant modification of the list of members.

8.2. Cepheus OB2

Pre-Hipparcos: The association Cep OB2 was discovered by Ambartsumian (1949). Later investigations (Morgan et al. 1953; Schmidt 1958; Ruprecht 1966; Humphreys[8] 1978; Keller 1970) confirmed its existence. The most detailed study to date is by Simonson (1968), who identified 75 bright members, including the runaway O6Iab star λ Cep (HIP109556), which we adopt as the classical members. The clusters NGC7160 and Trumpler 37 (Tr 37), with its associated HII region IC1396 (Patel et al. 1995), have similar distances as Cep OB2, ∼800 pc. Simonson & van Someren Greve (1976) suggested the division of Cep OB2 into two subgroups. One of these is Tr 37, with O6 as the earliest main-sequence member, one of the

[8] HD207306 in Humphreys' list has wrong coordinates; we suspect the correct entry should be HD207308. HD207538 is listed twice.

youngest known open clusters, with an age of 3–7 Myr (e.g., Marschall, Comins & Karshner 1990). However, its diameter of ∼40 pc suggests that Tr 37 is gravitationally unbound (e.g., Kun 1986). Garrison & Kormendy (1976) suggested that the bright star μ Cep (HIP107259; M2Ia) is a member of Tr 37. The main source of excitation of IC1396 is the O6 star HIP106886, which is a Trapezium-like system (e.g., Stickland 1995; Schulz, Berghöfer & Zinnecker 1997). IC1396 and neighbouring areas contain, besides a large number of Hα emission objects, most likely T Tauri stars (e.g., Kun 1986; Kun & Pásztor 1990; Balázs et al. 1996), several globules, possibly containing embedded young stellar objects (e.g., Duvert et al. 1990; Schwartz, Gyulbudaghian & Wilking 1991). The other subgroup is older, ∼10 Myr, consistent with the large number of evolved massive stars which are spread over a large area, and contains NGC7160. This subgroup is surrounded by a 9°-diameter infrared emission ring (Figure 22), which possibly resulted from a supernova explosion (Kun, Balázs & Tóth 1987). This supernova might have triggered star formation in this ring, as suggested by the presence of several HII regions, and a number of infrared sources which have the characteristics of embedded young stellar objects (Balázs & Kun 1989).

New results: We select 76 members, 1 O, 56 B, 10 A, 5 F, 1 G, 2 K, and 1 M-type, in the Cep OB2 field (Table A1 and Figure 22). The mean distance of Cep OB2 is 615±35 pc, making it the most distant association for which the Hipparcos measurements allow kinematic member selection (Table 2). All members with spectral type F or later have no luminosity class information or are (super)giants. Most of these may well be interlopers (Table A2). Of the 75 stars selected as Cep OB2 members by Simonson (1968), 61 are contained in the Hipparcos Catalogue. We select 20 of these as secure member, and also confirm the physical relation of the clusters Tr 37 and NGC7160 with Cep OB2. Neither μ Cep nor HIP106886 are selected as members. However, HIP106886 is physically connected to IC1396 and definitely belongs to Tr 37 and thus Cep OB2; our result may be affected by the multiple nature of this object. Most of the members around NGC7160 are evolved massive stars (Figure 22) supporting the claim that this part of the association is older than Tr 37 where no evolved stars are selected.

Besides the two classical subgroups we find one other clump at $(\ell, b) \sim (102\overset{\circ}{.}0, -1\overset{\circ}{.}5)$. The mean parallax for this clump, $\langle\pi\rangle = 1.6 \pm 0.3$ mas, is similar to that of all members, $\langle\pi\rangle = 1.9 \pm 0.1$ mas. It lies outside the Cepheus ring as well as outside the classical Cep OB2 field (Ruprecht 1966). Six of the 11 stars in the clump have radial velocities, taken from the Hipparcos Input Catalogue, of ~ -20 km s^{-1}, similar to the other Cep OB2 members, whereas 5 stars, HIP109996 (B1II), 110362 (B0.5IV:n), 110431 (F2Ib), 110504 (G8Ia var), and 111071 (B0IVn), have large radial velocities, $v_{\rm rad} < -67$ km s^{-1}. These are, in fact, classical members of Cep OB1 at ∼3.6 kpc (Ruprecht 1966; Humphreys 1978). We have omitted them from the list in Table C1. Fifteen other stars in the field $96° < \ell < 108°$ and $-5° < b < 0°$ have radial velocities $v_{\rm rad} < -50$ km s^{-1}; 9 of these are also classical Cep OB1 members. Selection of some Cep OB1 members as Cep OB2 members can partly be explained because the associations have similar projected kinematics: for distant objects, the observed proper motion is determined by differential Galactic rotation only and is, to first order, independent of distance. However, the radial velocities vary linearly with distance. Thus, Cep OB1 and Cep OB2 members have similar proper motions, but different radial velocities. Furthermore, some of the Cep OB1 members have observed parallaxes which are both consistent with the distance of Cep OB1 (∼0.3 mas) as well as Cep OB2 (∼1.8 mas).

The color-magnitude diagram of Cep OB2 (Figure 22) shows a broad main-sequence, with a number of evolved stars located at its tip, as expected. The width of the main sequence, as well as its overall shift towards positive $B-V$, indicates that (foreground) reddening is significant. The earliest spectral type suggests an age of ∼5 Myr. A more accurate age determination will be possible once intermediate band photometry is available for all members.

8.3. Cepheus OB3

Blaauw, Hiltner & Johnson (1959) made the first detailed photometric investigation of the association Cep OB3. They found 40 early-type members at ∼725 pc. Blaauw (1964a) found evidence for two subgroups, with ages of 4 and 8 Myr. Several photometric studies (Crawford & Barnes 1970; Garrison 1970; Jordi, Trullols & Galadí–Enríquez 1996) refined the Blaauw et al. membership list and extended it to fainter stars. Garmany (1973) suggested an expansion age of 0.72 Myr, based on the relative motion of the two subgroups. A detailed summary of all previous membership studies was given by Jordi et al. (1996), who obtained ages of 5.5 and 7.5 Myr for the two subgroups. Simonson & van Someren Greve (1976) found an expanding HI shell centered on the young subgroup in Cep OB3, but did not detect significant HI associated with the older subgroup. Sargent (1977, 1979) found several clumps in the Cep OB3 molecular cloud. Some of these, Cep A and Cep F, show signs of recent star formation (Hughes 1988). Cep B, the hottest CO component, is located closest to Cep OB3. The interaction of the early-type stars and the molecular cloud is clearly visible as the HII region S155. Elmegreen & Lada (1977) considered Cep OB3 as one of the examples of sequential star formation. Panagia & Thum (1981) suggested that the younger subgroup of Cep OB3 originated from the Cep B/S155 complex. Testi et al. (1995) presented evidence for young stars embedded in the Cep B cloud.

Seventeen of the 40 Cep OB3 members compiled by Blaauw et al. are contained in the Hipparcos Catalogue. Figure 23 shows that there is some evidence for two subgroups with a small difference in the magnitude of their mean proper motions. However, our selection procedure is

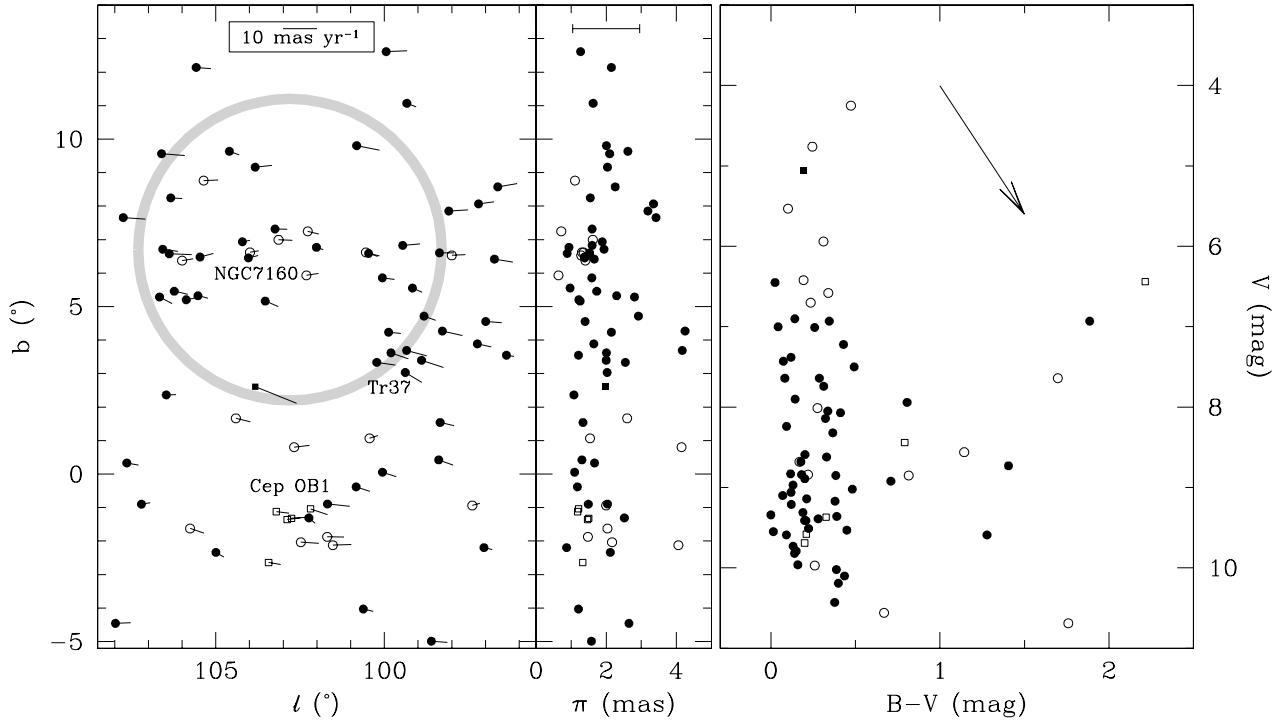

Figure 22: Positions and proper motions (left), parallaxes (middle), and color-magnitude diagram, not corrected for reddening (right), of the Cepheus OB2 members. Filled circles denote members with luminosity classes IV, V and undefined. Open circles denote stars with luminosity classes I, II and III. The filled square indicates the runaway O star λ Cep. The gray circle represents the Cepheus ring. The approximate position of Cep OB1 is indicated. The 5 open squares denote Cep OB1 members (see §8.2).

unable to identify a moving group in this field.

8.4. Cepheus OB4

Cep OB4 was discovered by Blanco & Williams (1959), who noticed the presence of 16 early-type stars in a small region, including the cluster Berkeley 59. Cep OB4 is related to a dense, irregular absorption cloud containing several emission regions, including the dense HII region S171 (e.g., Herschel 1833; Lozinskaya, Sitnik & Toropova 1987). A detailed description of the association and related objects was given by MacConnell (1968). He identified 42 members earlier than B8 at ∼845 pc. Furthermore, he found 11 Hα emission-line objects within the dark cloud, some of which may be T Tauri stars (e.g., Cohen & Kuhi 1976). Based on the absence of supergiants, an earliest spectral type of O7V, and the gravitational contraction time of a B8 star, he estimated an age between 0.6 and 6 Myr.

Lozinskaya et al. (1987) found two expanding shells in Cep OB4: one shell, of radius ∼0.°7, connects NGC7822 and S171. Most Cep OB4 members are located inside this shell; their energy input into the interstellar medium can account for its observed size and expansion velocity of ∼10 km s^{-1}. The other shell, of radius ∼1.°5, is centered on S171 and has an expansion velocity of ∼30–40 km s^{-1}; it may be the result of a supernova explosion or of the stellar wind of a massive star which so far has escaped detection.

Only 19 of the 42 classical members of Cep OB4 are listed in the Hipparcos Catalogue (Figure 24). We suspect this is caused by a combination of crowding effects and the large extinction towards Cep OB4, $A_V \gtrsim 3^{\rm m}$ (MacConnell 1968). Based on their proper motions and parallaxes, three MacConnell stars (HIP117724, 118192, 118194) are not associated with Cep OB4. The parallaxes of the other classical members are consistent with a distance of 800–1000 pc. Our member selection procedure fails to detect the association.

8.5. Cepheus OB6

New results: Hoogerwerf et al. (1997) reported the discovery of a new moving group in the Cepheus region, based on a subset of the Hipparcos Catalogue. Here we use all stars in the Catalogue in the field $100° < \ell < 110°$ and $-4° < b < 3°$ to examine this moving group in more detail. A poor sampling of this group can be expected as it was not part of our (or any other) 1982 proposal to the Hipparcos Input Catalogue (§2.2). We started by applying the Spaghetti method, and found a significant peak in velocity space at $(U, V, W) = (-14.00, -28.58, -5.67)$ km s^{-1}. We then searched for stars consistent with this velocity and corresponding convergent point, and found 27 co-movers. These showed a modest central concentration at $(\ell, b) \sim (104.°0, -0.°5)$. We therefore changed the field to $100° < \ell < 110°$

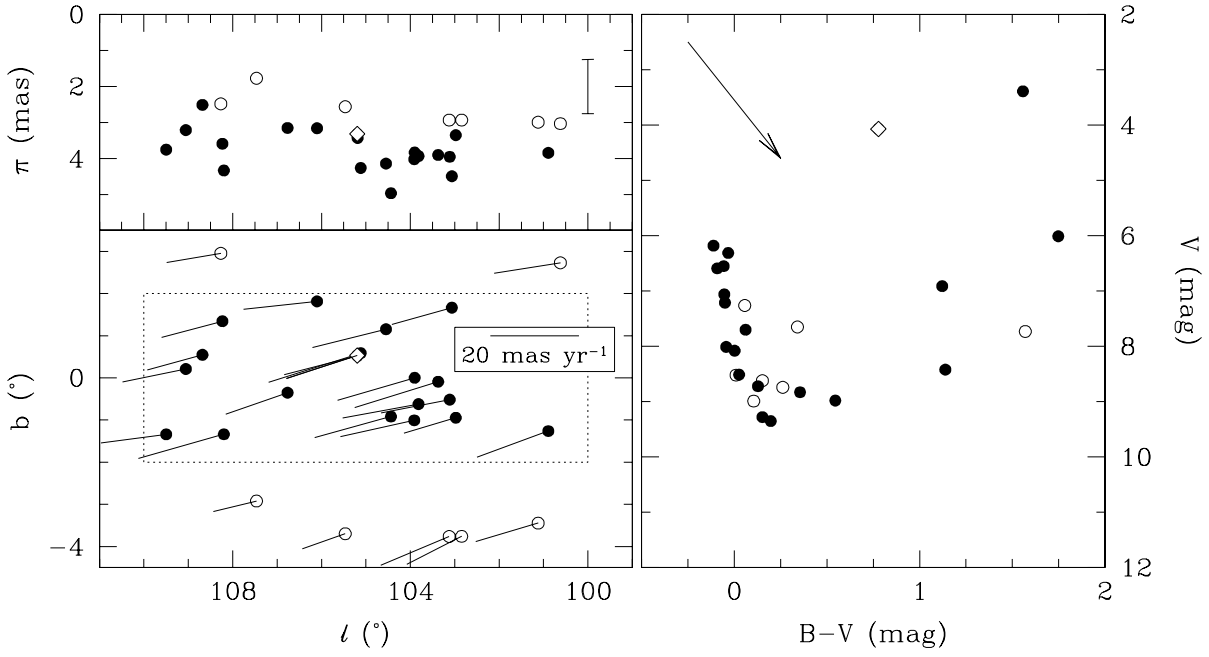

Figure 25: Left: positions and proper motions (bottom) and parallaxes (top) for the new moving group in Cepheus, which we call Cepheus OB6. Right: color-magnitude diagram, not corrected for reddening. Open circles denote stars which are kinematically selected to belong to Cep OB6 but fall outside the area $100^\circ < \ell < 110^\circ$ and $-2^\circ < b < 2^\circ$. The filled circles represent 20 members of Cep OB6. The open diamond denotes δ Cep.

and $-2^\circ < b < 2^\circ$ (Figure 25). This resulted in 20 members: 6 B, 7 A, 1 F, 2 G, 3 K-type, and 1 star without spectral classification. Eleven of these have no luminosity class information, one is a main-sequence star, while the remaining 8 are classified as giants. The brightest member is the K1Ibv supergiant ζ Cep (HIP109492). We expect only a few interlopers (Table A2). The color-magnitude diagram is very narrow and strengthens the evidence that these stars form a moving group. We suspect it is an old OB association: the earliest spectral type is B5III, suggesting an age of ∼50 Myr. We provisionally refer to this group as Cep OB6.

One of the red supergiants in Cep OB6 is HIP110991, the prototype classical Cepheid δ Cep. Its parallax, $\pi = 3.32 \pm 0.58$ mas (301^{+64}_{-45} pc), is consistent with the mean distance of Cep OB6 of 270±12 pc. Previous distance estimates of δ Cep agree well with the mean distance of Cep OB6, e.g., 240±24 pc (Mourard et al. 1997), 2.80 ± 0.96 mas (Gatewood, de Jonge & Stephenson 1993), 246±14 pc (Fernley, Skillen & Jameson 1989), and 290±17 pc (Gieren, Barnes & Moffett 1993).

8.6. Cygnus OB4

Membership of the association Cyg OB4 was studied by Morgan et al. (1953), Ruprecht[9] (1966) and Humphreys (1978). All three quote the same distance of 1 kpc, originally derived by Morgan et al., based on photometric distances of 4 luminous members: 3 main sequence stars earlier than B1, and the B9Iab supergiant σ Cyg. All 4 stars are included in the Hipparcos Catalogue and have parallaxes of ∼1 mas, consistent with the distance estimate of 1 kpc. However, Figure 26 shows no evidence of common motion: the proper motions differ considerably in magnitude. It also shows that it is impossible to make any kinematic member selection based on the Hipparcos measurements.

8.7. Cygnus OB7

Based on a survey of bright stars by Hiltner (1956), Schmidt (1958) put Cyg OB7 on the list of associations, and derived a distance of 740 pc. Subsequent studies by Schmidt–Kaler (1961), Ruprecht (1966) and Humphreys (1978) resulted in a list of 18 stars associated with Cyg OB7, located in a field of $12^\circ \times 14^\circ$. The dark cloud Kh141 (Khavtassi 1960), 'the Northern Coalsack', lies in the middle of the Cyg OB7 field, at a distance of ∼400 pc. It contains several T Tauri stars. Continuum sources seen projected onto the cloud are most likely HII regions behind the cloud complex (Simonson & van Someren Greve 1976).

The Hipparcos parallaxes and proper motions for 17 of the 18 classical Cyg OB7 members do not show evidence of common motion (Figure 26). As for Cyg OB4, we do not detect a moving group. However, the line of sight towards Cygnus runs parallel to the local spiral arm. Some of the previous claims for OB associations based on large numbers of supergiants and/or early-type stars in this di-

[9] Ruprecht's list contains a typographical error: HD201349 should be HD202349.

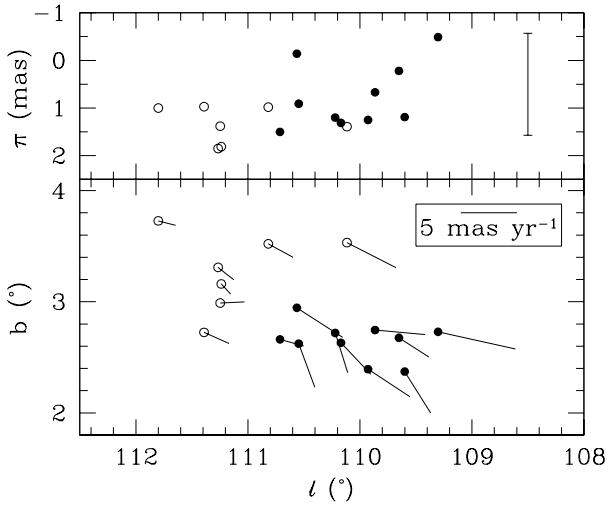

Figure 23: Positions and proper motions (bottom) and parallaxes (top) of the classical Cepheus OB3 members contained in the Hipparcos Catalogue (Blaauw et al. 1959). The open circles show the classical members of the older subgroup of Cep OB3, and the filled circles indicate the younger subgroup.

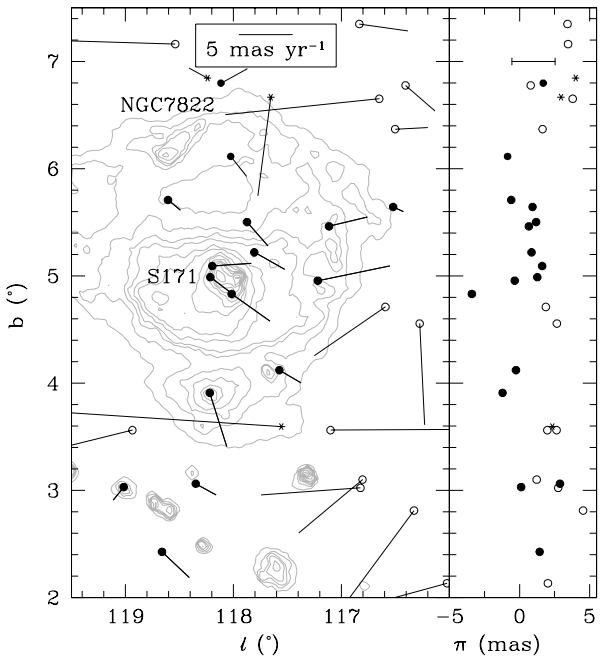

Figure 24: Positions and proper motions (left) and parallaxes (right) of the early-type stars in the Cepheus OB4 region. The Cep OB4 members as found by MacConnell (1968) are indicated by filled circles. The three asterisks are MacConnell members which, based on their proper motion or parallax, do not belong to Cep OB4. Open circles are the remaining stars earlier than A0, with $\pi < 5$ mas. The gray contours show the IRAS 60μm flux.

rection, e.g., Cyg OB4 and Cyg OB7, may therefore be the result of chance projections.

8.8. *Scutum OB2*

The first reference to the association Sct OB2 is by Ambartsumian (1949), who estimated a distance of 1250 pc, and suggested a possible physical connection to the open cluster NGC6705 (Meurers & Mikulitsch 1968). In his catalog of OB associations, Schmidt (1958) gave a distance of 730 pc. Ruprecht (1966) listed 6 photometric members (cf. Keller 1970). Humphreys (1978) found another 10 photometric members, and derived a distance of ∼1000 pc based on 4 stars. Reichen et al. (1990) found 17 photometric members, and suggested the presence of two groups: one at 510 pc (3 stars), the other at 1170 pc (14 stars). Of the combined list of 29 classical members, 9 are included in the Hipparcos Catalogue.

Figure 27 shows all O–B5 stars observed by Hipparcos in the field $15° \leq \ell \leq 30°$, $-7° \leq b \leq 4°$. Most stars have parallaxes $\pi \lesssim 2$ mas; only 3 of the 62 stars have $\pi \geq 5$ mas. No kinematic signature of Sct OB2 is evident.

9. MEAN DISTANCES AND MOTIONS

We postpone a full investigation of the physical properties of the nearby associations and their members, and the implications for scenarios for the formation of the Solar neighbourhood, to a future investigation. Here we limit ourselves to a derivation of the mean distances and mean space motions, present an improved map of the nearby associations (Figure 29), and discuss the kinematics of the Gould Belt.

9.1. *Mean distances*

We have derived the mean distances to all associations and subgroups for which our kinematic selection method has identified members in the Hipparcos Catalogue. The mean distances are derived from the mean parallax of the secure members, and are corrected for the bias introduced by discarding stars with negative parallaxes in the member selection (§3.6 and Appendix B). The results are summarized in Table 2, where we give the mean distance determined for the early- and late-type members separately (specified in Table A1), and for the entire set of members. The errors are derived from the formal errors in the mean parallaxes. We adopt as the best estimate of the mean distance, underlined in Table 2, the value derived for all members, except for Vel OB2, Tr 10, Col 121 and Per OB2 for which we only consider the early-type members. In these groups the number of selected late-type stars is similar to the expected number of interlopers.

Figure 28 compares the resulting distances to the distances in Table 1, which are taken from a variety of sources. These generally are not the most recent (or best) values, but are the most widely used, and are mostly based on early calibrations of M_V versus spectral type for upper main-sequence stars. The open triangles are the Hipparcos mean distances, uncorrected for the bias described above. The open circles include this correction, $D_{\rm sys}$, which is

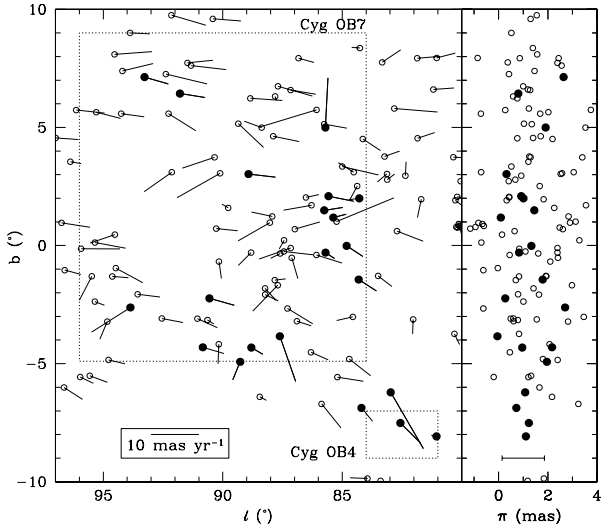

Figure 26: Positions and proper motions (left) and parallaxes (right) of the classical Cygnus OB4 (Ruprecht 1966) and Cygnus OB7 (Schmidt–Kaler 1961; Ruprecht 1966; Humphreys 1978) members (filled circles). The open circles represent all stars earlier than B5, with parallaxes $\pi < 4$ mas. The dotted lines indicate the association boundaries given by Ruprecht. Two of the classical Cyg OB4 members fall outside the field. The lack of stars around $(\ell, b) \sim (92\overset{\circ}{.}5, 2\overset{\circ}{.}0)$ is due to the foreground dark cloud Kh141 (see §8.7).

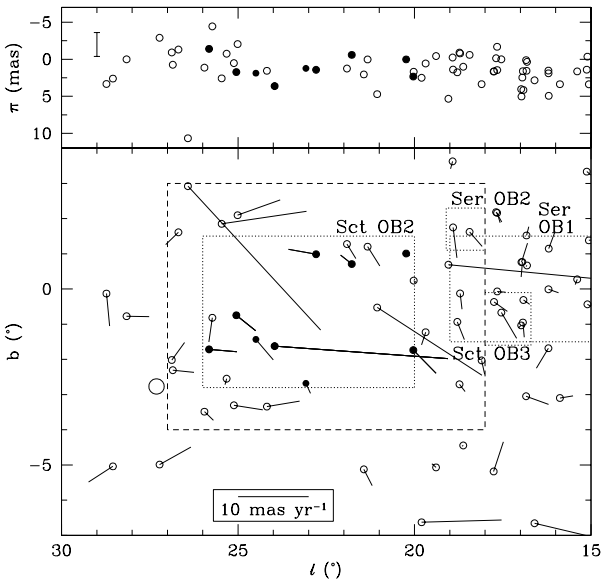

Figure 27: Positions and proper motions (bottom) and parallaxes (top) of all Hipparcos O–B5 stars (17 O; 45 B0–B5) in and around the Scutum OB2 field. Filled circles denote 9 classical photometric Sct OB2 members (see §8.8). The large circle denotes the open cluster NGC6705. The dashed rectangle denotes our Sct OB2 field. The dotted rectangles refer to the IAU boundaries of all OB associations in the field (Ruprecht 1966): Ser OB1: $D = 1.7$ kpc, Ser OB2: $D = 2.0$ kpc, Sct OB3: $D = 1.6$ kpc.

based on our Monte Carlo simulations (§3.6). $D_{\rm sys}$ is negligible for the nearest associations, but changes the distance estimate by ∼15 per cent for Col 121 and Cep OB2. With the exception of Lac OB1 (cf. §8.1), the pre- and corrected post-Hipparcos distances are correlated remarkably tightly, with the latter showing a modest systematic offset towards smaller distances. This tight relation is perhaps surprising at first, as in many cases our kinematic member selection method has halved the number of classical members, while at the same time at least tripling the total number of members. However, the early distance estimates were often based on a few of the brightest stars, and these have in most cases been confirmed as members.

A small systematic offset in distance modulus may have a number of reasons, the improved member lists being one (especially for the more distant associations). Another possibility is that the correction for interstellar extinction is inaccurate, perhaps caused by local variations in the value of the ratio R of total to selective extinction. We suspect however that the principle reason for the discrepancies is likely to be found in the calibration of the upper main sequence, which is based to a large extent on the bright members of the nearest associations (e.g., Blaauw 1956). Hipparcos parallaxes for individual stars, and for open clusters, have given similar indications that stars on the upper main sequence may be a few tenths of a magnitude fainter than assumed previously (cf. Lamers et al. 1997; Mermilliod et al. 1997). This is not surprising, as the classical calibration is based on a patching together of the upper main sequences of nearby young groups — including many of those studied here. The short lifetimes of the most massive stars make it likely that the calibration stars have evolved away from the zero-age main sequence, so that they are a little brighter than a main-sequence star of similar spectral type. A more quantitative investigation of the calibration of the upper main sequence requires homogeneous spectral types and intermediate band photometry, and is beyond the scope of this paper.

9.2. Mean motions

Table 2 also lists the mean proper motions of the kinematically selected nearby OB associations. The means are based on the individual measurements for all secure members, except for Vel OB2, Tr 10, Col 121 and Per OB2, for which they are based on the early-type members only (as in §9.1). The errors are the formal errors on the mean. The Hipparcos Input Catalogue lists radial velocities from a variety of sources. They are not available for all secure association members, and we therefore list the median radial velocity in Table 2, and do not attach an error estimate to it. The Spaghetti method predicts a mean radial velocity for each moving group based on the positions, proper motions and parallaxes of the members (§3.2). The uncertainties on these predicted values are considerable, and all we can conclude is that they are consistent with the measured median values.

We have derived the mean space motions of the nearby

Table 2. Mean distances and mean motions of the OB associations

Name	$D_{\rm early-type}$	N	$D_{\rm late-type}$	N	$D_{\rm all}$	N	$D_{\rm sys}$	$\langle\mu_\ell\cos b\rangle$	$\langle\mu_b\rangle$	$v_{\rm rad}$
Upper Scorpius	144 ± 3	83	148 ± 5	37	$\underline{145}\pm 2$	120	0	-24.5 ± 0.1	-8.1 ± 0.1	-4.6
Upper Centaurus Lupus	142 ± 2	134	137 ± 3	87	$\underline{140}\pm 2$	221	0	-30.1 ± 0.1	-9.1 ± 0.1	4.9
Lower Centaurus Crux	116 ± 2	97	120 ± 2	83	$\underline{118}\pm 2$	180	0	-32.1 ± 0.1	-13.1 ± 0.1	12.0
Vela OB2	$\underline{410}\pm12$	87	435 ± 45	6	411 ± 12	93	20	-10.4 ± 0.1	-1.3 ± 0.1	18.0
Trumpler 10	$\underline{366}\pm23$	22	558 ± 238	1	372 ± 23	23	13	-14.3 ± 0.2	-4.9 ± 0.2	21.0
Collinder 121	$\underline{592}\pm28$	87	389 ± 39	16	543 ± 23	103	74	-5.1 ± 0.1	-1.5 ± 0.1	26.0
Perseus OB2	$\underline{318}\pm27$	17	282 ± 21	24	296 ± 17	41	8	8.4 ± 0.2	-2.3 ± 0.3	20.1
α Persei	185 ± 5	30	173 ± 5	49	$\underline{177}\pm 4$	79	1	33.5 ± 0.1	-8.7 ± 0.1	-1.0
Lacerta OB1	364 ± 22	36	371 ± 23	60	$\underline{368}\pm17$	96	14	-2.3 ± 0.1	-3.4 ± 0.1	-13.3
Cepheus OB2	624 ± 42	54	588 ± 62	17	$\underline{615}\pm35$	71	84	-4.1 ± 0.1	-0.5 ± 0.1	-21.4
Cepheus OB6					$\underline{270}\pm12$	20	4	15.9 ± 0.2	-4.4 ± 0.2	-20.0

Note. — All distances, in pc, include a correction $D_{\rm sys}$ for systematic effects as described in §3.6 and Appendix B. The first column lists the association. The second column contains the mean distance and error on the mean distance of the early-type members (cf. Table A1), and the third column gives the number of early-type members identified by our selection procedure. Columns 4–5 and 6–7 give the mean distance and corresponding number of late-type and all (early- plus late-type) members, respectively. We adopt as *the* distance D to the associations the underlined distances; default is the value derived for all members, except for Vel OB2, Tr 10, Col 121 and Per OB2 (§9.1). Column 8 gives the systematic correction $D_{\rm sys}$, in pc, that is included in the underlined distance estimate. Columns 9 and 10 list the average proper motions in the directions of Galactic longitude and latitude, and the formal errors on the mean in mas yr^{-1} for all secure members which were used in the determination of the underlined distances. Column 11 contains the median radial velocity in km s^{-1} compiled from the Hipparcos Input Catalogue for the same stars. Due to its large physical size and unknown orientation, the Cas–Tau association (§7.2) cannot be represented adequately by a single mean distance, proper motion, and radial velocity, and has hence been excluded from this table.

OB associations in km s^{-1} from the mean proper motions, mean distances, and the median radial velocities. We also determined values for the OB stars in Ori OB1 although we used an *ad hoc* selection procedure (§6.4). The Ori OB1 radial velocity of 23.0 km s^{-1} is taken from Morrell & Levato (1991), while the mean proper motion $\langle\mu_\ell\cos b\rangle = 0.8$ mas yr^{-1}, $\langle\mu_b\rangle = 0.1$ mas yr^{-1} corresponds to the mean proper motion in equatorial coordinates as given in eq. (8). Figure 29 shows the result, after subtraction of Solar motion (Dehnen & Binney 1998) and differential Galactic rotation (Feast & Whitelock 1997). Some of the associations in Figure 29 seem to fit a coherent pattern of expansion and rotation, which is very similar to that derived by Lindblad et al. (1997; their figure 4) and Torra et al. (1997) from Hipparcos measurements of OB stars with ages less than ∼30 Myr. This large-scale kinematic feature is known as Gould's Belt, which is the flat system of early-type stars within ∼500 pc (Gould 1874), associated with a large structure of interstellar matter, including reflection nebulae, dark clouds, and HI. Its most striking feature is a tilt of ∼18° with respect to the Galactic plane. We refer the reader to Pöppel (1997) for a comprehensive review of this structure, with emphasis on the role and characteristics of the interstellar medium.

Following a suggestion by Blaauw (1965), who studied the mean space motions of the nearby OB associations, Lindblad (1967) interpreted the observations of the local HI gas ('feature A') associated with Gould's Belt in terms of a ballistically expanding ring. Subsequent kinematic models combined with new observations confirmed this picture (e.g., Lindblad et al. 1973; Elmegreen 1982; Olano 1982). However, these models seem inadequate for a description of the space motions of the clumpy distribution of early-type stars, as no unique expansion center and/or expansion age can be defined for them (e.g., Blaauw 1965; Lesh 1968, 1972; Stothers & Frogel 1974; Frogel & Stothers 1977; Westin 1985; Comerón & Torra 1994). The lack of a homogeneous set of accurate radial velocities for all local early-type stars prevents an optimal exploitation of the Hipparcos data, and a full kinematic model is not yet available. Even so, we can use the mean motions of the OB associations to shed light on the systemic motions in the Gould Belt.

The associations Sco OB2, Ori OB1, Per OB2, and Lac OB1 are thought to be components of the Gould Belt (e.g., Olano 1982). The pattern displayed in Figure 29 seems to be shared by Tr 10, and perhaps also by Vel OB2 and Col 121, suggesting that these may all belong to the same coherent structure. The new distance of Lac OB1 reduces the extent of the Belt in the direction $\ell\sim90°$. Cep OB2 is not located in the plane of the Belt, and its motion is parallel to the Galactic plane. We conclude that it does not seem to belong to the Belt. The Cas–Tau complex which surrounds the α Persei cluster and shares its motion, as well as Cep OB6, are located inside the main ring of associations, have a different space motion, and are both significantly older at ∼50 Myr.

10. SUMMARY AND FUTURE WORK

10.1. Main conclusions

We have carried out a comprehensive census of the stellar content of the known OB associations within 1 kpc from the Sun (Table 1), based on the globally accurate Hipparcos positions, proper motions and parallaxes. We

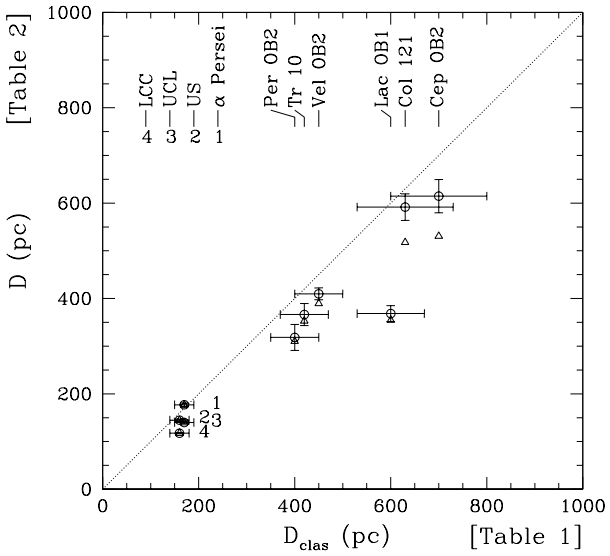

Figure 28: Distances D derived from the mean parallax of the Hipparcos members of the OB associations (Table 2) versus the classical distances $D_{\rm clas}$ (Ruprecht 1966; Table 1), open circles. For three associations $D_{\rm clas}$ was taken from another source: Col 121 (Feinstein 1967), Vel OB2 (Brandt et al. 1971) and Tr 10 (Lyngå 1959, 1962). The distances D have been corrected for systematic effects due to our selection procedure and the Hipparcos completeness limit (§3.6 and Appendix B). The open triangles indicate the distances *uncorrected* for these systematic effects.

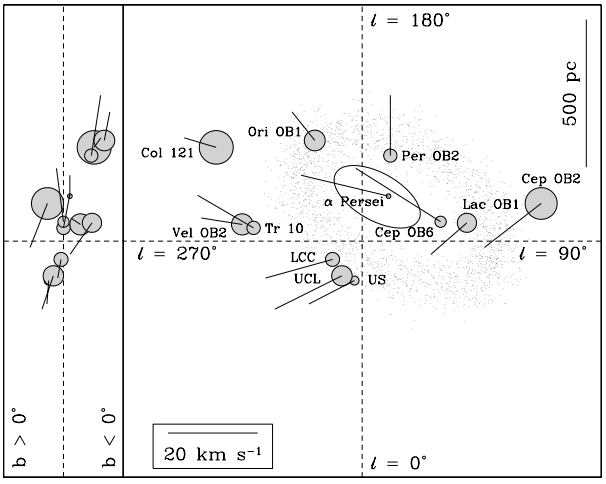

Figure 29: Locations of the kinematically detected OB associations projected onto the Galactic plane (right) and a corresponding cross section (left) (cf. Figure 1). The gray circles indicate the physical dimensions as obtained from the angular dimensions and mean distances, on the same scale. The lines represent the streaming motions, derived from the average proper motions, mean distances and median radial velocities of the secure members, corrected for 'standard' Solar motion and Galactic rotation (see §9.2). The ellipse around the α Persei cluster indicates the Cas–Tau association. The small dots schematically represent the Olano (1982) model of the Gould Belt.

have used a combination of de Bruijne's (1998) refurbished convergent point method and the 'Spaghetti method' of Hoogerwerf & Aguilar (1998) to search for moving groups in fields along the Galactic plane centered on nearby OB associations. The selection procedure is objective and reliable. Monte Carlo simulations provide an estimate of the expected number of interlopers. The resulting census significantly improves the description of the ensemble of OB associations in the Solar neigbourhood.

We have found a clear kinematic signature of a moving group in twelve cases, all at distances less than 650 pc. These are the three subgroups Upper Scorpius, Upper Centaurus Lupus, and Lower Centaurus Crux of Sco OB2, Vel OB2, Tr 10, Col 121, Per OB2, α Persei (Per OB3), Cas–Tau, Lac OB1, Cep OB2, and a new group in Cepheus, which we have designated as Cep OB6. Astrometric evidence for moving groups in the fields of R CrA, CMa OB1, Mon OB1, Ori OB1, Cam OB1, Cep OB3, Cep OB4, Cyg OB4, Cyg OB7, and Sct OB2 is inconclusive. Previous photometric and spectroscopic studies indicate that many of these are physical groups, but they are either at distances where the Hipparcos parallaxes are of limited use and the number of members bright enough to be included in the Hipparcos Catalogue is small, or they have unfavorable kinematics, so that the group proper motion does not stand out from that of the field stars in the Galactic disk (e.g., Ori OB1).

Our member selection procedure has extended the firmly established kinematic members of the nearby OB associations to fainter magnitudes than before. The previously established member lists for the earliest spectral types have been corrected and improved, and many members with later spectral type have been added. These include evolved giants and supergiants, amongst which the famous Wolf–Rayet stars γ^2 Vel (WR11) in Vel OB2 and EZ CMa (WR6) in Col 121, and δ Cep in Cepheus OB6. In some cases the new members extend well into the regime of the F dwarfs, which is the range where the stars in these young groups are expected to be in the final pre-main sequence phase. Our list of astrometric members of Sco OB2 indeed contains such objects, providing a direct link between the classical high-mass stellar content, and the lower-mass objects which are still approaching the main sequence. This suggests strongly that the mass functions of all OB associations extend to low masses, so that their individual total masses are likely to be of order a few thousand $M_\odot$ or more.

Six of the moving groups we have detected do not appear in the classical list of nearby OB associations (Table 1; Ruprecht 1966). For Upper Centaurus Lupus and Lower Centaurus Crux this is due to the absence of O stars. Tr 10 and Col 121 were known as open clusters, but we have shown that they are in fact extended moving groups with all the characteristics of unbound OB associations. The sparse group of stars previously known as Vel OB2 has similarly been transformed into a full-fledged association, which is identical to Col 173, and to the young

stellar group postulated by Sahu (1992) to explain the observed properties of an IRAS shell in this region. Cep OB6 is a serendipitous discovery in our Cep OB2 field, and is an (old) OB association that was completely overlooked. We have also confirmed the existence of Cas–Tau, which was previously considered as a doubtful association, and shown that it is connected kinematically to the α Persei cluster. Cas–Tau can be considered as an extended halo of α Persei, or the cluster as a bound component in the otherwise unbound complex. It follows that the number of unbound young stellar groups in the Solar neighbourhood may be significantly larger than thought previously, especially those without bright O and early B-type stars. Such groups are older than the classical OB associations, but may well form the missing link between the youngest groups such as Upper Scorpius and Ori OB1, and the old dispersed associations like Cas–Tau and Cep OB6.

The measured distances of the associations, based on the mean Hipparcos parallaxes of the astrometric members, and corrected for the known biases (§9.1), are systematically smaller than the previous photometric determinations. Whereas part of this effect must be caused by the much improved membership lists, especially for the more distant groups, we suspect that the upper main sequence may be a few tenths of a magnitude fainter than assumed previously.

We have used the mean distances of the 12 moving groups to obtain an improved map of the Solar neighbourhood. Together with the mean proper motions, and the median radial motion derived from the radial velocities in the Hipparcos Input Catalogue, this also provides a more reliable description of the motions in the Gould Belt.

Elmegreen (1993) suggested that fragmentation and (the first generation of recent) star formation in the Solar neighbourhood was triggered by the passage of the Carina spiral arm ∼60 Myr ago, and that Cas–Tau is one of the associations that formed in this process. The high-mass stars in Cas–Tau then blew a large bubble which resulted in Lindblad's ring, i.e., the Gould Belt, out of which ∼20 Myr ago the molecular clouds and associations in Scorpio–Centaurus–Lupus–Crux, Orion, Perseus, and Lacerta were formed as the second generation. The present star formation seen in Taurus–Auriga, and in Ophiuchus, is regarded as the third generation. The results of our census are in qualitative agreement with this picture. The traditional boundary between bound open cluster and unbound expanding association is maybe not as clear-cut as is commonly assumed (cf. Elmegreen & Efremov 1998), and the total amount of mass in the young stellar groups may have been underestimated. A reassesment of the star formation history in the Solar neighbourhood is clearly warranted.

10.2. Future work

The discovery of Cep OB6 in our Cep OB2 field suggests that there might be other previously unidentified nearby associations. A systematic search in regions of the strip $-30^\circ \leq b \leq 30^\circ$ not covered in the current study, might reveal such groups. We suspect this will not yield a rich harvest because the sampling of possible members is likely to be sparse. Whereas many candidate members of the known associations were included deliberately in the Hipparcos Catalogue, in particular in the magnitude range where the Catalogue is incomplete, this will generally not be the case in other areas. We have generally ignored the known open clusters. Their membership is well-defined in many cases, and is based on relative proper motions from photographic studies in small fields. The limit on stellar number density of about 3 per square degree results in the Catalogue being significantly incomplete in the areas of open clusters, even for the brightest members. Even so, it is interesting to investigate whether extended halos can be found around other clusters.

We have presented color-magnitude diagrams based on the V and $B-V$ data reported in the Hipparcos catalog, but have not used these data in the member selection. We have also not discussed the physical parameters of the member stars in detail, mostly because the required homogeneous multi-color photometry (and spectral classification) is incomplete (§2.3). Now that the astrometric member selection has reduced the number of candidates in a given field by an order of magnitude, it is relatively straightforward to obtain the missing photometry, and we are carrying out a program to do so. This is particularly interesting in Sco OB2, where the faintest astrometric members can be connected directly to the populations of pre-main sequence objects discovered through X-ray searches. This will provide accurate ages, initial mass functions (Brown 1998), and the energy and momentum input into the interstellar medium, and will allow a detailed investigation of the influence of the young stellar group on the surrounding distribution of gas and dust (e.g., de Geus 1992). The Leiden–Dwingeloo HI survey (Hartmann & Burton 1997) delineates the HI distribution and kinematics with unprecedented accuracy over the entire sky north of $\delta = -30^\circ$. It has already been used to study the shell around Ori OB1 (Brown et al. 1995). It will be interesting to look for similar structures around other nearby associations.

It is highly desirable to complement the uniform astrometric measurements provided by Hipparcos with homogeneous radial velocities with accuracies of ∼3 km s^{-1} or better. While this is relatively easy for spectral types F and later, it is a considerable challenge for earlier spectral types, because of the modest number of suitable spectral lines, the fast stellar rotation, and the large number of spectroscopic binaries (e.g., Verschueren et al. 1997; Brown & Verschueren 1997). An unbiased member selection based only on radial velocities is still impractical, but measurement of the radial velocity of the proper motion members identified here is feasible. This will allow removal of a significant number of remaining interlopers: for a typical measurement error in radial velocity of 3 km s^{-1}, our

Monte Carlo simulations (§3.4) suggest that the expected reduction of the number of interlopers is typically about a factor of 4. We are in the process of obtaining radial velocities for this purpose. These will also provide further information on the distribution of spectroscopic binaries in these groups. The many new astrometric binaries discovered by Hipparcos are also a source for a follow-up study.

The Hipparcos proper motions have an accuracy of $\sim$1 mas yr^{-1}, which corresponds to $\sim$1 km s^{-1} at the distance of Sco OB2. It is natural to ask whether the data can resolve an overall expansion. This has been attempted from the ground for a number of associations, and has led to the derivation of kinematic ages, defined as the time since the group occupied a minimum volume (e.g., Blaauw 1978). However, the relative motion of the Sun with respect to the association also introduces a virtual expansion or contraction in the measured proper motions, and hence unambiguous measurement of internal motions and expansion ages requires radial velocities for all group members that are significantly more accurate than the internal dispersion of the group. Even then, it will not be easy to define an expansion age (Brown et al. 1997). It follows that all previously determined kinematic ages should be considered as provisional.

The Hipparcos parallaxes are not sufficiently accurate to resolve the internal structure of even the nearest associations. This would be interesting, as it might help to delineate substructure, and hence shed light on the details of the star formation process throughout an interstellar cloud. However, it is possible to improve the individual distance estimates further by using the proper motions (and radial velocities) of the established members to compute secular parallaxes (e.g., Dravins et al. 1997).

Hipparcos has provided a much improved description of the ensemble of young stellar groups in the Solar neighbourhood, out to a distance of $\sim$650 pc. Like the Hipparcos Catalogue, the lists of members given in Table C1 are incomplete beyond $V\sim7\overset{\mathrm{m}}{.}3$, and may have excluded a few genuine members (including some long-period binaries) that are brighter (§3.5). Our lists extend to $V\sim10\overset{\mathrm{m}}{.}5$, and include a few pre-main sequence objects in the nearest groups. It is natural to ask whether the member lists can be completed, and extended to even fainter stars, by use of available large-scale ground-based studies which can now be put on the Hipparcos reference system. Unfortunately, the space motions of the young groups are not large, and as a result the proper motions of the group members do not differ very much from those of the field stars except in a few cases, such as the α Persei cluster. For example, if we degrade the vector point diagram for the Upper Scorpius field (Figure 5) to, e.g., the PPM accuracy of 3–4 mas yr^{-1} (Röser & Bastian 1991; Bastian et al. 1993; Röser, Bastian & Kuzmin 1994), the group hardly stands out. Reliable extension of our lists requires proper motions with accuracies of order 2 mas yr^{-1} or better. These are provided by the ACT Catalog (Urban, Corbin & Wycoff 1998) and the TRC Catalogue (Høg et al. 1998), through a combination of the positions in the Astrographic Catalog with the Tycho positions to $V\sim11^{\mathrm{m}}$. The individual stellar positions in these two catalogs have modest accuracy, but the $\sim$80 yr epoch difference results in quite accurate proper motions. The first installment of the ACT and TRC catalogs both contain about 1 million measurements. The completion of the second edition of the Tycho Catalogue (see Høg 1997) will provide proper motions of similar quality for about 2.5 million objects to $V\sim12^{\mathrm{m}}$. The ACT/TRC will also allow us to investigate the astrometric membership for those long-period binaries for which the Hipparcos measurements are suspect (§3.5). However, the 1 mas accuracy parallaxes obtained by Hipparcos play a crucial role in culling interlopers from the membership lists (Figure 4). With few exceptions, such parallaxes are not available for fainter association members. A complete study of all OB associations in the Solar neighbourhood (extent, distance, structure, kinematics) has to await the future GAIA space astrometry mission (e.g., Perryman, Lindegren & Turon 1997; Gilmore et al. 1998).

It is a pleasure to thank Luis Aguilar, Eugène de Geus, Rudolf Le Poole, Jan Lub, Michael Perryman, and Noël Robichon for stimulating discussions and detailed comments on the manuscript. Ernest Stavro Blofeld, Jan Brand, Marijn Franx, Frank Israel, Jan van Paradijs, and Cor de Vries made significant contributions to the 1982 SPECTER proposal. This work has made extensive use of SIMBAD, ADS, and SKYVIEW, and was supported in part by ESA, NWO and the Leids Kerkhoven Bosscha Fonds.

REFERENCES

Abt H.A., Hunter J.H., 1962, ApJ, 136, 381
Abt H.A., Landolt A.U., Levy S.G., Mochnacki S., 1976, AJ, 81, 541
Adelman S.J., 1968, PASP, 80, 329
Adelman S.J., 1973, PASP, 85, 676
Abt H.A., Hunter J.H., 1962, ApJ, 136, 381
Abt H.A., Landolt A.U., Levy S.G., Mochnacki S., 1976, AJ, 81, 541
Adelman S.J., 1968, PASP, 80, 329
Adelman S.J., 1973, PASP, 85, 676
van Albada T.S., Klomp M., 1969, BAN, 20, 208
van Albada T.S., Sher D., 1969, BAN, 20, 204
Alcalá J.M., et al., 1996, A&AS, 119, 7
Alcalá J.M., Chavarría–K. C., Terranegra L., 1998, A&A, 330, 1017
van Altena W.F., Cudworth K.M., Johnston K., Lasker B., Platais I., Russell J.L., 1993, in *Workshop on databases for Galactic structure*, eds A.G.D. Philip, B. Hauck, A.R. Upgren (Schenectady: L. Davis Press), p. 250
Alter G., Ruprecht J., Vanýsek V., 1970, *Catalogue of Star Clusters and Associations, 2nd Edition*, eds G. Alter, B. Balázs, J. Ruprecht (Budapest: Akadémiai Kiadó)
Ambartsumian V.A., 1947, in *Stellar Evolution and Astrophysics*, Armenian Acad. of Sci. (German translation, 1951, Abhandl. Sowjetischen Astron., 1, 33)
Ambartsumian V.A., 1949, Dokl. Akad. Nauk SSR, 68, 22
Ambartsumian V.A., 1954, IAU Trans., 8, 665

Andreazza C.M., Vilas–Boas J.W.S., 1996, A&AS, 116, 21
Artyukhina N.M, 1972, Sov. Astron., 16, 317
Balázs L.G., Kun M., 1989, AN, 310, 385
Balázs L.G., Garibjanyan A.T., Mirzoyan L.V., Hambaryan V.V., Kun M., Frontó A., Kelemen J., 1996, A&A, 311, 145
Barnard E.E., 1927, *A photographic atlas of selected regions of the Milky Way*, Washington: Carnegie Inst.
Bastian U., Röser S., Yagudin L.I., Nesterov V.W., 1993, PPM Star Catalogue III, IV., Heidelberg, Spektrum Akad. Verlag
Becker W., 1963, ZfA, 57, 117
Bertiau F.C., 1958, ApJ, 128, 533
Bijaoui A., Lacoarret M., Granes P., 1981, A&AS, 45, 483
Blaauw A., 1944, BAN, 10, 29
Blaauw A., 1946, *PhD Thesis*, Groningen Univ. (Publ. Kapteyn Astron. Lab., 52, 1)
Blaauw A., 1952a, BAN, 11, 405
Blaauw A., 1952b, BAN, 11, 414
Blaauw A., 1952c, AJ, 57, 199
Blaauw A., 1956, ApJ, 123, 408
Blaauw A., 1958, AJ, 63, 186
Blaauw A., 1960, in *Present Problems Concerning the Structure and Evolution of the Galactic System* (Nuffic Intern. Summer Course, The Hague), 3, p. 1
Blaauw A., 1961, BAN, 15, 265
Blaauw A., 1964a, ARA&A, 2, 213
Blaauw A., 1964b, in *The Galaxy and the Magellanic Clouds*, IAU Symp. 20, eds F.J. Kerr & A.W. Rodgers, p. 50
Blaauw A., 1965, Proc. Royal Neth. Acad. of Sciences, 74, 54
Blaauw A., 1978, in *Problems of Physics and Evolution of the Universe*, ed. L.V. Mirzoyan (Yerevan), p. 101
Blaauw A., 1991, in *The Physics of Star Formation and Early Stellar Evolution*, eds C.J. Lada & N.D. Kylafis, NATO ASI Ser. C, Vol. 342, p. 125
Blaauw A., 1993, in *Massive Stars: Their Lives in the Interstellar Medium*, eds J.P. Cassinelli & E.B. Churchwell, ASP Conf. Ser., 35, p. 207
Blaauw A., van Albada T.S., 1963, ApJ, 137, 791
Blaauw A., van Albada T.S., 1964, preprint
Blaauw A., Morgan W.W., 1953, ApJ, 117, 256
Blaauw A., Morgan W.W., Bertiau F.C., 1955, ApJ, 121, 557
Blaauw A., Hiltner W.A., Johnson H.L., 1959, ApJ, 130, 69
Blanco V.M., Williams A.D., 1959, ApJ, 130, 482
Blitz L., 1978, *PhD Thesis*, Columbia Univ.
Blitz L., Fich M., Stark A.A., 1982, ApJS, 49, 183
Bohnenstengel H.–D., Wendker H.J., 1976, A&A, 52, 23
Bok B.J., 1934, Harvard College Obs. Circ., 384, 1
Borgman J., Blaauw A., 1964, BAN, 17, 358
Boss B., 1910, AJ, 26, 163
Botley C.M., 1980, Observatory, 100, 211
Braes L.L.E., 1962, BAN, 16, 297
Brand J., Blitz L., 1993, A&A, 275, 67
Brandner W., Köhler R., 1998, ApJ, 499, L79
Brandner W., Alcalá J.M., Kunkel M., Moneti A., Zinnecker H., 1996, A&A, 307, 121
Brandt J.C., Stecher T.P., Crawford D.L., Maran S.P., 1971, ApJ, 163, L99
Brown A., 1950, ApJ, 112, 225
Brown A., 1987, ApJ, 322, L31
Brown A.G.A., 1998, in *The Stellar Initial Mass Function*, eds G.F. Gilmore & D. Howell, ASP Conf. Ser., 142, p. 45
Brown A.G.A., Verschueren W., 1997, A&A, 319, 811
Brown A.G.A., de Geus E.J., de Zeeuw P.T., 1994, A&A, 289, 101
Brown A.G.A., Hartmann D., Burton W.B., 1995, A&A, 300, 903
Brown A.G.A., Dekker G., de Zeeuw P.T., 1997, MNRAS, 285, 479
Brown A.G.A., Arenou F., van Leeuwen F., Lindegren L., Luri X., 1997b, ESA SP–402, p. 63
Brown A.G.A., Walter F.M., Blaauw A., 1998, in *The Orion Complex Revisited*, eds M.J. McCaughrean & A. Burkert, ASP Conf. Ser., in press
de Bruijne J.H.J., 1998, MNRAS, submitted
de Bruijne J.H.J., Hoogerwerf R., Brown A.G.A., Aguilar L.A., de Zeeuw P.T., 1997, ESA SP–402, p. 575
van Bueren H.G., 1952, BAN, 11, 385
Burrows D.N., Singh K.P., Nousek J.A., Garmire G.P., Good J., 1993, ApJ, 406, 97
Buscombe W., 1963, MNRAS, 126, 29
Campbell B., Persson S.E., McGregor P.J., 1986, ApJ, 305, 336
Canavaggia R., Fribourg M.–L., 1934, Bull. Astron., 2e Serie, Tome 9, 259
Cappa de Nicolau C.E., Pöppel W.G.L., 1991, A&AS, 88, 615
Catalog of Open Clusters, 1997, *http://heasarc.gsfc.nasa.gov/W3Browse/all/openclust.html*
Cernicharo J., Bachiller R., Duvert G., 1985, A&A, 149, 273
Černis K., 1990, Ap&SS, 166, 315
Černis K., 1993, Baltic Astronomy, 2, 214
Chen H., Grenfell T.G., Myers P.C., Hughes J.D., 1997, ApJ, 478, 295
Chereul E., Crézé M., Bienaymé O., 1997, ESA SP–402, p. 545
Clariá J.J., 1974a, AJ, 79, 1022
Clariá J.J., 1974b, A&A, 37, 229
Cohen M., Kuhi L.V., 1976, ApJ, 210, 365
Cohen M., Kuhi L.V., 1979, ApJS, 41, 743
Collinder P., 1931, Ann. Obs. Lund, 2, No. 1
Comerón F., Torra J., 1994, A&A, 281, 35
Comerón F., Torra J., Gómez A.E., 1998, A&A, 330, 975
Coyne G., Burley–Mead J., Kaufman M., 1969, AJ, 74, 103
Crampton D., 1968, AJ, 73, 338
Crawford D.L., 1960, AJ, 65, 487
Crawford D.L., 1961, ApJ, 133, 860
Crawford D.L., 1963, ApJ, 137, 523
Crawford D.L., Barnes J.V., 1970, AJ, 75, 952
Crawford D.L., Warren W.H., 1976, PASP, 88, 930
Cudworth K.M., 1998, in *Proper Motions and Galactic Astronomy*, ed. R.M. Humphreys, ASP Conf. Ser., 127, p. 91
Dame T.M., Ungerechts H., Cohen R.S., de Geus E.J., Grenier I.A., May J., Murphy D.C., Nyman L.–Å., Thaddeus P., 1987, ApJ, 322, 706
Dehnen W., Binney J.J., 1998, MNRAS, 298, 387
Delhaye J., Blaauw A., 1953, BAN, 12, 72
Digel S.W., Lyder D.A., Philbrick A.J., Puch D., Thaddeus P., 1996, ApJ, 458, 561
Dravins D., Lindegren L., Madsen S., Holmberg J., 1997, ESA SP–402, p. 733
Duvert G., Cernicharo J., Bachiller R., Gómez–González J., 1990, A&A, 233, 190
Eddington A.S., 1910, MNRAS, 71, 43
Eddington A.S., 1914, *Stellar movements and the structure of the universe*, London: MacMillan & Co.
Eggen O.J., 1961, Royal Obs. Bull., No. 41
Eggen O.J., 1978, PASP, 90, 436
Eggen O.J., 1980, ApJ, 238, 627
Eggen O.J., 1981, ApJ, 247, 507
Eggen O.J., 1982, ApJS, 50, 199
Eggen O.J., 1983, AJ, 88, 197
Eggen O.J., 1986, AJ, 92, 1074
Elmegreen B.G., 1982, in *Submillimeter wave astronomy*, eds J.E. Beckman & J.P. Phillips, p. 3

Elmegreen B.G., 1993, in *Protostars and Planets III*, eds E.H. Levy & J.I. Lunine (Tucson: Univ. of Arizona Press), p. 97
Elmegreen B.G., Efremov Y.N., 1998, in *The Orion Complex Revisited*, eds M.J. McCaughrean & A. Burkert, ASP Conf. Ser., in press
Elmegreen B.G., Lada C.J., 1977, ApJ, 214, 725
ESA, 1989, The Hipparcos Mission, ESA SP–1111
ESA, 1997, The Hipparcos and Tycho Catalogues, ESA SP–1200
Feast M., Whitelock P., 1997, MNRAS, 291, 683
Feigelson E.D., Lawson W.A., 1997, AJ, 113, 2130
Feinstein A., 1967, ApJ, 149, 107
Fernley J.A., Skillen I., Jameson R.F., 1989, MNRAS, 237, 947
Fitzgerald M.P., Harris G.L.H., Reed B.C., 1990, PASP, 102, 865
Fredrick L.W., 1954, AJ, 59, 321
Fredrick L.W., 1956, AJ, 61, 437
Fresneau A., 1980, AJ, 85, 66
Frink S., Röser S., Neuhäuser R., Sterzik M.F., 1997, A&A, 325, 613
Frogel J.A., Stothers R., 1977, AJ, 82, 890
Gaposchkin S., Greenstein J.L., 1936, Harvard College Obs. Bull., 904, 8
Garmany C.D., 1973, AJ, 78, 185
Garmany C.D., Stencel R.E., 1992, A&AS, 94, 211
Garrison R.F., 1967, ApJ, 147, 1003
Garrison R.F., 1970, AJ, 75, 1001
Garrison R.F., Kormendy J., 1976, PASP, 88, 865
Gatewood G., de Jonge J.K., Stephenson B., 1993, PASP, 105, 1101
de Geus E.J., 1992, A&A, 262, 258
de Geus E.J., de Zeeuw P.T., Lub J., 1989, A&A, 216, 44
de Geus E.J., Lub J., van der Grift E., 1990, A&AS, 85, 915
Gieren W.P., Barnes T.G., Moffett T.J., 1993, ApJ, 418, 135
Gilmore G.F., et al., 1998, in *Astronomical Interferometry*, SPIE Proc. 3350, eds R.D. Reasenberg & M. Shao, in press [astro–ph/9805180]
Giménez A., Clausen J.V., 1994, A&A, 291, 795
Gingrich C.H., 1922, ApJ, 56, 139
Glaspey J.W., 1971, AJ, 76, 1041
Glaspey J.W., 1972, AJ, 77, 474
Glass I.S., Penston M.V., 1975, MNRAS, 172, 227
Goss W.M., Manchester R.N., Brooks J.W., Sinclair M.W., Manefield G.A., Danziger I.J., 1980, MNRAS, 191, 533
Goudis C., 1982, *The Orion Complex: A case study of interstellar matter*, Ap&SSL, p. 90
Gould B.A., 1874, Proc. AAAS, p. 115
Grasdalen G.L., Strom K.M., Strom S.E., 1973, ApJL, 184, L53
Greene T.P., Young E.T., 1992, ApJ, 395, 516
Greenstein J.L., 1948, ApJ, 107, 375
Gregorio–Hetem J., Lépine J.R.D., Quast G.R., Torres C.A.O., de la Reza R., 1992, AJ, 103, 549
Grillmair C.J., Freeman K.C., Irwin M., Quinn P.J., 1995, AJ, 109, 2553
Guetter H.H., 1976, AJ, 81, 1120
Guetter H.H., 1977, AJ, 82, 598
Guillout P., Sterzik M.F., Schmitt J.H.M.M., Motch C., Egret D., Voges W., Neuhäuser R., 1998, A&A, 334, 540
Gutiérrez–Moreno A., Moreno H., 1968, ApJS, 15, 459
Hardie R.H., Crawford D.L., 1961, ApJ, 133, 843
Hardie R.H., Seyfert C.K., 1959, ApJ, 129, 601
Hardie R.H., Seyfert C.K., Grenchik R.T., 1957, AJ, 62, 143
Harju J., Haikala L.K., Mattila K., Mauersberger R., Booth R.S., Nordh H.L., 1993, A&A, 278, 569
Haro G., 1953, ApJ, 117, 73
Harris D.L., 1955, ApJ, 121, 554
Harris D.L., 1956, ApJ, 123, 371
Harris D.L., Morgan W.W., Roman N.G., 1954, ApJ, 119, 622
Harris D.L., Morgan W.W., Roman N.G., 1955, AJ, 60, 53
Hartmann D., Burton W.B., 1997, *Atlas of Galactic Neutral Hydrogen*, Cambridge Univ. Press
Hartquist T.W., Morfill G.E., 1983, ApJ, 266, 271
Hauck B., Mermilliod M., 1990, A&AS, 86, 107
Haug U., 1970, A&AS, 1, 35
Heckmann O., Lübeck K., 1958, ZfA, 45, 243
Heckmann O., Dieckvoss W., Kox H., 1956, AN, 283, 109
Heeschen D.S., 1951, ApJ, 114, 132
Herbig G.H., 1954, PASP, 66, 19
Herbig G.H., Rao N.K., 1972, ApJ, 174, 401
Herbst W., 1980, in *Star Clusters*, IAU Symp. 85, ed. J.E. Hesser, p. 33
Herbst W., Assousa G.E., 1977, ApJ, 217, 473
Herbst W., Racine R., Richer H.B., 1977, PASP, 89, 663
Herbst W., Racine R., Warner J.W., 1978, ApJ, 223, 471
Herbst W., Miller D.P., Warner J.W., Herzog A., 1982, AJ, 87, 98
van Herk G., 1959, AJ, 64, 348
Herschel J.F.W., 1833, Phil. Trans., p. 481
Herschel J.F.W., 1847, *Results of Astron. Observations made during the years 1834–1838 at the Cape of Good Hope*, London, p. 385
Hiltner W.A., 1956, ApJS, 2, 389
Hoag A.A., Johnson H.L., Iriarte B., Mitchell R.I., Hallam K.L., Sharpless S., 1961, Publ. Naval Obs., 17, 345
Høg E., 1997, ESA SP–402, p. 25
Høg E., Kuzmin A., Bastian U., Fabricius C., Kuimov K., Lindegren L., Makarov V.V., Röser S., 1998, A&A, 335, L65
Hoogerwerf R., Aguilar L.A., 1998, MNRAS, submitted (HA)
Hoogerwerf R., de Bruijne J.H.J., Brown A.G.A., Lub J., Blaauw A., de Zeeuw P.T., 1997, ESA SP–402, p. 571
Howard W.E., 1958, AJ, 63, 50
Howarth I.D., Schmutz W., 1995, A&A, 294, 529
Hubble E., 1922a, ApJ, 56, 162
Hubble E., 1922b, ApJ, 56, 400
van der Hucht K.A., et al., 1997, New Astronomy, 2, 245
Hughes J.D., Hartigan P., Clampitt L., 1993, AJ, 105, 571
Hughes J.D., Hartigan P., Krautter J., Kelemen J., 1994, AJ, 108, 1071
Hughes V.A., 1988, ApJ, 333, 788
Humphreys R.M., 1978, ApJS, 38, 309
Jones D.H.P., 1971, MNRAS, 152, 231
Jordi C., Trullols E., Galadí–Enríquez D., 1996, A&A, 312, 499
Jung J., Bischoff M., 1971, Bull. Inf. Centre Donn. Stell., 2, 8
Kalas P., Jewitt D., 1997, Nature, 386, 52
Kaper L., van Loon J.T., Augusteijn T., Goudfrooij P., Patat F., Waters L.B.F.M., Zijlstra A.A., 1997, ApJ, 475, L37 (err. ApJ, 479, L153)
Kapteyn J.C., 1911, Trans. Int. Solar Union, 3, 215
Kapteyn J.C., 1914, ApJ, 40, 43
Kapteyn J.C., 1918, ApJ, 47, pp 104, 146, 255
Keller H.–U., 1970, Wien. Ann., 29, No. 3
Kenyon S.J., Dobrzycka D., Hartmann L., 1994, AJ, 108, 1872
Khavtassi D.S., 1960, *Atlas of Galactic Dark Nebulae*, Abastumani Astrophys. Obs.
Klochkova V.G., Kopylov I.M., 1985, Bull. Spec. Astrophys. Obs., 20, 3
Knacke R.F., Strom K.M., Strom S.E., Young E.T., Kunkel W., 1973, ApJ, 179, 847
Kodaira K., Greenstein J.L., Oke J.B., 1970, ApJ, 159, 485

Koyama K., Hamaguchi K., Ueno S., Kobayashi N., Feigelson E.D., 1996, PASJ, 48, L87
Krelowski J., Megier A., Strobel A., 1996, A&A, 308, 908
Krzemínski W., Oskanjan V., 1961, Act. Astr., 11, 1
Kulikovsky P., 1940, Bull. Sternberg State Astr. Inst., No. 2
Kun M., 1986, Ap&SS, 125, 13
Kun M., Pásztor L., 1990, Ap&SS, 174, 13
Kun M., Balázs L.G., Tóth I., 1987, Ap&SS, 134, 211
Kutner M.L., Dickman R.L., Tucker K.D., Machnik D.E., 1979, ApJ, 232, 724
Lada C.J., Gottlieb C.A., Litvak M.M., Lilley A.E., 1974, ApJ, 194, 609
Lada C.J., Alves J., Lada E.A., 1996, AJ, 111, 1964
Lada E.A., Lada C.J., 1995, AJ, 109, 1682
Ladd E.F., Lada E.A., Myers P.C., 1993, ApJ, 410, 168
Lamers H.J.G.L.M., Harzevoort J.M.A.G., Schrijver H., Hoogerwerf R., Kudritzki R.P., 1997, A&A, 325, L25
van Leeuwen F., 1985, in *Dynamics of Star Clusters*, IAU Symp. 113, eds J. Goodman & P. Hut, p. 579
van Leeuwen F., 1994, in *Galactic and Solar System Optical Astrometry: Observation and Application*, eds L.V. Morrison & G.F. Gilmore (Cambridge Univ. Press), p. 223
Lesh J.R., 1968, ApJS, 17, 371
Lesh J.R., 1969, AJ, 74, 891
Lesh J.R., 1972, A&AS, 5, 129
Levato H., Abt H.A., 1976, PASP, 88, 141
Levato H., Malaroda S., 1975, PASP, 87, 173
Levato H., Malaroda S., Morrell N., Solivella G., 1987, ApJS, 64, 487
Lindblad P.O., 1967, BAN, 19, 34
Lindblad P.O., Grape K., Sandqvist Aa., Schober J., 1973, A&A, 24, 309
Lindblad P.O., Palouš J., Lodén K., Lindegren L., 1997, ESA SP–402, p. 507
Lindegren L., 1989, ESA SP–1111, Vol. 3, p. 311
Lindegren L., 1997, ESA SP–402, p. 13
Lissauer J.L., 1997, Nature, 386, 18
Loren R.B., 1976, ApJ, 209, 466
Loren R.B., 1979, ApJ, 227, 832
Lozinskaya T.A., Sitnik T.G., Toropova M.S., 1987, Sov. Astron., 31, 493
Lub J., Pel J.W., 1977, A&A, 54, 137
Lynds B.T., 1962, ApJS, 7, 1
Lynds B.T., 1969, PASP, 81, 496
Lyngå G., 1959, AfA, 2, 379
Lyngå G., 1962, AfA, 3, 65
Lyngå G., Wramdemark S., 1984, A&A, 132, 58
Machnik D.E., Hettrick M.C., Kutner M.L., Dickman R.L., Tucker K.D., 1980, ApJ, 242, 121
MacConnell D.J., 1968, ApJS, 16, 275
Maeder A., Meynet G., 1994, A&A, 287, 803
Malaroda S., 1981, PASP, 93, 614
Margulis M., et al., 1990, ApJ, 352, 615
Markarian B.E., 1952, Proc. Acad. Sci. Armenian SSR, 15, 13
Marraco H.G., 1978, A&A, 70, L61
Marraco H.G., Rydgren A.E., 1981, AJ, 86, 62
Marschall L.A., Comins N.F., Karshner G.B., 1990, AJ, 99, 1536
Mathieu R.D., 1986, in *Highlights of Astronomy*, Vol. 7, p. 481
May J., Murphy D.C., Thaddeus P., 1988, A&AS, 73, 51
McCaughrean M.J., Burkert A., 1998, *The Orion Complex Revisited*, ASP Conf. Ser., in press
Mermilliod J.–C., 1998, *http://obswww.unige.ch/webda/*
Mermilliod J.–C., Mermilliod M., 1994, *Catalog of Mean UBV Data on Stars*, Springer Verlag
Mermilliod J.–C., Turon C., Robichon N., Arenou F., Lebreton Y., 1997, ESA SP–402, p. 643
Meurers J., Mikulitsch W., 1968, Wien Ann., 27, No. 5
Meynet G., Mermilliod J.–C., Maeder A., 1993, A&AS, 98, 477
Morgan W.W., Sharpless S., Osterbrock D., 1952a, Sky & Telescope, 11, 138
Morgan W.W., Sharpless S., Osterbrock D., 1952b, AJ, 57, 3
Morgan W.W., Whitford A.E., Code A.D., 1953, ApJ, 118, 318
Morrell N., Levato H., 1991, ApJS, 75, 965
Mourard D., Bonneau D., Koechlin L., Labeyrie A., Morand F., Stee Ph., Tallon–Bosc I., Vakili F., 1997, A&A, 317, 789
Murphy D.C., May J., 1991, A&A, 247, 202
Murphy D.C., Cohen R., May J., 1986, A&A, 167, 234
Nakano M., Wiramihardja S.D., Kogure T., 1995, PASJ, 47, 889
Neuhäuser R., 1997, Science, 276, 1363
Neuhäuser R., Brandner W., 1998, A&A, 330, L29
Odenwald S.F., 1988, ApJ, 325, 320
Ogura K., 1984, PASJ, 36, 139
Olano C.A., 1982, A&A, 112, 195
Olano C.A., Walmsley C.M., Wilson T.L., 1994, A&A, 290, 235
Öpik E.J., 1953, IrAJ, 2, 219
Panagia N., Thum C., 1981, A&A, 98, 295
Pannekoek A., 1929, Publ. Astron. Inst. Amsterdam, No. 2, p. 63
Patel N.A., Goldsmith P.F., Snell R.L., Hezel T., Xie T., 1995, ApJ, 447, 721
Pérez M.R., 1991, RMxAA, 22, 99
Perryman M.A.C., Lindegren L., Turon C., ESA SP–402, p. 743
Perryman M.A.C., et al., 1998, A&A, 331, 81
Petrie R.M., 1958, MNRAS, 118, 80
Petrie R.M., 1962, MNRAS, 123, 501
Pinsonneault M.H., Stauffer J., Soderblom D.R., King J.R., Hanson R.B., 1998, ApJ, 504, 170
Plaskett J.S., 1928, MNRAS, 88, 395
Plaskett J.S., Pearce J.A., 1934, MNRAS, 94, 679
Plummer H.C., 1913, MNRAS, 73, 492
Pöppel W.G.L., 1997, Fund. of Cosmic Phys., 18, 1
Poveda A., Ruiz J., Allen C., 1967, Bol. de los Obs. Tonantzintla y Tacubaya, Vol. 4, No. 28, 86
Preibisch T., 1997, A&A, 324, 690
Preibisch T., Zinnecker H., Herbig G.H., 1996, A&A, 310, 456
Preibisch T., Guenther E., Zinnecker H., Sterzik M., Frink S., Röser S., 1998, A&A, 333, 619
Prosser C.F., 1992, AJ, 103, 488
van Rensbergen W., Vanbeveren D., de Loore C., 1996, A&A, 305, 825
Racine R., 1968, AJ, 73, 233
Rajamohan R., 1976, Pramāna, 7, 160
Rasmuson N.H., 1921, Lund Medd., Ser. II, 26, 1
Rasmuson N.H., 1927, Lund Medd., Ser. II, 47b, 1
Reichen M., Lanz T., Golay M., Huguenin D., 1990, Ap&SS, 163, 275
Reynolds R.J., Ogden P.M., 1978, ApJ, 224, 94
Robichon N., Arenou F., Turon C., Mermilliod J.–C., Lebreton Y., 1997, ESA SP–402, p. 567
Roman N.G., Morgan W.W., 1950, ApJ, 111, 426
Röser S., Bastian U., 1991, PPM Star Catalogue I, II., Heidelberg, Spektrum Akad. Verlag
Röser S., Bastian U., Kuzmin A., 1994, A&AS 105, 301
Rossano G.S., 1978, AJ, 83, 234
Ruprecht J., 1966, IAU Trans., 12B, 348
Ruprecht J., Balázs B., White R.E., 1981, *Catalogue of Star*

Clusters and Associations, Supplement to 2nd *Edition*, ed. B. Balázs (Budapest: Akadémiai Kiadó)
http://obswww.unige.ch/webda/
Rydgren A.E., 1971, PASP, 83, 656
Sahu M.S., 1992, *PhD Thesis*, Groningen Univ.
Sahu M.S., Blaauw A., 1994, The Messenger, 76, 48
Sancisi R., 1970, A&A, 4, 387
Sancisi R., 1974, in *Galactic radio astronomy*, IAU Symp. 60, eds F.J. Kerr & S.C. Simonson, p. 115
Sancisi R., Goss W.M., Anderson C., Johansson L.E.B., Winnberg A., 1974, A&A, 35, 445
Sandqvist Aa., Tomboulides H., Lindblad P.O., 1988, A&A, 205, 225
Sargent A.I., 1977, ApJ, 218, 736
Sargent A.I., 1979, ApJ, 233, 163
Schaerer D., Schmutz W., Grenon M., 1997, ApJ, 484, L153
Schmidt K.H., 1958, AN, 284, 76
Schmidt–Kaler T., 1961, ZfA, 53, 28
Schreur J.J., 1970, AJ, 75, 38
Schulz N.S., Berghöfer T.W., Zinnecker H., 1997, A&A, 325, 1001
Schwartz R.D., Gyulbudaghian A.L., Wilking B.A., 1991, ApJ, 370, 263
Sciortino S., Damiani F., Favata F., Micela G., 1998, A&A, 332, 825
Seyfert C.K., Hardie R.H., 1957, AJ, 62, 146
Seyfert C.K., Hardie R.H., Grenchik R.T., 1960, ApJ, 132, 58
Simonson S.C., 1968, ApJ, 154, 923
Simonson S.C., van Someren Greve H.W., 1976, A&A, 49, 343
Skinner S.L., Itoh M., Nagase F., 1998, New Astronomy, 3, 37
Slawson R.W., Hill R.J., Landstreet J.D., 1992, ApJS, 82, 117
Slettebak A., Bahner K., Stock J., 1961, ApJ, 134, 195
Smart W.M., 1936, MNRAS, 96, 568
Smart W.M., 1939, MNRAS, 100, 60
Smith H., Eichhorn H., 1996, MNRAS, 281, 211
Snell R.L., Scoville N.Z., Sanders D.B., Erickson N.R., 1984, ApJ, 284, 176
Snow T.P., Hanson M.M., Seab C.G., Saken J.M., 1994, ApJ, 420, 632
Stauffer J.R., Hartmann L.W., Burnham J.N., Jones B.F., 1985, ApJ, 289, 247
Stauffer J.R., Hartmann L.W., Jones B.F., 1989, ApJ, 346, 160
Stauffer J.R., Hartmann L.W., Prosser C.F., Randich S., Balachandran S., Patten B.M., Simon T., Giampapa M., 1997, ApJ, 479, 776
Steffey P.C., 1973, PASP, 85, 520
Stickland D.J., 1995, Observatory, 115, 180
Stock J., 1984, RMxAA, 9, 127
Stothers R., Frogel J.A., 1974, AJ, 79, 456
Straka W.C., 1971, in *The Gum Nebula and Related Problems*, eds S.P. Maran, J.C. Brandt, T.P. Stecher, NASA SP–332, p. 126
Straka W.C., 1973, ApJ, 180, 907
Strom K.M., Strom S.E., Grasdalen G.L., 1974, ApJ, 187, 83
Strom S.E., Grasdalen G.L., Strom K.M., 1974, ApJ, 191, 111
Strom S.E., Strom K.M., Carrasco L., 1974, PASP, 86, 798
Taylor K.N.R., Storey J.W.V., 1984, MNRAS, 209, 5P
Testi L., Olmi L., Hunt L., Tofani G., Felli M., Goldsmith P., 1995, A&A, 303, 881
Tian K.P., van Leeuwen F., Zhao J.L., Su C.G., 1996, A&AS, 118, 503
Torra J., Gómez A.E., Figueras F., Comerón F., Grenier S., Mennessier M.O., Mestres M., Fernández D., 1997, ESA SP–402, p. 513
Trullols E., Jordi C., 1997, A&A, 324, 549
Turner D.G., 1976, ApJ, 210, 65
Turon C., et al., 1992, Hipparcos Input Catalogue, ESA SP–1136
Upton E.K.L., 1971, in *The Gum Nebula and Related Problems*, eds S.P. Maran, J.C. Brandt, T.P. Stecher, NASA SP–332, p. 119
Urban S.E., Corbin T.E., Wycoff G.L., 1998, AJ, 115, 2161
Vasilevskis S., Sanders W.L., Balz A.G.A., 1965, AJ, 70, 797
Verschueren W., David M., Brown A.G.A., 1996, in *The Origins, Evolution, and Destinies of Binary Stars in Clusters*, eds E.F. Milone & J.–C. Mermilliod, ASP Conf. Ser., 90, p. 131
Verschueren W., Brown A.G.A., Hensberge H., David M., Le Poole R.S., de Geus E.J., de Zeeuw P.T., 1997, PASP, 109, 868
Vrba F.J., Strom S.E., Strom K.M., 1976, AJ, 81, 317
Wackerling L.R., 1972, PASP, 84, 827
Walker M.F., 1956, ApJS, 2, 365
Walker M.F., 1969, ApJ, 155, 447
Walter F.M., Boyd W.T., 1991, ApJ, 370, 318
Walter F.M., Vrba F.J., Mathieu R.D., Brown A., Myers P.C., 1994, AJ, 107, 692
Walter F.M., Vrba F.J., Wolk S.J., Mathieu R.D., Neuhäuser R., 1997, AJ, 114, 1544
Walter F.M., Wolk S.J., Sherry W., 1998, in *Cool Stars, Stellar Systems, and the Sun*, eds R. Donahue & J. Bookbinder, in press
Warren W.H., Hesser J.E., 1977a, ApJS, 34, 115
Warren W.H., Hesser J.E., 1977b, ApJS, 34, 207
Warren W.H., Hesser J.E., 1978, ApJS, 36, 497
Weaver W.B., 1970, AJ, 75, 938
Welin G., 1979, A&A, 79, 334
Wendker H.J., Higgs L.A., Landecker T.L., 1991, A&A, 241, 551
Westin T.N.G., 1985, A&AS, 60, 99
Whiteoak J.B., 1961, MNRAS, 123, 245
Wichmann R., Bastian U., Krautter J., Jankovics I., Rucinski S.M., 1997a, ESA SP–402, p. 359
Wichmann R., Krautter J., Covino E., Alcalá J.M., Neuhäuser R., Schmitt J.H.M.M., 1997b, A&A, 320, 185
Wielen R., Schwan H., Dettbarn C., Jahreiß H., Lenhardt H., 1997, ESA SP–402, p. 727
Wilking B.A., Harvey P.M., Joy M., Hyland A.R., Jones T.J., 1985, ApJ, 293, 165
Wilking B.A., Greene T.P., Lada C.J., Meyer M.R., Young E.T., 1992, ApJ, 397, 520
Wilking B.A., McCaughrean M.J., Burton M.G., Giblin T., Rayner J.T., Zinnecker H., 1997a, AJ, 114, 2029
Wilking B.A., Schwartz R.D., Fanetti T.M., Friel E.D., 1997b, PASP, 109, 549
Woolley R.v.d.R., Eggen O.J., 1958, Observatory, 78, 149
de Zeeuw P.T., Brand J., 1985, in *Birth and Evolution of Massive Stars and Stellar Groups*, eds W. Boland & H. van Woerden (Dordrecht: Reidel), p. 95
de Zeeuw P.T., Brown A.G.A., Verschueren W., 1994, in *Galactic and Solar System Optical Astrometry: Observation and Application*, eds L.V. Morrison & G.F. Gilmore (Cambridge Univ. Press), p. 215
de Zeeuw P.T., Brown A.G.A., de Bruijne J.H.J., Hoogerwerf R., Le Poole R.S., Lub J., Blaauw A., 1997, ESA SP–402, p. 495

A. RECIPE FOR MEMBERSHIP DETERMINATION

Here we specify the parameters of our astrometric member selection procedure for a moving group, following the principles set out in §§3.1–3.3. Table A1 lists the values for these parameters for the 12 associations and subgroups which we have identified in the Hipparcos Catalogue (§§4–8).

First, we fix the parameters $D_{\rm guess}$, $D_{\rm range}$, $\sigma_{\rm int}$, $\epsilon_{\rm min}$, $t_{\rm min}$ and $S_{\rm min}$. Here $D_{\rm guess}$ is the initial guess for the mean distance (in pc) of the association, and $D_{\rm range}$ denotes the range in distance (in pc) over which we expect to find association members (§3.2). The default value for $D_{\rm range}$ is 100 pc. If the association was detected by de Zeeuw et al. (1997), this distance is taken as the initial guess; otherwise, $D_{\rm guess}$ is taken from de Zeeuw et al. (1994). The quantity $\sigma_{\rm int}$ is the internal velocity dispersion in the association (one-dimensional, in km s^{-1}). We choose $\sigma_{\rm int} = 3.0$ km s^{-1} (cf. Mathieu 1986; Tian et al. 1996; §3.3). The quantity $\epsilon_{\rm min}$ is the stop criterion for the convergent point method, as defined by de Bruijne (1998); it sets an acceptable value of χ^2 (§3.1) by requiring that $\epsilon \geq \epsilon_{\rm min}$, where

$$\epsilon = \frac{1}{\Gamma(\frac{N}{2}-1)} \int_{\chi^2}^{\infty} x^{\frac{N}{2}-2} {\rm e}^{-x} \, {\rm d}x. \qquad (9)$$

We set $\epsilon_{\rm min}$ equal to 0.954, based on a Monte Carlo analysis (de Bruijne 1998). The parameter $t_{\rm min}$ is the minimum ratio of total proper motion and related 1σ error required for a star to enter the convergent point method (eq. 1). Finally, the quantity $S_{\rm min}$ is the Spaghetti method membership criterion limit for a star to be selected as member (§3.2); it was fixed at $S_{\rm min} = 0.1$ based on a Monte Carlo analysis (Hoogerwerf & Aguilar 1998).

Before starting the member selection, we discard all stars which do not satisfy $(\mu_\alpha \cos\delta)_{\rm min} \leq \mu_\alpha \cos\delta \leq (\mu_\alpha \cos\delta)_{\rm max}$ and $\mu_{\delta,{\rm min}} \leq \mu_\delta \leq \mu_{\delta,{\rm max}}$. We also check the quality of the astrometric parameters: stars with 15 per cent or more rejected data, or a goodness-of-fit indicator larger than 3.0 (fields H29 and H30 in the Hipparcos Catalogue, respectively), are discarded. Typically, this excludes less than 0.5 per cent of the total sample. We then apply the convergent point and Spaghetti method independently to a sample of early-type stars, e.g., all OB stars (see Table A1 for the precise definition of 'early-type'). The results of the two methods are combined by intersecting the individual membership lists. Next, we consider the vector point diagram for all stars in the intersection. This vector point diagram contains association members as well as a small number of field stars. These field stars have astrometric properties which make them indistinguishable from the association members. However, the association members generally define a clear concentration in this diagram whereas the field stars have a much broader distribution. In order to remove as many field stars as possible while, at the same time, rejecting as few as possible genuine members, we define a lower and upper cutoff in $\mu \equiv \sqrt{\mu_\ell^2 \cos^2 b + \mu_b^2}$, $\mu_{\rm min}$ and $\mu_{\rm max}$, respectively, such that the range $\mu_{\rm min} \leq \mu \leq \mu_{\rm max}$ mainly corresponds to the association members. We construct the resulting parallax distributions to make sure that our proper motion cutoffs efficiently separate the foreground and background stars from the association members. We then define as secure members all stars in the intersection of the individual membership lists which lie within the range $\mu_{\rm min} \leq \mu \leq \mu_{\rm max}$.

The convergent point and Spaghetti method are then applied to the secure early-type members to determine their convergent point and space motion, respectively. This convergent point is used to define the membership probability, $P = p_{\rm cp}$, for each star (cf. §3.1). We then fix the convergent point and space motion to those of the secure early-type members and apply both methods to the remaining (late-type) stars in the field to search for 'comoving members'. The individual membership lists are again intersected. Using the same proper motion cutoffs as for the early-type members, we define the secure late-type members and their membership probabilities.

Given the final list of all secure members we determine the association distance D and the related value for the systematic underestimate $D_{\rm sys} \geq 0$ (§3.6). If the corrected distance $D_{\rm cor} \equiv D + D_{\rm sys}$ deviates more than 25 per cent of the value of $D_{\rm guess}$, we repeat the whole member selection process starting with $D_{\rm guess} = D_{\rm cor}$. This turned out to be required only in the case of Cep OB2 (§8.2), where we replaced the initial $D_{\rm guess} = 559$ pc by $D_{\rm guess} = 657$ pc.

Table A1 also gives the convergent points and space velocities found by the convergent point and Spaghetti method, respectively. These values must be interpreted with great care. Most importantly, the convergent point and space motion may contain an unknown component due to expansion or contraction of the association (cf. §3.7). Furthermore, the uncertainty of the space motion in the line-of-sight direction is large, and can be up to several tens of km s^{-1}; compare the large difference in the V-component of the space motion of α Persei and Cep OB6 (Table A1) with their similar mean motion displayed in Figure 29 (§9.2). Moreover, the space motions are biased due to the use of the parallax in the calculation of the tangential velocity (Hoogerwerf & Aguilar 1998). The typical uncertainty in the convergent points is several degrees along the great circle connecting the convergent point with the association, and much smaller, less than a degree, in the perpendicular direction (de Bruijne 1998).

Our procedure to estimate the expected number of interlopers in the list of association members produced by the above selection method is described in detail in §3.4. Table A2 summarizes the results as a function of spectral type, for the 12 fields where the Hipparcos measurements allow identification of a moving group.

Table A1. Selection parameters

	US	UCL	LCC	Vel OB2	Tr 10	Col 121	Per OB2	α Persei	Cas–Tau	Lac OB1	Cep OB2	Cep OB6
$l_{\rm min}$	343	312*	285	255	255	228	145	140	118	90	96	100
$l_{\rm max}$	360	343	312	270	270	244	170	165	220	110	108	110
$b_{\rm min}$	10	0	−10	−15	−2	−15	−27	−17	−45	−25	−5	−2
$b_{\rm max}$	30	25	21	−2	4	−2	−13	3	12	−5	14	2
N	945	3132	3897	874	392	840	876	1588	2348	1436	923	181
$(\mu_\alpha \cos\delta)_{\rm min}$	−1500	−500	−1500	−1500	−1500	−1500	−1500	−1500	−1500	−15	−100	−1500
$(\mu_\alpha \cos\delta)_{\rm max}$	1500	500	1500	1500	1500	1500	1500	1500	1500	15	100	1500
$\mu_{\delta,\rm min}$	−1500	−500	−1500	−1500	−1500	−1500	−40**	−1500	−1500	−15	−100	−1500
$\mu_{\delta,\rm max}$	1500	500	1500	1500	1500	1500	1500	1500	1500	15	100	1500
early-type	O–A	O–A	O–A	O–A	O–B	O–B	O–B	O–B	O–B	O–B	O–B	O–R
late-type	F–R	F–R	F–R	F–R	A–R	A–R	A–R	A–R		A–R	A–R	
$D_{\rm guess}$	145	140	118	415	362	546	310	176	140	373	657	243
$t_{\rm min}$	3.0	3.0	3.0	3.0	3.0	2.5	2.5	3.0	3.0	1.0	1.0	3.0
$\mu_{\rm min}$	0	22	25	8	13	0	0	30	0	2	0	10
$\mu_{\rm max}$	37	45	45	14	18	7	15	40	1000	7	7	25
$\ell_{\rm cp}$	270	249	234	152	251	198	297	207	244	300	346	244
$b_{\rm cp}$	-16	-15	-19	-4	-4	-17	1	-16	-13	-14	-7	-10
U	-1	-9	-12	-16	-24	-13	1	-11	-13	5	7	-14
V	-16	-17	-13	6	-24	-4	-11	-26	-20	-7	2	-29
W	-5	-6	-7	-1	-8	-4	-1	-7	-6	-4	-1	-6

Note. — Input parameters for the member selection of the nearby OB associations based on Hipparcos data, and resulting convergent points and space motions. We consider all N stars in the field defined by the boundaries $\ell_{\rm min}$, $\ell_{\rm max}$, $b_{\rm min}$, and $b_{\rm max}$, units in degrees, as candidate members. We exclude stars which do not satisfy proper motion criteria set by $(\mu_\alpha \cos\delta)_{\rm min}$, $(\mu_\alpha \cos\delta)_{\rm max}$, $\mu_{\delta,\rm min}$, and $\mu_{\delta,\rm max}$, units in mas yr^{-1}. The convergent point method excludes all stars with insignificant proper motions: $t \leq t_{\rm min}$ (eqs 1 and 5). We first apply our procedure to the 'early-type' stars, and use $D_{\rm guess}$, in pc, as initial guess for the distance of the group. This gives a convergent point $(\ell, b)_{\rm cp}$, in degrees, and space motion (U, V, W), in km s^{-1} (see Appendix A for details). We then search for 'late-type' comoving members. We accept as members all stars with $\mu_{\rm min} \leq \mu$ (mas yr^{-1}) $\leq \mu_{\rm max}$. *The UCL field is not rectangular: it includes the small extension $343° < \ell \leq 350°$ and $0° \leq b \leq 10°$ (Figure 9). **Limit set in order to exclude the Pleiades.

B. MEAN DISTANCES

The conversion from parallax to distance introduces a bias in the distance (Smith & Eichhorn 1996; Brown et al. 1997b). Consider a sphere of radius R with its center at a distance D_0 ($R < D_0$), with a homogeneous distribution of stars. An observer who measures distances D to the individual stars in the group will derive a number density as a function of distance, $F(D)\,{\rm d}D$, with

$$F(D) = \frac{3D^2}{2R^3}\Big(1 - \frac{D_0^2 + D^2 - R^2}{2D_0 D}\Big). \qquad (10)$$

The mean distance $\langle D \rangle$ of the group, computed by integrating $DF(D)\,{\rm d}D$, then is

$$\langle D \rangle = D_0\Big(1 + \frac{1}{5}\frac{R^2}{D_0^2}\Big). \qquad (11)$$

Thus, the mean of the individual distances is an overestimate of the true mean distance D_0, and it depends on the angular size of the group.

The number density distribution as a function of parallax, $F^{\star}(\pi)\,{\rm d}\pi$, is given by

$$F^{\star}(\pi) = \frac{1}{\pi^2}F(\frac{1}{\pi}) = \frac{3}{2R^3}\Big(\frac{1}{\pi^4} - \frac{1}{2D_0\pi^5} + \frac{R^2 - D_0^2}{2D_0\pi^3}\Big), \qquad (12)$$

and the mean parallax $\langle \pi \rangle$ is

$$\langle \pi \rangle = \frac{1}{D_0}. \qquad (13)$$

The errors in the Hipparcos parallaxes are distributed as a Gaussian. As this is a symmetric function, convolution of the parallax distribution, and then computing the mean parallax of the group, again produces $1/D_0$. It follows that the mean parallax of a spherical homogeneous group is an unbiased estimator of the mean distance of the group. Any spherically symmetric density distribution can be written as the sum of homogeneous spheres with different radii. The inverse of the mean parallax therefore is an unbiased estimator of the distance for all spherical star clusters.

The OB associations studied in this paper are gravitationally unbound, and not likely to be exactly spherical. We have computed the observed mean parallax for ellipsoidally stratified groups, as a function of viewing angle, and find that in this case there is a small bias in the mean parallax. However, to an accuracy of about 1 per cent, the corresponding mean distance is equal to the true distance for realistic shapes and for all viewing angles. We conclude that the inverse of the mean parallax is an essentially unbiased estimator of the distance to the associations.

The calculation of mean distances for open clusters based on Hipparcos data must be done with care, as it needs to take into account the correlated measurements for stars located in a small area. This can be achieved by using Hipparcos intermediate data. Mermilliod et al. (1997) have done so, and find a distance of 184.2±7.5 pc for 32 members of the α Persei cluster, which is the highest-density group investigated in our census. Our method yields the same distance for the early-type stars, which gives confidence that the distances of the low-density as-

Table A2. Interloper analysis

SP	US	UCL	LCC	Vel OB2	Tr 10	Col 121	Per OB2	α Persei	Cas–Tau	Lac OB1	Cep OB2	Cep OB6
O+	0 0 0	0 0 0	0 0 0	0 0 0	0 0 0	0 0 1	0 0 0	0 0 0	0 0 0	0 0 0	0 1 1	0 0 0
O−	0 0 0	0 0 0	0 0 0	0 0 0	0 0 0	0 0 0	0 0 0	0 0 0	0 0 0	0 0 0	0 1 1	0 0 0
OV	−	4	20	0	29	20	0	33	30	50	25	14
B+	4 5 6	9 12 14	5 7 9	30 34 39	3 4 5	27 29 34	1 2 5	1 2 3	48 52 57	8 11 13	13 16 19	0 0 1
B−	0 1 2	3 5 6	3 4 5	19 22 26	1 2 3	14 17 20	1 1 2	0 0 1	43 46 51	4 6 8	8 10 12	0 0 1
BV	62	47	49	66	58	47	29	33	26	22	26	21
A+	4 6 8	13 15 19	9 11 14	4 6 7	0 1 2	3 5 6	9 11 13	4 5 7		21 24 27	9 11 13	0 1 2
A−	1 2 5	9 10 13	6 8 10	4 6 8	0 0 1	3 4 5	8 10 13	3 4 5		18 21 24	8 11 13	0 0 1
AV	49	60	53	70	51	51	9	9		5	3	2
F+	5 6 8	14 17 20	10 12 14	0 0 1	0 0 0	0 0 0	0 1 2	1 2 3		0 1 1	0 0 1	0 0 0
F−	4 5 7	13 15 17	7 9 12	0 0 0	0 0 0	0 0 0	0 1 2	1 2 3		0 1 1	0 0 1	0 0 0
FV	82	72	61	63	79	66	14	13		6	9	17
G+	1 2 3	5 6 8	2 3 4	0 1 2	0 0 0	0 0 1	0 0 1	0 0 1		0 0 0	0 1 1	0 0 0
G−	1 2 3	5 6 8	2 3 4	0 1 2	0 0 0	0 0 0	0 1 1	0 0 1		0 0 0	0 0 1	0 0 0
GV	61	47	38	35	40	39	5	8		0	5	16
K+	1 2 3	2 4 5	1 2 3	1 1 2	0 0 1	0 1 1	1 2 3	0 1 1		2 3 4	1 1 2	0 0 0
K−	1 1 2	2 4 5	1 2 3	1 1 2	0 0 1	0 1 1	1 1 3	0 1 2		2 3 4	1 1 2	0 0 0
KV	13	10	8	7	6	4	2	3		1	1	14
M+	0 0 1	0 0 0	0 0 0	0 0 0	0 0 0	0 0 0	0 0 0	0 0 0		0 0 1	0 0 0	0 0 0
M−	0 0 0	0 0 1	0 0 0	0 0 0	0 0 0	0 0 0	0 0 0	0 0 0		0 0 1	0 0 0	0 0 0
MV	0	6	3	3	11	26	0	3		4	9	50
R+	0 0 0	0 0 0	0 0 0	0 0 0	0 0 0	0 0 0	0 0 0	0 0 0		0 0 0	0 0 0	0 0 0
R−	0 0 0	0 0 0	0 0 0	0 0 0	0 0 0	0 0 0	0 0 0	0 0 0		0 0 0	0 0 0	0 0 0
RV	0	0	0	0	0	0	0	0		0	5	0
T+	19 22 26	51 55 60	32 36 40	40 43 48	4 6 7	33 37 41	15 18 21	9 12 14	48 53 58	37 40 44	28 31 34	1 2 4
T−	10 14 17	36 40 46	22 27 30	28 32 36	2 4 5	19 22 26	13 15 19	7 9 11	43 46 52	27 31 35	21 24 29	1 1 2
TV	54	45	39	45	42	40	9	12	26	6	10	13

Note. — Expected number of field stars in the membership lists of the nearby OB associations, as a function of spectral type SP ('R' indicates remainder, 'T' indicates total). The interquartile range and the median are given, based on 100 Monte Carlo realisations of the Galactic field star distribution. The symbol '+' refers to the results of the analysis in which the members of the associations were retained; the symbol '−' refers to the situation in which the members were removed beforehand. The lines labeled 'V' give the percentage of stars which are explicitly classified as main sequence stars (luminosity class V) in the Hipparcos Catalogue. Severe observational selection effects are present in the latter numbers for the northern associations. See §3.4 for more details. We only consider OB stars for the Cas–Tau association (§7.2).

sociations obtained in this paper are unbiased. This agrees with the conclusions of, e.g., Lindegren (1989) and Pinsonneault et al. (1998).

C. MEMBERSHIP LISTS

Rather than give lengthy lists with properties of the selected member stars, and cross references to the different numbering systems used in previous studies, we simply tabulate in Table C1 the entry numbers in the Hipparcos Catalogue for all secure members found by our selection procedure, together with the membership probability defined in eq. (6). All other properties, including HR and HD numbers, as well as spectral types, V and $B-V$ photometry, and indication of multiplicity, can be found in the Hipparcos Catalogue. Radial velocities can be found in the Hipparcos Input Catalogue, or in SIMBAD.

Many classical proper motion members of the nearby associations are not confirmed by our selection procedure, and hence do not appear in Table C1. However, as described in §3.5, some of these 'rejects' are in fact long-period binaries, for which the Hipparcos measurements do not necessarily reflect the mean space motion but rather an instantaneous orbital motion. The ground-based proper motions used in the classical studies generally are based on a much longer timespan. It is likely that a significant number of these astrometric binaries are in fact members. They are identified in the main text in §§4–8.

Figure C1 illustrates the cumulative membership probabilities for all secure members. In general, ∼45–65 per cent of all members have membership probabilities $P \geq 90$ per cent, while ∼10–15 per cent have $P \geq 99.7$ per cent. The median membership probabilities for α Persei and Cep OB6 are higher than for the other associations, but the small number of Cep OB6 members (20 stars) combined with the special member selection for this case (§8.5) call for caution.

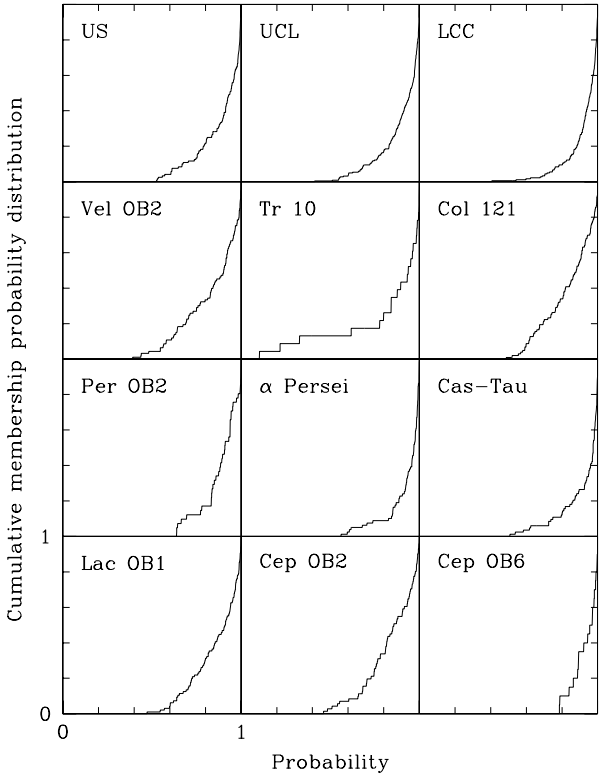

Figure 30: Cumulative membership probability distributions of the secure members of the associations listed in Table C1.

Table C1. Membership lists

HIP	*P*	HIP	*P*	HIP	*P*	HIP	*P*	HIP	*P*	HIP	*P*	HIP	*P*	HIP	*P*	HIP	*P*	HIP	*P*
Upper Scorpius												120: 0 O, 49 B, 34 A, 22 F, 9 G, 4 K, 2 M, 0 R								
76071	83	77911	80	78702	92	79156	100	79739	99	80130	53	80799	91	78977	98	79644	98	82319	56
76310	61	77939	97	78809	88	79250	70	79771	100	80196	96	81266	98	79054	95	79910	98	82534	96
76503	96	77960	84	78820	57	79366	98	79785	88	80238	99	81474	76	79083	92	79977	100	83456	67
76633	75	78099	99	78847	96	79374	90	79860	93	80311	86	81624	98	79097	95	80320	77	83542	61
77457	84	78104	89	78877	81	79392	95	79878	100	80324	92	82397	94	79247	100	80535	100		
77545	94	78168	97	78933	98	79404	99	79897	100	80338	99			79252	75	80586	92		
77635	99	78196	80	78956	99	79410	96	79987	90	80371	61	75916	75	79258	95	80763	100		
77815	90	78207	74	78963	61	79439	67	80019	91	80425	93	77813	91	79288	100	80896	65		
77840	96	78246	99	78968	75	79476	80	80024	96	80461	99	78233	100	79369	94	81392	100		
77858	99	78265	98	78996	88	79530	98	80059	86	80473	53	78271	92	79462	90	81455	80		
77859	99	78494	98	79031	92	79599	91	80088	99	80474	79	78483	99	79596	99	81851	100		
77900	100	78530	99	79098	90	79622	99	80112	94	80493	76	78581	54	79606	84	82140	100		
77909	99	78549	100	79124	79	79733	79	80126	100	80569	67	78663	97	79643	87	82218	90		
Upper Centaurus Lupus												221: 0 O, 66 B, 68 A, 55 F, 25 G, 6 K, 1 M, 0 R								
66447	98	70441	100	72627	100	74657	100	76945	97	79631	100	67970	100	73742	77	76472	99	79610	87
66722	100	70455	100	72630	76	74752	100	77086	83	80142	100	68328	73	73777	99	76501	92	79673	85
66908	98	70626	74	72683	97	74797	78	77150	97	80208	88	68335	90	73783	95	76875	89	79710	100
67464	99	70690	94	72800	87	74950	99	77286	99	80390	83	68726	91	74177	100	77015	90	79742	100
67472	97	70697	100	72940	94	74985	91	77295	100	80591	99	69291	99	74224	60	77038	83	79908	78
67973	98	70809	100	72984	95	75056	98	77315	79	80897	55	69327	96	74499	91	77081	91	80636	98
68080	99	70904	98	73145	95	75077	97	77317	96	81136	90	69395	100	74501	63	77135	97	80663	98
68245	98	70918	100	73147	83	75141	99	77388	55	81316	99	69720	87	74688	94	77144	86	80921	100
68282	100	70998	89	73266	92	75151	100	77523	94	81472	97	70350	94	74772	97	77157	99	81380	84
68532	88	71140	97	73334	94	75210	99	77968	67	81751	100	70376	85	74865	87	77432	77	81447	98
68722	73	71271	90	73341	98	75264	84	78150	94	81914	99	70558	96	74959	87	77502	100	81775	68
68781	98	71321	98	73393	99	75304	100	78324	89	81949	97	70689	99	75367	55	77520	94	82135	60
68862	96	71453	100	73559	60	75476	100	78384	97	81972	98	70833	68	75459	51	77524	55	82569	100
68867	96	71498	98	73807	83	75509	100	78533	75	82154	98	70919	68	75480	87	77656	87	82747	57
68958	91	71536	84	73913	89	75647	95	78541	41	82430	90	71023	93	75491	100	77713	68	83159	77
69113	96	71708	97	73937	92	75915	99	78641	89	82545	93	71178	99	75683	100	77780	80		
69302	83	71724	81	73990	84	75957	99	78655	99	82560	98	71767	86	75824	67	78043	94		
69605	100	71727	93	74066	97	76001	86	78754	67	83457	96	72033	95	75891	95	78133	100		
69618	85	71860	80	74100	97	76048	93	78756	93	83693	92	72070	89	75924	90	78432	88		
69749	98	71865	98	74104	98	76297	83	78853	72			72099	99	75933	66	78555	88		
69845	99	72140	69	74117	60	76371	80	78918	77	67497	100	72164	97	76084	72	78684	92		
70149	98	72192	76	74449	99	76395	97	79044	92	67522	100	73666	97	76197	85	78881	80		
70300	100	72584	88	74479	88	76600	95	79400	99	67957	97	73667	90	76457	96	79516	100		
Lower Centaurus Crux												180: 0 O, 42 B, 55 A, 61 F, 15 G, 6 K, 1 M, 0 R								
50083	98	57809	100	60084	95	62179	100	64892	99	67260	100	59084	54	61087	94	63527	91	65891	70
50520	84	57851	90	60183	96	62205	96	64925	100	67919	72	59481	99	61241	85	63797	87	66001	92
50847	68	58416	99	60320	95	62322	91	64933	90			59603	99	61248	80	63836	100	66285	60
51991	90	58452	99	60379	96	62327	96	65021	87	55334	89	59693	93	62032	87	63847	78	66782	100
52357	83	58465	100	60561	92	62703	100	65089	95	56227	88	59716	94	62056	81	63886	98	66941	98
53524	41	58680	95	60577	98	63003	99	65112	100	56420	99	59764	97	62134	92	63962	93	67003	92
53701	99	58720	94	60710	98	63005	90	65178	98	56673	96	59781	98	62171	96	63975	99	67068	88
54231	95	58859	93	60823	100	63007	98	65219	96	56814	93	59854	99	62427	78	64044	88	67230	97
55188	98	58884	99	60851	93	63204	100	65271	87	57524	92	59960	98	62428	98	64184	99	67428	95
55425	96	59173	100	61257	97	63210	98	65394	100	57595	99	60205	100	62431	84	64216	75	68534	90
55899	97	59282	97	61265	98	63236	98	65426	100	57950	93	60245	96	62445	76	64316	90		
56354	99	59397	99	61585	95	63839	94	65822	100	58075	100	60348	96	62657	99	64322	100		
56379	100	59413	97	61639	100	63945	100	65965	92	58146	100	60459	89	62674	100	64877	90		
56543	76	59502	93	61684	97	64004	99	66068	100	58167	100	60513	76	62677	86	64995	100		
56561	73	59505	99	61782	94	64053	94	66454	95	58220	93	60567	93	63022	92	65136	99		
56963	89	59724	95	61796	80	64320	100	66566	100	58528	100	60885	75	63041	85	65423	88		
56993	99	59747	98	62002	99	64425	82	66651	91	58899	96	60913	97	63272	97	65517	91		
57238	69	59898	97	62026	86	64515	100	67036	100	58921	100	61049	99	63435	70	65617	92		
57710	85	60009	89	62058	100	64661	62	67199	93	58996	99	61086	92	63439	97	65875	96		
Vel OB2												93: 1 O, 81 B, 5 A, 0 F, 3 G, 3 K, 0 M, 0 R								
35832	93	37926	76	38795	86	39182	97	39623	96	39974	58	40594	98	41442	100	42036	99	39493	90
35970	64	37953	99	38816	96	39185	64	39691	91	39981	81	40600	99	41486	99	42069	83	39754	98
36219	99	38020	55	38879	67	39231	90	39694	90	40109	96	40662	99	41498	92	42073	69	39979	92
36299	99	38133	69	38936	100	39246	57	39717	85	40183	62	40921	90	41559	93	42154	100	42340	62
36856	83	38290	91	38957	58	39349	44	39810	84	40357	100	41039	99	41601	100	42698	100		
37008	83	38370	96	39054	95	39371	85	39845	80	40389	83	41052	92	41616	75	43011	71		
37318	99	38425	98	39084	73	39431	84	39861	39	40397	83	41186	100	41621	91	43057	97		
37577	55	38438	91	39107	100	39573	44	39873	100	40515	71	41249	64	41668	48				
37637	99	38510	94	39142	100	39576	92	39953	61	40574	71	41295	75	41828	88	38152	77		
37663	63	38584	69	39162	56	39584	89	39970	77	40586	97	41332	92	42007	93	38400	94		

Note. — Identification of Hipparcos members of the OB associations studied in the main text. The odd columns list the Hipparcos numbers of the members, and the even columns give the associated membership probability P (in per cent). For each association the total number of members as well as the distribution over spectral types is given in the first line. Wolf–Rayet stars have been counted as O stars. The early-type members (see Table A1) are listed first, and are separated from the later types by a blank entry.

Table C1. Continued

HIP	*P*	HIP	*P*	HIP	*P*	HIP	*P*	HIP	*P*	HIP	*P*	HIP	*P*	HIP	*P*	HIP	*P*	HIP	*P*
Trumpler 10												23: 0 O, 22 B, 1 A, 0 F, 0 G, 0 K, 0 M, 0 R							
42295	88	42559	10	43055	96	43182	94	43326	99	43536	78	44019	33	44996	62				
42398	84	42653	100	43059	22	43240	100	43450	93	43807	100	44034	95						
42477	100	42685	80	43085	99	43285	96	43520	84	43987	90	44598	100	44631	98				
Collinder 121												103: 2 O, 85 B, 8 A, 1 F, 1 G, 3 K, 3 M, 0 R							
31125	64	33062	93	33316	96	33686	99	34041	91	34412	79	35168	96	35996	99	31919	91	35746	78
31436	98	33070	96	33343	79	33695	88	34067	94	34579	82	35267	97	36009	56	31935	59	35940	96
31901	64	33083	81	33414	67	33721	74	34074	70	34784	81	35316	57	36222	85	32335	89	36267	90
31959	98	33092	78	33447	67	33769	91	34097	86	34898	96	35329	62	36293	99	33152	90	36929	88
32084	61	33165	100	33522	77	33770	98	34153	93	34937	60	35342	99	36605	94	33504	97	36987	93
32101	100	33200	67	33523	90	33804	96	34167	91	34940	100	35412	100	36646	76	33511	84		
32292	86	33208	100	33532	86	33814	85	34219	92	34954	98	35413	100	36707	93	33610	82		
32591	52	33211	74	33611	59	33846	100	34227	62	34968	93	35421	100	36944	92	34161	60		
32823	74	33260	97	33621	100	33865	99	34281	100	35026	87	35453	81	36972	88	34444	98		
32911	85	33276	49	33666	58	33888	72	34303	69	35051	61	35887	76	37025	81	34483	66		
33007	82	33294	76	33673	91	33975	70	34331	99	35110	65	35920	88			35289	99		
Per OB2												41: 0 O, 17 B, 16 A, 2 F, 2 G, 3 K, 1 M, 0 R							
14552	94	17561	100	18081	87	19201	100	14458	77	16164	100	17474	94	18392	97	19240	94		
14713	83	17698	95	18111	94	19659	100	14824	69	16705	84	17498	83	18397	94	20324	100		
15895	90	17735	88	18246	84			14869	64	16784	100	17596	64	18578	94				
15984	85	17845	78	19039	98	14145	100	15601	89	17113	91	18258	88	18610	83				
17313	95	17998	91	19178	64	14207	66	15696	91	17172	86	18330	99	18886	93				
α Persei (Per OB3)												79: 0 O, 30 B, 33 A, 12 F, 2 G, 2 K, 0 M, 0 R							
14566	92	15531	100	16118	98	16450	71	13409	88	15160	74	15821	62	16318	94	16995	100	18716	96
14845	93	15556	95	16137	99	16470	84	13488	100	15363	96	15863	97	16403	99	17254	61	18808	56
14980	100	15770	94	16147	97	16782	99	13820	97	15388	98	15878	97	16426	93	17549	96	19563	99
15040	100	15819	93	16210	98	16826	98	14661	99	15420	98	15898	99	16452	100	17577	100	19648	98
15259	100	15988	98	16244	87	17548	89	14697	85	15499	97	15911	92	16455	83	18037	92	19686	85
15338	90	16011	99	16252	85	19343	98	14853	100	15505	94	16036	99	16574	93	18161	100	20403	60
15404	99	16047	99	16340	99			14923	85	15654	96	16211	99	16966	99	18214	68	21111	96
15444	98	16079	98	16430	89	13155	99	14949	97	15814	98	16258	92	16972	99	18640	98	21376	86
Cas–Tau (OB stars only)																		83: 0 O, 83 B	
1921	100	5566	51	8704	98	12453	99	15531	98	19466	82	21135	100	23130	98	25657	97	30180	95
2377	100	5813	97	8886	93	12477	100	15627	100	19720	73	21177	100	23745	90	25695	84	31278	98
2474	98	6480	99	9656	100	13003	74	17563	80	19860	96	21192	97	23767	99	26034	100		
2505	80	7457	98	9890	98	13124	93	17681	98	20063	100	21640	86	24740	80	26640	94		
2647	97	7988	88	10924	99	13327	86	17707	93	20171	97	21973	81	24836	99	27421	87		
2866	97	8068	100	10944	89	13330	100	17907	95	20229	96	22034	97	25157	58	27723	100		
3504	99	8108	100	10974	95	14887	100	18033	100	20354	100	22109	73	25499	97	27746	93		
4437	99	8387	54	11295	99	15065	75	18067	97	20424	96	22128	100	25555	62	27962	62		
5062	100	8551	100	12218	100	15520	87	18190	98	20884	94	22415	100	25561	99	29038	100		
Lac OB1												96: 1 O, 35 B, 46 A, 1 F, 0 G, 8 K, 3 M, 2 R							
108508	79	111308	99	112144	97	113469	76	110033	72	111055	62	111916	85	113145	60	114134	77	116088	65
109082	93	111337	90	112148	47	113835	55	110373	80	111207	71	112016	95	113187	64	114153	99	116135	64
110476	92	111429	99	112167	82	114097	99	110448	71	111292	57	112017	99	113188	73	114441	94	116411	69
110790	100	111491	98	112293	91	114106	74	110473	92	111329	87	112182	99	113208	97	114554	60	116457	67
110835	99	111546	85	112906	93	115067	72	110664	87	111340	98	112212	94	113237	100	114593	96	116522	89
110849	98	111576	79	113003	96	115334	96	110700	94	111375	87	112213	70	113288	97	114625	76	116540	80
110953	91	111589	99	113110	94			110804	78	111552	100	112639	89	113411	91	114642	95	116681	84
111080	78	111683	99	113226	100	106656	64	110929	85	111591	99	112700	85	113474	97	114890	97		
111104	81	111841	97	113281	95	108841	97	111022	100	111762	100	112710	91	113731	82	114909	72		
111139	82	112031	100	113371	86	108933	100	111038	90	111814	60	112805	100	113950	99	115441	94		
Cep OB2												71: 1 O, 53 B, 10 A, 4 F, 0 G, 2 K, 1 M, 0 R							
102771	92	105925	94	106801	86	107316	97	108073	70	109687	82	110200	96	103539	60	108427	75		
104021	85	106059	66	106843	46	107374	99	108372	54	109701	97	110441	90	104515	81	108603	100		
104605	94	106202	93	106896	90	107480	100	108605	78	109803	91	111089	95	104775	70	109393	98		
105091	87	106210	83	106937	68	107733	68	108902	78	110025	76	111785	75	106022	96	109451	98		
105222	96	106227	66	106956	100	107777	68	109130	76	110026	85	112558	88	106874	85	109586	93		
105545	100	106265	82	107164	48	107961	94	109253	82	110090	51	113908	73	107418	71	109798	100		
105621	77	106349	99	107209	55	107984	81	109416	95	110125	75			107755	97	111972	87		
105699	99	106689	82	107276	99	108054	98	109603	76	110186	99	103385	81	108096	98	112430	99		
Cep OB6												20: 0 O, 6 B, 7 A, 1 F, 2 G, 3 K, 0 M, 1 R							
109426	94	110266	96	110356	100	110497	98	110807	92	110988	100	111060	100	112141	89	112998	98	113316	99
109492	97	110275	89	110459	100	110648	84	110925	86	110991	89	111069	79	112473	97	113255	99	113993	79